INTEGRATION OF AN INTER TURBINE BURNER TO A JET TURBINE ENGINE

THESIS

Matthew M. Conrad, Captain, USAF

AFIT-ENY-13-M-06

DEPARTMENT OF THE AIR FORCE
AIR UNIVERSITY
AIR FORCE INSTITUTE OF TECHNOLOGY

Wright-Patterson Air Force Base, Ohio

INTEGRATION OF AN INTER TURBINE BURNER TO A JET TURBINE ENGINE

THESIS

Presented to the Faculty

Department of Aeronautics and Astronautics

Graduate School of Engineering and Management

Air Force Institute of Technology

Air University

Air Education and Training Command

In Partial Fulfillment of the Requirements for the

Degree of Master of Science in Aeronautical Engineering

Matthew M. Conrad, BS

Captain, USAF

March 2013

INTEGRATION OF AN INTER TURBINE BURNER TO A JET TURBINE ENGINE

Matthew M. Conrad, BS

Captain, USAF

Approved:

_____   _____
Marc D. Polanka, PhD (Chairman)   Date

_____   _____
Maj. James L. Rutledge, PhD (Member)   Date

_____   _____
Mark F. Reeder, PhD (Member)   Date

AFIT-ENY-13-M-06

Abstract

As aircraft power requirements continue to grow, whether for electrical systems or increased thrust, improved engine efficiency must be found. An Ultra-Compact Combustor (UCC) is a proposed apparatus for accomplishing this task by burning in the circumferential direction as a main combustor or an Inter-Turbine Burner (ITB). In order for the UCC to be viable it is important to study the effects of feeding the core and circumferential flows from a common gas reservoir. This research effort has developed a diffuser, for the AFIT Combustion Laboratory, that is capable of 80/20, 70/30, and 60/40 mass flow splits between the core and cavity for flow emanating from a single source. The diffuser was fabricated robustly so that the single flow source may consist of a vitiated air, such as that from a small jet engine, or a clean air source of compressed air. Chemical analysis software (CHEMKIN) was applied to assist in the prediction of which flow split would produce the best results and testing of this prediction was initiated. A second important issue for UCC development is the assessment of the effects of g-loading on atomized fuel sprays within a UCC because it is important to stabilize the flame in the cavity. To this end, fuel spray experiments have been conducted over a g-load range of 0 to 3000 to examine how atomized fuel behaves within the circumferential cavity. Results gathered from high speed imaging showed that as g-load increased, fuel carried toward the outside diameter of the circumferential cavity. Results were obtained for combinations of fuel pressure, and cavity air mass flow rate. In summary, a new rig has been developed that will facilitate future endeavourers into UCC research.

Table of Contents

List of Figures

List of Tables

List of Abbreviations

AFIT	=	Air Force Institute of Technology
AFRL	=	Air Force Research Laboratory
EGV	=	Exit Guide Vane
HPT	=	High-Pressure Turbine
ID	=	Inner Diameter
IGV	=	Inlet Guide Vane
ITB	=	Inter-Turbine Burner
LPT	=	Low-Pressure Turbine
MD	=	Middle Diameter
OD	=	Outer Diameter
RVC	=	Radial Vane Cavity
STE	=	Small Turbine Engine
UCC	=	Ultra-Compact Combustor

List of Symbols

CO	=	Carbon Monoxide
CO_2	=	Carbon Dioxide
H_2O	=	Water
NO_x	=	Nitrous Oxide
O_2	=	Oxygen
Φ	=	Equivalence Ratio
$(\Delta p/q)$	=	Change in pressure over dynamic pressure

INTEGRATION OF AN INTER TURBINE BURNER TO A JET TURBINE ENGINE

1   Introduction

1.1   Ultra-Compact Combustor

Combustor design in jet engines has not changed greatly since the first jet engine was made. The traditional jet engine combustor is axial in flow. The air is diffused as it leaves the compressor so the flow is at a low Mach number when entering the combustor. Fuel is introduced to the airflow, mixed, and burned in the combustor. The hot combusted gas is then sent to the turbine to be transferred into work to power the compressor and the electrical systems of the aircraft. The combustor must be long enough for the air fuel mixture to burn completely before entering the turbine.

One way to improve the turbine engine is by increasing the thrust-to-weight ratio, which can be accomplished by reducing the weight of the engine. Shortening engine components or combining engine stages into a more compact system can reduce engine weight. One potential way of achieving a lighter engine is the Ultra-Compact Combustor (UCC) as shown in Figure 1.1. In the figure a comparison of a traditional turbine engine and a turbine engine with a UCC are shown side by side. The shorter UCC engine will be lighter due to a smaller engine size than a comparable traditional engine. The Ultra Compact Combustor is being developed jointly by the Air Force Research Laboratory (AFRL) and the Air Force Institute of Technology (AFIT).

Centripetal acceleration is the fundamental principle of how the UCC functions. Combustion in the UCC occurs in the circumferential direction in the circumferential cavity. By burning circumferentially, the centripetal acceleration in the cavity causes the g-load to increase. The centripetal acceleration induces a buoyant force in the cavity. The buoyant force causes the heavier non-combusted reactants toward the outside of the cavity while the lighter combusted products move inward toward the core of the UCC. The products can then rejoin the core flow and continue to the turbine.

A traditional combustor must be long enough to allow for combustion to complete before entering the turbine. The UCC has the added benefit of burning in the circumferential direction, which means the combustor has a theoretically infinite length because it is a circle. The combustor section of the engine can now be made much shorter because the flame length is burning in the circumferential direction. To achieve flow in the circumferential direction, the air leaving the compressor must be injected into the circumferential cavity at an angle to induce the swirl and mixing with the fuel. Once the fuel-air mixture is moving in the circumferential direction, centripetal acceleration causes the buoyant force to keep the combustion in the circumferential cavity. Lewis [1] found that as g-loading is increased, flame speed is also increased. The increase in flame speed allows for an axially shorter combustion cavity due to the increased reaction rate. By designing the combustor this way it is estimated that the combustor could be 1/3rd the length of a traditional combustor as seen in Figure 1.1. The UCC shown in Figure 1.1 is idealized in that it not all of the components to integrate the UCC into the engine have been accounted for, such as a diffuser to bring flow from the compressor into the UCC.

The diffuser need to slow down the flow to enter the UCC was not addressed in the past and therefore is now of concern when integrating the UCC into a turbine engine. Therefore the reduction to the length of the combustor will be less than what has been predicted in the past. However, any reduction in the combustor length would lead to less material or simply weight, increasing the thrust-to-weight ratio.
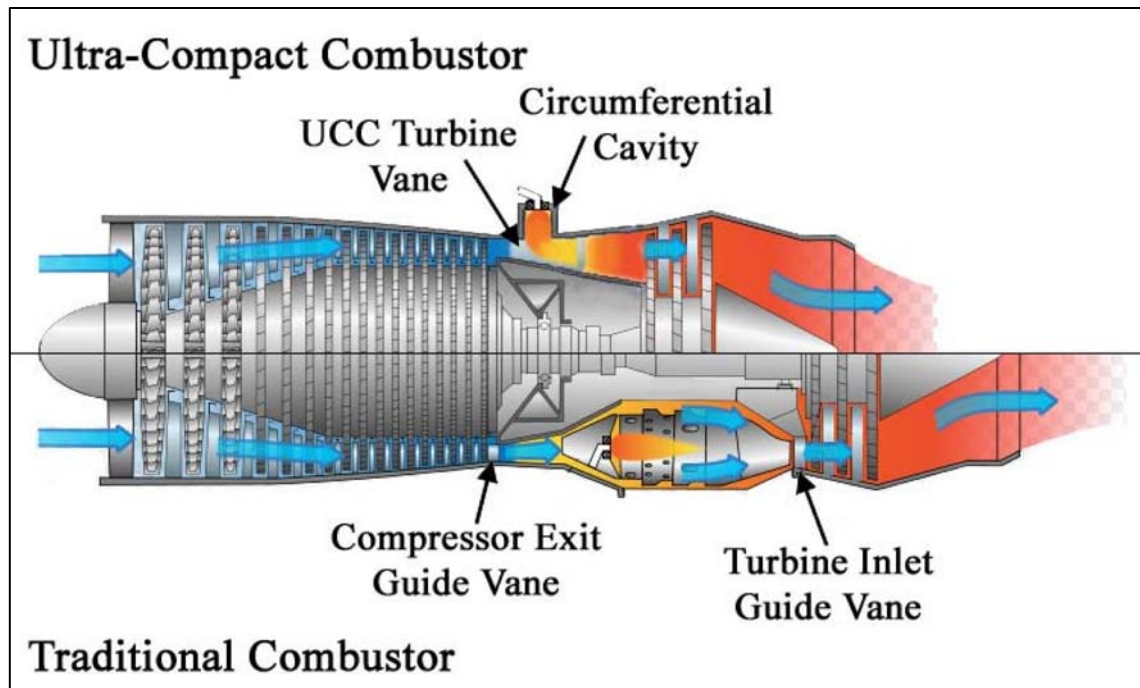
Figure 1.1: Axial length comparison of traditional & ultra-compact combustors [2]

A challenge of the UCC design that is explored in this thesis is the integration of the UCC to a common flow source. The UCC has two flows, a core and circumferential. Both of these flows come from the exit of the compressor. The flow exiting the compressor therefore must be split to provide the two flows to the UCC. Previous research, which will be discussed later, used a separate feed for the core and circumferential cavity flows. An important aspect of splitting the flow from a common

3

source is to minimize pressure losses through the flow splitting process and through the UCC. This thesis discusses a diffuser that has been fabricated to have the core and circumferential flows come from a common source. The new UCC diffuser will be important toward accomplishing this goal as it will provide real pressure loss data for flow through the UCC.

A second challenge of UCC design is the integration of liquid fuels to the UCC. The effect of g-loading on fuel sprays in the circumferential cavity is also important to understand for integration into a turbine engine. Aircraft turbine engines use liquid fuels and therefore it is important to understand how liquid fuels will act inside of the circumferential cavity under g-loads. Fuel spray testing has been conducted in the circumferential cavity to begin examining liquid fuels under g-loads in a UCC.

Most UCC research up to this point has been conducted with clean air. If the UCC design were to be applied as an Inter-Turbine Burner (ITB), the incoming air to the circumferential cavity would originate from the flow exiting the high pressure turbine. As such it would have already been burned in the main combustor. Therefore studying the impact of vitiated air on the combustion dynamics is of current concern.

1.2   Inter-Turbine Burner

Second stage combustion is already used in many modern military engines through the use of afterburners. An ITB is another type of second stage combustion which could be used to provide similar thrust while using less fuel. Aircraft are also incorporating more advanced electronics which require larger amounts of electricity. This additional power must come from somewhere. An ITB again might be the answer.

4

In the past, adding an additional combustor in between turbine sections would have not been worth the additional weight gain to the engine, but now with the development of the UCC, an ITB may become practical.

As stated above, the ITB would be located between the high-pressure and low-pressure turbines. The ITB could provide a small increase in temperature to the flow before entering the low-pressure turbine. The additional energy provided by the low-pressure turbine could then be used to operate larger fans or generate additional electricity for the aircraft. In addition to the challenges of the UCC, the ITB also functions with a vitiated air source. The vitiated air contains higher concentrations of carbon dioxide, water vapor, NO_x and unburned hydrocarbons, while having less available oxygen for combustion in a secondary combustion chamber. In a traditional afterburner large amounts of fuel are injected into the augmenter section of the engine to maximize the temperature gain and therefore increase thrust. Not all of the fuel is combusted inside the engine and any combustion outside the engine does not go toward thrust production. In an ITB, less fuel would be necessary, when compared to the main combustor, because centripetal acceleration would keep unburned fuel in the circumferential cavity until it is burned. The flow exiting the ITB would then be able to enter a second turbine to have more work extracted out to provide more power to the compressor and fan, or generate addition electrical power for the aircraft.

1.3   Objectives

There are several objectives to this research. The first is to examine how to integrate the UCC into a common flow source. In past UCC research, the core flow and

circumferential flow have had different sources. The core flow entered axially and the circumferential flow was injected from the top of the rig to induce the swirl in the combustion cavity. For this research a flow splitter has been designed and fabricated to allow the core and circumferential flows to come from a common source. The splitter takes a specified amount of the common source and directs it to the circumferential cavity. The flow enters from the side of the circumferential cavity rather than from outer diameter (OD) of the circumferential cavity. The diffuser is designed to have modular mass flow splits by replacing a single component. The diffuser is able to accept flow from a clean or vitiated source which will be able to provide a valuable comparison of the different air types while keeping the diffuser geometry the same. More on the diffuser design will be discussed in Chapter 3.

The second objective is focused on examining the effect g-loading has on fuel sprays in the circumferential cavity. It is important to understand how atomized fuel acts in the circumferential cavity as part of the integration of the UCC to a turbine engine. It would be expected that due to the higher density of the atomized particles, the g-load would cause them to stay toward the OD of the circumferential cavity. This would improve efficiency as unburned fuel would stay in the cavity until combustion is complete which is highly desired.

The last objective is to create a vitiated air source for the UCC inlet. The vitiated air source is needed to begin using the UCC to be used as an ITB. A small jet engine is the vitiated air source for the engine. The combination of the diffuser and the small jet engine will allow future research to examine how vitiated air affects the combustion

process in the UCC. Due to the reduced amount of oxygen available in the

circumferential chamber, lower amounts of fuel will be needed to achieve complete

combustion. In addition air-to-fuel ratios will be kept below stochiometeric to reduce

burning in the core flow. The low air-to-fuel ratios will be very important to

understanding if the UCC concept is a good option for an ITB.

2   Background

2.1   Introduction

The major push in jet engine design is in reducing the size and weight of the engine while maximizing efficiency and thrust. One option that is being considered is a constant temperature cycle engine. While having combustion continue through the turbine section of the engine would be excellent in terms of performance gain, it is impractical [3]. Combustion in the turbine section is impractical because it is too difficult to continually add fuel injectors between components. An alternative consists of staged burning within the stator sections of the turbine limiting combustion to this region. An ITB can accomplish burning between turbine stages as required. This needs to be accomplished over a short axial length to not increase the size of the engine. The Ultra-Compact Combustor (UCC) is a viable option for meeting this requirement. The specific research goals of this endeavor are to examine how to integrate the UCC into a common flow source, effects of g-load on atomized fuel sprays, and the creation of a vitiated oxidizer source for the UCC. These three goals will be discussed in greater detail throughout the chapter.

2.2   Diffuser

The purpose of a diffuser upstream of a combustion chamber is to decelerate the flow to allow combustion to occur in the combustion chamber and to allow air to bypass around the combustor for cooling purposes. A diffuser can be designed by looking at data from existing diffusers and interpolating or extrapolating to achieve a new design or by simply selecting values of ($\Delta p/q$) for different diffuser applications [4]. When

designing a diffuser, the three most important characteristics to consider are the diffuser

cross sectional area, the ratio of length to inlet hydraulic diameter, and the size and shape

of inlet boundary layers. Mach number and direction of inlet flow are also evaluated, as

well as whether the flow is steady, periodic or fluctuating. Finally, straight or curved

wall shape, and roughness, and downstream conditions are considered. With such a vast

amount of diffuser variables to consider a method would be needed to design a diffuser

for the ITB.

Pressure losses are a major concern in diffuser design. If the diffuser opens up

too quickly, then separation can occur as seen in Figure 2.1. Separation occurs in a

diffuser when the diffuser opens up too quickly. For a diffuser length to inlet ratio of 10,

separation will not be present with a diffuser wall angle of less than 8° [4]. Appreciable

separation will begin to appear from 8° to 11° and separation will occur after 11°. When

separation occurs in the diffuser, losses in pressure will result. Even if the diffuser walls

angle in such a way that the flow can reattach downstream, the pressure loss will not be

recovered. The goal is to open up the diffuser enough to achieve the desired flow without

creating separation and incurring a loss in pressure.

(a) Small area ratio: moderate pressure recovery

(b) Moderate area ratio: higher pressure recovery

(c) Higher area ratio: no pressure recovery
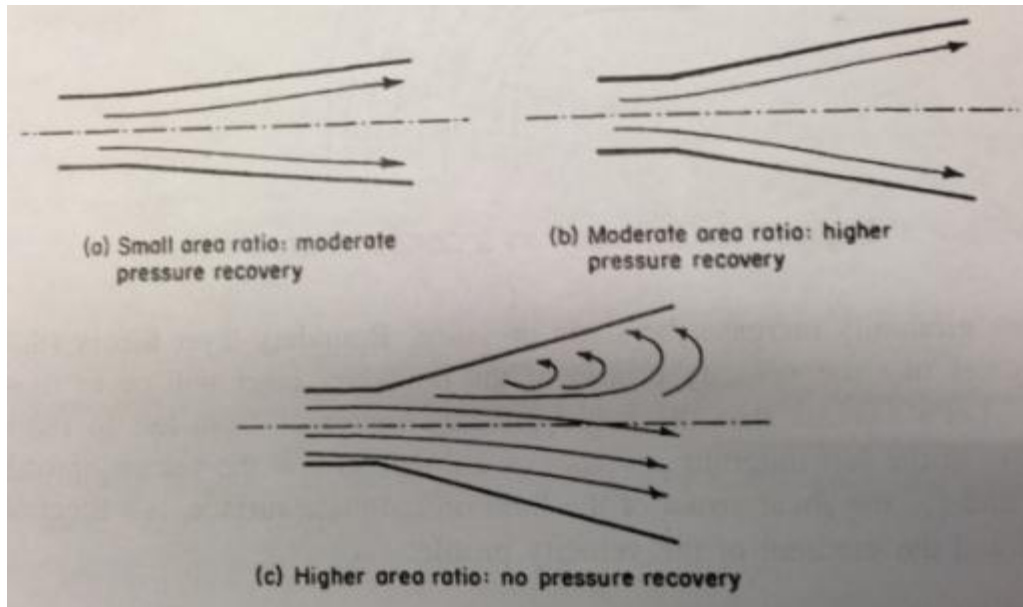
Figure 2.1: Diffuser design pressure loss risk [4]

2.3 UCC and ITB

An idea for achieving a higher thrust-to-weight ratio while maintaining engine efficiency was proposed by Sirignano et al. in 1997 [5]. They showed that the traditional turbine engine augmenter could be removed and replaced with an ITB. Sirignano et al. were able to accomplish this without sacrificing any thrust and becoming more fuel efficient at the same time. The UCC was one option for fulfilling their proposal.

The fundamentals of the UCC ITB are based on two different research areas. The first consists of mechanisms for maintaining swirl from the upstream flow with minimal pressure losses. Bohan [2] has been able to show computationally that the compressor exit guide vane (EGV) and the turbine inlet guide vane (IGV) could be combined into a single "hybrid" vane. This design allowed the air to maintain swirl as it entered the UCC section. This same concept could be applied to an ITB where the vane would direct the

flow leaving the high-pressure turbine (HPT) through the ITB and then into the low-pressure turbine (LPT).

UCC research in flame stability limits have been conducted by Zelina et al. for a range of g-loads and equivalence ratios [6]. The equivalence ratio is defined in Equation 1. Maximum g-loading with a stable flame occurs at an equivalence ratio of one as seen in Figure 2.2. Within the ITB much lower equivalence ratios will be used forcing lower g-loading. A lower equivalence ratio is desired for the ITB because all of the fuel must be combusted prior to leaving the ITB to ensure unburned fuel does not ignite with film cooling flows on the turbine blades. An additional benefit of a UCC that was also found by Zelina et al. is the flame lengths were 50% shorter [7]. This is a major benefit for the ITB in terms of increased turbine life.

Equation 1: Equivalence ratio

$$\Phi = \frac{m_{fuel}/m_{air}}{\left(m_{fuel}/m_{air}\right)_{stoichiometric}}$$
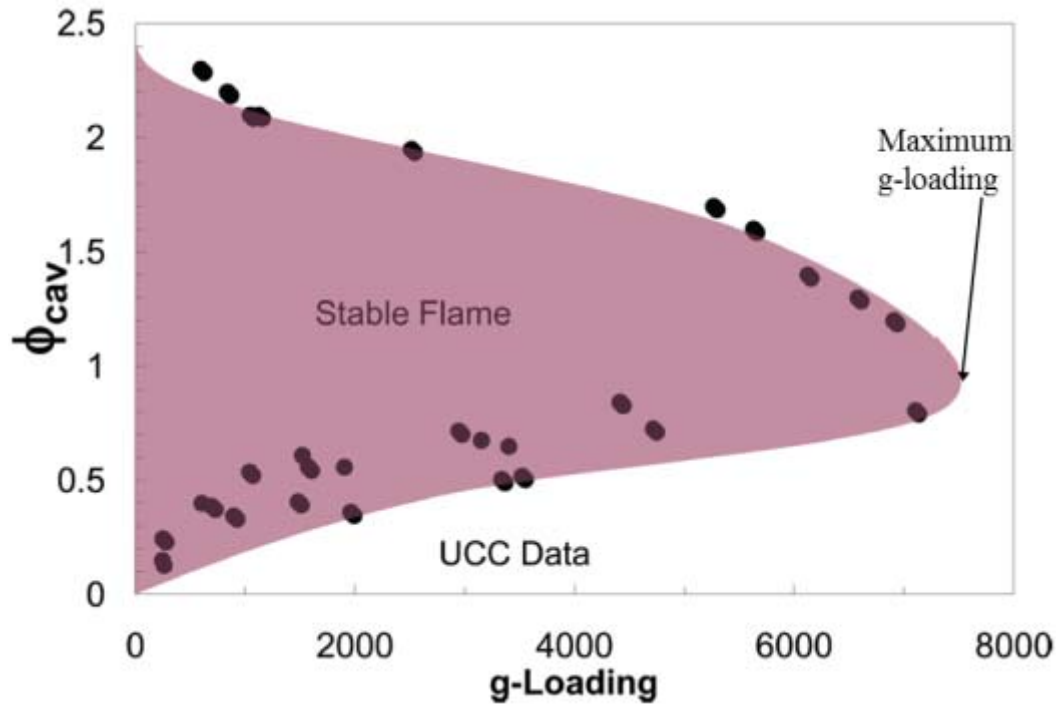
Figure 2.2: UCC LBO as a function of section g-loading using JP-8+100 as fuel [7]

The UCC is currently being developed by the Air Force Research Laboratory (AFRL) [6], [7] and the Air Force Institue of Technology (AFIT) [2] jointly. Figure 2.3 compares a conventional engine with a axial combustor to that of an engine with a UCC and UCC based ITB. The lower part the figure shows a conventional gas turbine engine hot section. The red slashed out sections are, from left to right, the compressor exit vane, HPT IGV, and the stator between the HPT and LPT. These components would be incorporated into the UCC and the ITB. The upper part of the figure is a potential gas turbine engine with a UCC for the main combustion chamber and a UCC for an ITB.
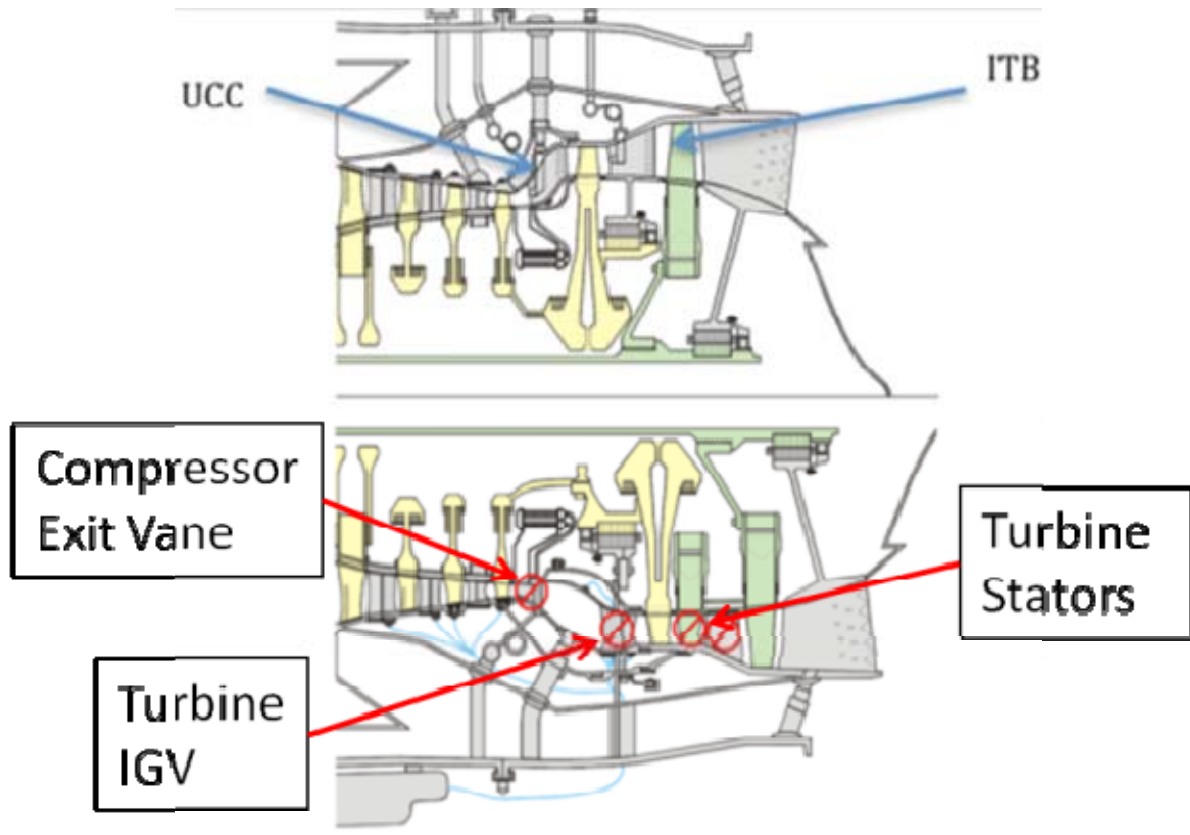
Figure 2.3: Conventional Combustor (lower) and UCC and ITB (upper) [8]

The purpose of adding a UCC to a jet engine in an ITB configuration has two practical mission applications. First, the engine can then be optimized for cruise and the ITB can be activated when additional thrust is required for takeoff, evasive maneuvers, or when trying to maximize speed. This configuration could replace an afterburner if enough thrust could be generated while also providing more flexibility in operation. Second, the addition of an ITB can be used to generate extra power when needed for short duration, high power requirement missions. The Airborne Laser would be an example of this when the additional power is only required just before and during firing

of the laser. This could represent an efficient mechanism to generate short duration power without inducing a weight penalty.

A cycle analysis of an ideal jet engine with and without an ITB is shown in Figure 2.4. The solid line represents a jet engine without a ITB, showing the rise in temperature in the compressor, the rise in temperature and entropy in the main combustor and then the decrease of pressure and temperature in the high and low pressure turbines. If an ITB is added in between the high and low pressure turbines, a rise in temperature and entropy can be achieved before heading to the low pressure turbine. This gain translates to additional work which can be extracted in the low pressure turbine.
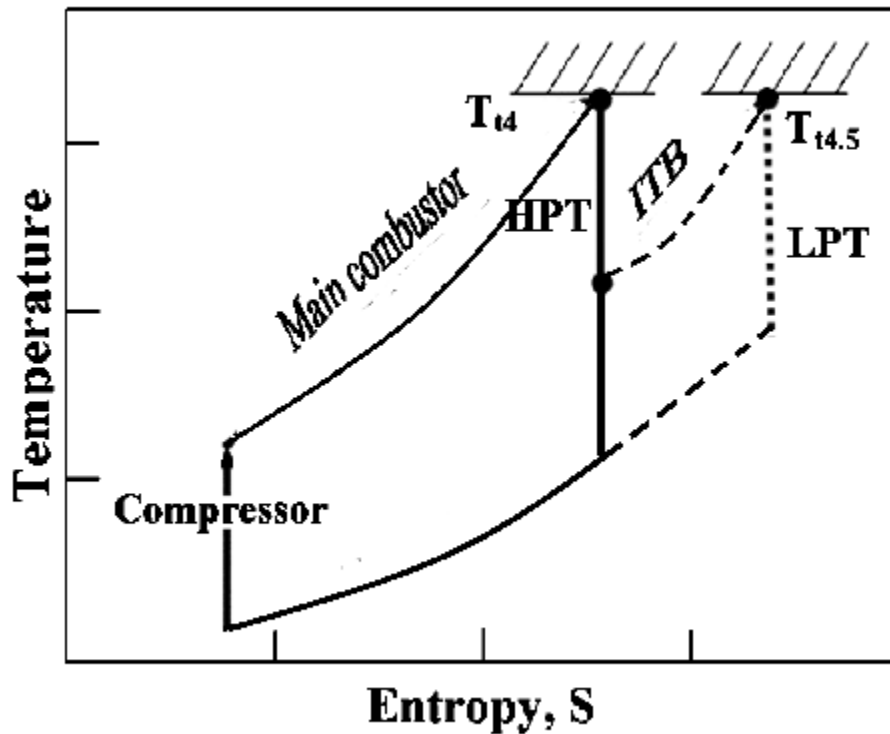
Figure 2.4: T-S diagram with ITB addition [9]

14

Fuel injection and type of fuel are also important to consider. Liquid JP-8+100 has been successfully used in a UCC [10]. Using JP-8 more accurately simulates operating conditions, as opposed to propane, as many military aircraft use JP-8. Another result from the work in UCC fuel injector design is that lean blowout performance and combustion efficiency were improved when fuel was injected at an angle into the UCC cavity. This can then be incorporated into the ITB for an improved chance of success.

CFD analysis has shown that a radial vane cavity (RVC), shown in Figure 2.5, can benefit an ITB [11]. An RVC is a passage cut into the side of a vane within the UCC to draw flow out of the circumferential cavity into the core flow. It was found that multiple combustion zones form in the UCC cavity, which is due to the airflow jets as they entered the flow. Hot combustion products were able to mix well with the main flow through the shear layer. The curved RVC performed well in mixing the combustion products and main flow, which allowed for peak temperatures to be in the center of the flow. This was an improvement over the straight RVC. The added gain from this design is an improved temperature field and radial profile at the exit of the ITB. A non-uniform temperature field can be detrimental to turbine blade life as well as turbine performance.
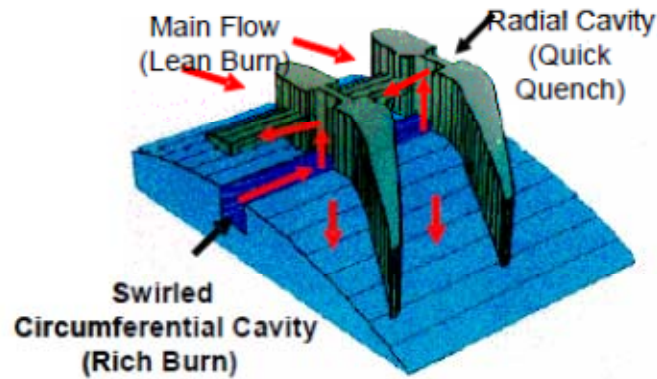
Figure 2.5: Curved RVC [11]

Liew et al. has conducted an off design performance-cycle analysis for a two spool turbofan engine with an ITB [9]. It was found that the engine with an ITB performed better than a non-ITB baseline engine in several areas. At full throttle, the ITB engine outperformed the baseline engine. Based on my interpretation of the data, Liew et al. found that thrust was increased by 10.9%, thrust specific fuel consumption was increased by 2.9% and thermal efficiency was increased by 4.5% at sea level static conditions.

2.4 Vitiated Air

The third goal is to look at flame stability and g-loading effects in the presence of vitiated air. A UCC has also been demonstrated, by Zelina et al., to operate with vitiated air in laboratory setting using laboratory supplied air and a vitiator [8]. The vitiator burned the air and used a "cyclone" type swirler. The oxygen levels in the vitiator were then controlled by adding additional shop air to the vitiated flow. The flow was then piped into the UCC cavity and the core flow area. Zelina et al. found that this ITB could

operate with extremely low overall fuel to air ratios. This allowed the ITB to have low fuel flow rates and maintain combustion. They also learned that at low equivalence ratios and high g-loading the combustion efficiency reached near 99.5%. One thing that was lacking from the study was the use of an actual turbine for the gas stream. Using an actual jet engine to supply the vitiated air would provide a more accurate UCC inlet condition for an ITB. The jet engine would have a more accurate temperature profile leaving the turbine for an ITB. Also the species that are produced would be that of a real jet engine.

2.5   Summary

UCC research up to this point has produced some excellent results. The UCC concept has shown the thrust-to-weight ratio of an engine can be improved with the use of a UCC. The UCC can also be applied as an ITB which will result in increased engine performance. More research still lies ahead before the design is ready to be implemented in a turbine engine on an aircraft. The overarching goal of my research was to advance UCC technology toward this overall goal in three ways. A common flow source for the UCC was important to the integration of the UCC into a turbine engine and needed to be investigated further. The examination of the effect g-loading had on the atomized fuel also needed to be conducted. Providing a vitiated air source to use the UCC in an ITB application was important towards advancing UCC technology.

3 Methodology

3.1 Introduction

A new test rig has been designed and built to examine the objectives of integrating the UCC to a common source, conduct fuel spray tests to examine the effect g-loading has on the atomized fuel, and setup a vitiated air source for the ITB. The new rig has several features to meet the objectives. First, a diffusing flow splitter has been made to bring clean or vitiated flow into the UCC. Second, the rig has been designed as a full annular model. Third, large observation windows have been incorporated into the design to allow for flow visualization and measurements. Fourth, the rig has been designed with ports throughout the UCC to acquire pressure and temperature measurements.

The experiment is located in the Combustion Optimization and Analysis Laser (COAL) Laboratory at the Air Force Institute of Technology. The lab has been used for many years to run various student experiments, including sectional UCC rigs. This is the first time a full annular UCC rig will be run in the COAL lab. The lab is equipped with three air lines of different sizes, can run various types of fuels, has the capability to make laser diagnostics measurement, and is equipped for determining combustion emissions. More detail of the COAL lab capabilities will be discussed throughout the chapter.

The testing rig consists of several components: a small turbine engine (STE), diffuser, the UCC, thrust stand, and instrumentation. The details of these components are discussed in the following sections. The JetCat P-200 turbojet engine has been chosen as the STE. The JetCat P-200 is used because it has been proven to be a reliable platform

by AFRL [12]. It is also roughly the correct geometry and mass flow rates for the UCC that has been designed by Wilson [13]. The vitiated air then proceeds into the diffuser, where the flow splits into a core flow and a circumferential cavity flow. The diffuser allows the UCC to run from a common source. The two flows will then enter the UCC where the circumferential cavity flow will be burned to produce additional thrust. The thrust stand will be used to hold all of the components in place and will be used to measure the thrust generated by the STE/ITB integrated system and then compared to baseline thrust measurements of the unaugmented STE. The instrumentation on the ITB will consist of temperature and pressure probes, cameras, and emissions collectors. The temperature and pressure probes will be used to collect data inside of the UCC. A camera will be used to examine the flow and combustion occurring in the circumferential cavity. Emissions measurements will also be used to examine the products of combustion and completeness of combustion. The pressure probes will be critical to examining pressure losses through the system.

3.2   ITB Design

Figure 3.1 shows a potential configuration for an ITB in a turbojet engine. The ITB is located downstream of the HPT and upstream of the LPT. Flow comes in the inlet to the compressor, is burned in the main combustor, and has work extracted from it in the HPT. After passing through the HPT, the flow enters the ITB where additional fuel is burned before heading to the LPT for further work extraction before exiting the engine. In this experimental setup the STE is being used as the primary engine. I.E. the STE's compressor, combustor, and turbine serve as the components to the left of the ITB in

19

Figure 3.1. This provides the high temperature, vitiated air to the ITB. The ITB is then connected via a diffuser aft of the STE as shown in Figure 3.2. The flow that exits the STE enters the diffuser where the flow is split into the core and circumferential flows. Additional fuel is added at high g-loading to the circumferential flow. The two flows then rejoin and exit the ITB. A low pressure turbine would follow the ITB, but was not added to this experimental setup as it would increase the complexity of the system beyond what is required to meet the objectives of the research.
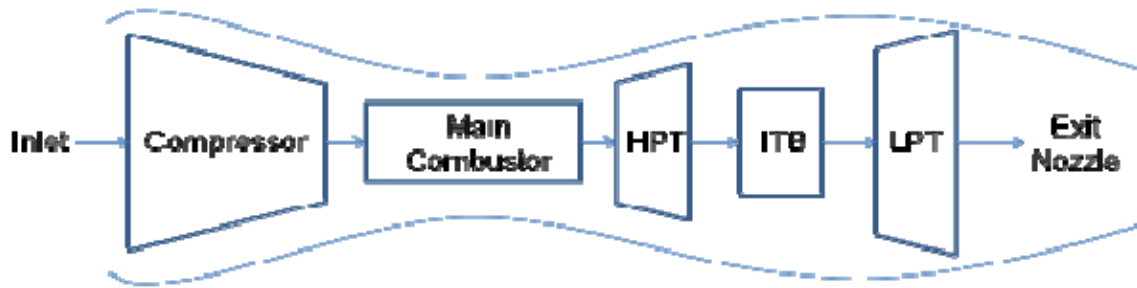
Figure 3.1: Turbine engine with ITB
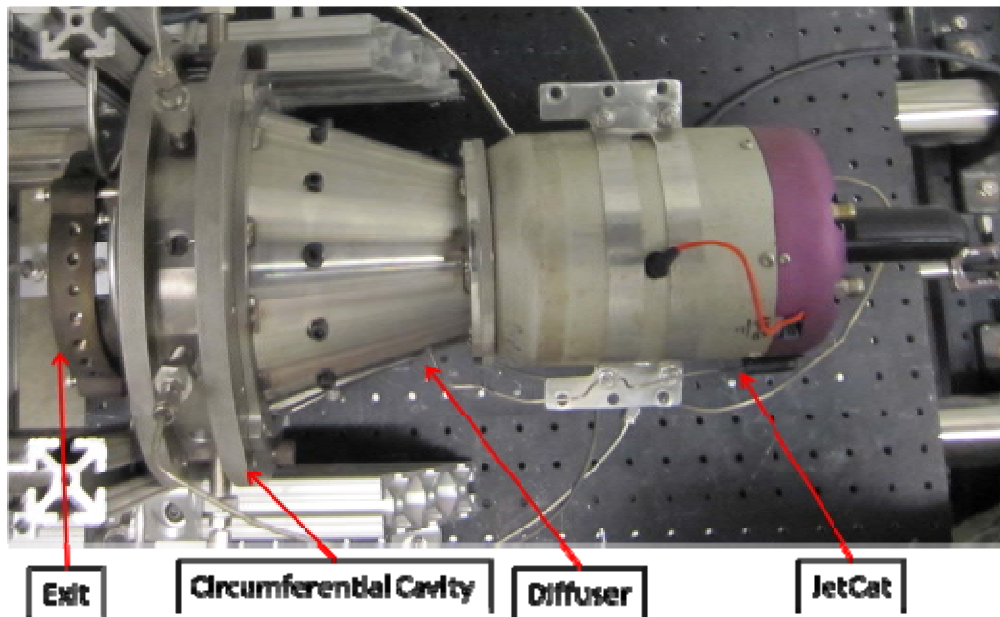
Figure 3.2: STE and ITB

The STE exit condition are a mass flow rate 1 lb/s, temperature of 1023 K, Mach 0.76, and a approximately zero swirl. The STE exit conditions are inlet conditions to the ITB. The equivalence ratio desired for the ITB is between 0.3 and 0.6. This range of equivalence ratio has been chosen because a small gain of 300 K is desired as output from the ITB while using minimal fuel. The g-load in the circumferential cavity is desired to be 1500. The ITB can be operated using two different configurations, as a standard ITB minus the low pressure turbine or as an augmenter. The Mach numbers and flow angles through the engine will vary with the configuration of the ITB and will be outlined in the next two sections.

3.2.1   Standard ITB Configuration

The standard ITB configuration is used to examine how vitiated air would act in the typical ITB environment depicted in Figure 3.1. In an ITB the flow exits the HPT at an angle. For the ITB used for this research an angle of 35° has been used based off of data from AFRL's HEETE program.   The 35° angle is induced in the diffuser, as the STE exhaust is approximately axial, to simulate flow coming off the HPT. Three mass flow splits have been designed and are discussed in Section 3.4.1. The Mach number exiting the diffuser is shown in Table 1 for the three mass flow splits. The flow then enters the center body at 35° and the appropriate Mach number for the flow split. The center body rotates the flow further and exits at 70°. The 70° angle would be the inlet angle to the LPT. The exit Mach numbers are show in Table 1. The mass Mach numbers were calculated using continuity. The locations of the Mach numbers in Table 1 are show visually in Figure 3.3. The red vertical lines in Figure 3.3 are the planes where the Mach numbers were calculated.

Table 1: Standard ITB Mach numbers

Core / Cavity Flow Percentage	Diffuser Exit Mach Number	Center body Mach Number	Exit Mach Number
80 / 20 Split	0.28 / 0.04	0.41	0.22
70 / 30 Split	0.24 / 0.06	0.35	0.22
60 / 40 Split	0.21 / 0.07	0.30	0.22
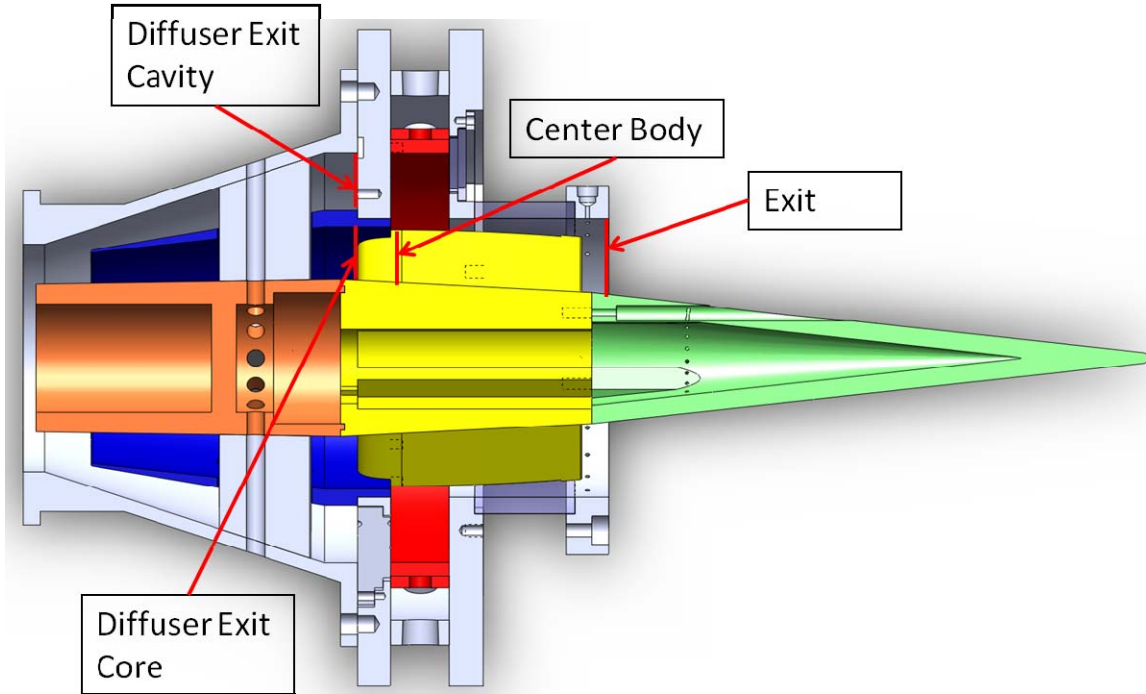
Figure 3.3: Mach number locations

3.2.2   Augmenter Configuration

For the augmenter configuration the flow through the engine is kept axial as much

as possible. The purpose of keeping the flow axial through the core is to reduce the

pressures losses from having to turn the flow. This has been done to produce as much

thrust as possible by reducing losses through the diffuser and the center body. The only

point where flow is not axial is in the circumferential cavity where flow is flowing in the

circumferential direction.   Therefore all of the flow angles through the diffuser and the

core are at 0°. The Mach numbers at the exit of the diffuser are show in Table 2. The

Mach number through in the center body and the exit Mach number are also shown in

Table 2. The exit Mach number for the augmenter is low because a nozzle has not been

designed to optimize the exit flow. The locations of the Mach numbers in Table 2 are

show visually in Figure 3.3.

Table 2: Augmenter ITB Mach numbers

	Diffuser Exit Mach Number	Center body Mach Number	Exit Mach Number
80 / 20 Split Point	0.28 / 0.04	0.36	0.22
70 / 30 Split Point	0.24 / 0.06	0.31	0.22
60 / 40 Split Point	0.21 / 0.07	0.27	0.22

3.3   Small Turbine Engine

For this experiment the JetCat P-200 engine was selected as the STE needed to

provide a vitiated air generator for the ITB. The JetCat engine is typically designed for

use in remote controlled model aircraft. The STE is mounted on the stand in front of the

ITB. JP-8 will be used as the primary fuel for the STE. In addition to JP-8, the STE also

requires propane as a starter fuel. The STE is capable of starting with JP-8, but it is not

as reliable and can be significantly more messy to clean up from failed starts. A

dedicated fuel pump is used for the STE for the JP-8. The fuel pump is used to keep the

STE running as close to its normal operation as possible. The JetCat P-200 turbojet

engine is able to consume 1 lbs/s of air and the maximum fuel flow rate is 24.7 fluid

ounces per minute. The RPM range for the engine is 33,000 to 112,000. The exit

temperature of the STE is 1023 K at maximum RPM. The engine weights 5.53 lbs, has a

diameter of 5.07 inches, and is 13.65 inches long. The maximum thrust the engine can

produce is 52 lbf. A full list of the manufacturer rated performance specification can be

seen in Table 3.

Table 3: JetCat P-200 performance specifications [12]

Engine Performance Parameter	Manufacturer Rating
Speed Idle (rpm)	33,000
Speed maximum (rpm)	112,000
Thrust Idle (lbf)	2.0
Thrust maximum (lbf)	52.0
EGT minimum (°C)	480
EGT maximum (°C)	750
Pressure ratio	4.0
Total mass flow (lb./s)	1.0
Exhaust gas velocity (m/s)	490.0
Power output (hp.)	72.1
Fuel consumption at idle speed (lb./hr.)	13.46
Fuel consumption at maximum speed (lb./hr.)	76.16
Thrust specific fuel consumption at idle speed (lb./hr. lbf)	6.66
Thrust specific fuel consumption at maximum speed (lb./hr. lbf)	1.54
Engine weight (lb.)	5.22
Engine outer diameter (in)	5.20
Engine overall length (including Starter) (in)	13.98

A fuel component box seen in Figure 3.4 was fabricated to house the fuel pump,

filters and shut off valves of the STE fuel system. This box was made to improve safety

in the event of a fuel leak so it would have limited contact with oxygen. The STE's fuel

pump provides JP-8 to the engine from a 5-gallon JP-8 fuel container. A small propane

can supplies the propane starting gas for which no pump is needed. Both the propane and

JP-8 fuel lines have JetCat shut off valves which are controlled electronically by JetCat's

software. Manual shut off values have also been installed downstream of the fuel

component box to ensure fuel cannot flow into the STE in the event of a failed JetCat

shut off valve. Procedures for starting and operating the STE engine can be found in

Appendix A.
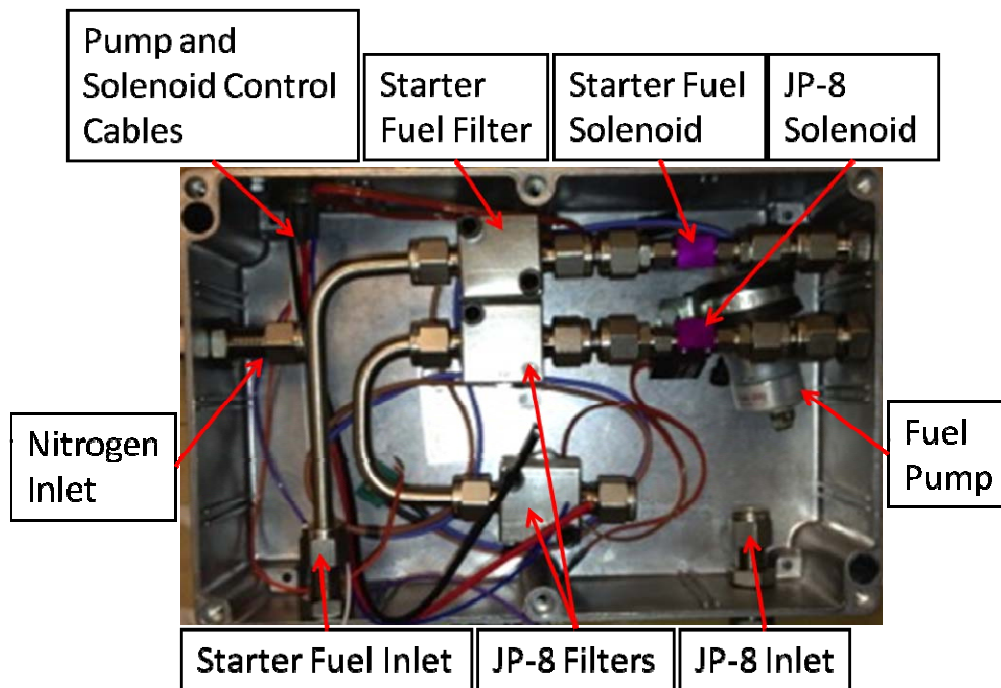
Figure 3.4: STE fuel component box

An electrical component box was also created to house the STE's electronic

control unit (ECU) which is seen in Figure 3.5. The ECU was also placed in a box to

reduce the risk of a spark from the ECU igniting any leaked fuel. Power for the ECU is

provided by a 7.2 VDC system run off of the lab power supply. The ECU has outlets

connecting to the fuel shut off valves and the fuel pump inside the fuel box. The STE

connects to the ECU by a RJ-25 communication cable and a power cable. A second

communication cable from the ECU goes to the control panel computer. The STE is

controlled from the control station using the LabVIEW software. The STE will be set to

the throttle position that is required to achieve the desired mass flow through the ITB.
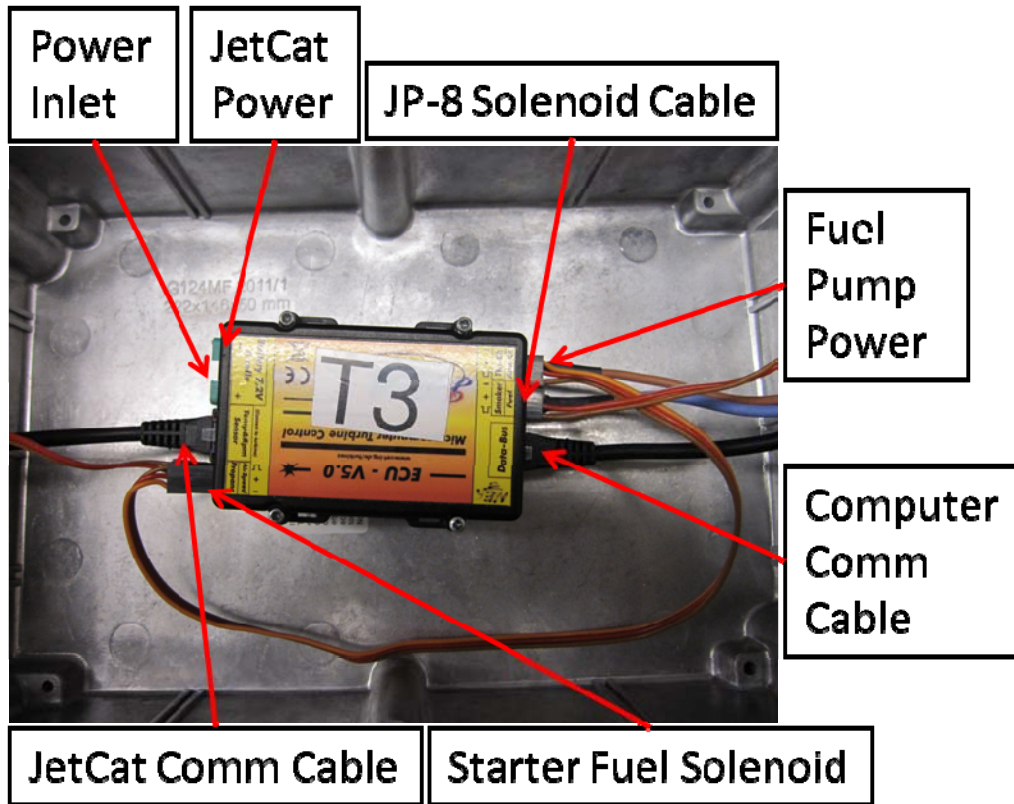
Figure 3.5: STE electrical component box

The STE is run in two configurations. The first is without the ITB rig to establish

a baseline. Then subsequently, the ITB is added to evaluate its performance. When

running the STE alone the engine is kept in its normal operating configuration. The

nozzle is removed from the STE to allow the STE to mount onto the ITB. An exploded

view of the STE engine can be seen in Figure 3.6, including the nozzle that was removed

for integration with the ITB.
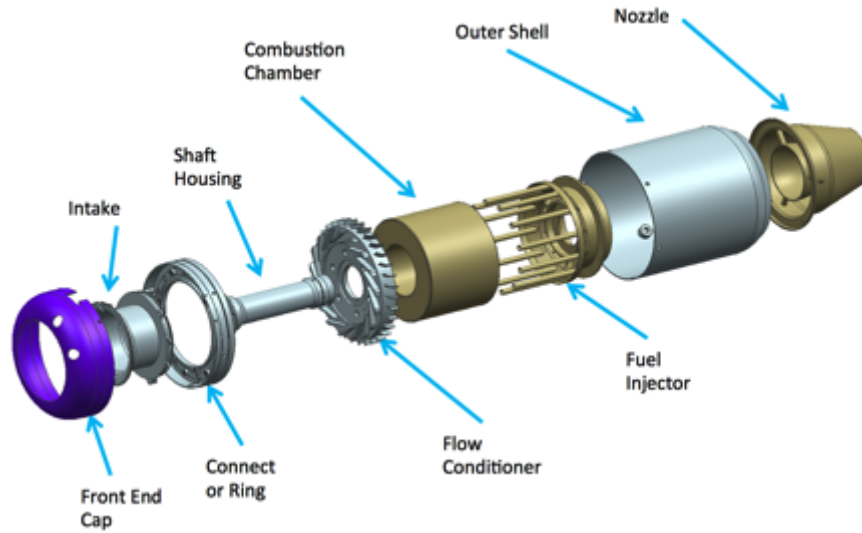
Figure 3.6: Exploded view of JetCat P-200 engine

Baranski et al. has used the JetCat P-200 engine at AFRL to examine the use of bio-fuels [12]. The air and fuel mass flow rates for the JetCat P-200 were determined for the range 33,000 to 112,000 RPM for JP-8 seen in Figure 3.7. Knowing the angular velocity required to achieve a given mass flow rate will be important when varying the g-load in the circumferential cavity of the ITB.
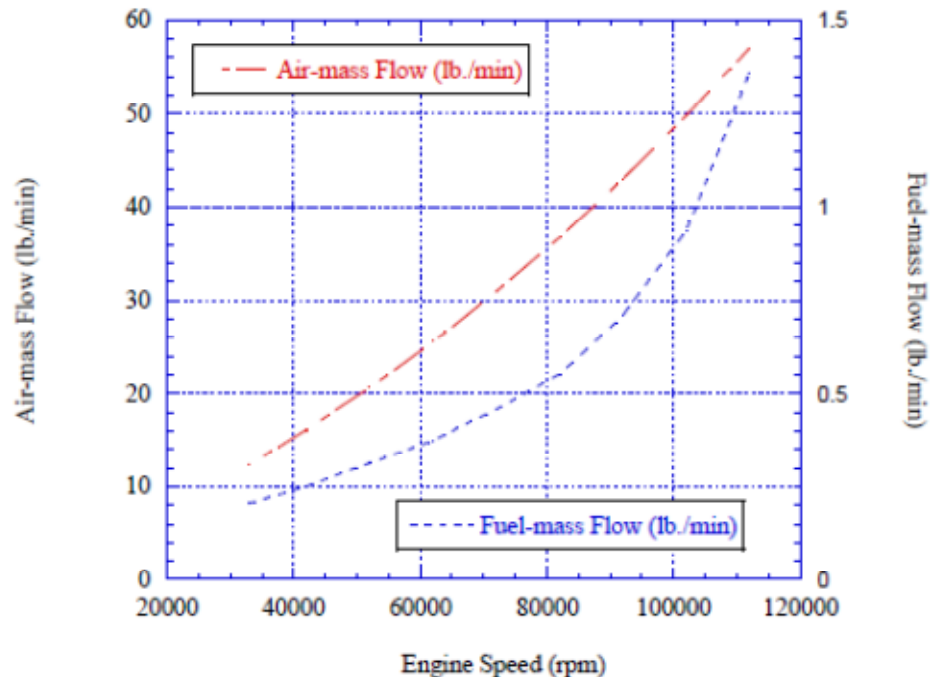
Figure 3.7: JetCat P-200 flow rates for varied engine speed

3.4 ITB Components

The ITB that was designed for the experiment is made of several components, including the diffuser, center body, combustion chamber, and exit as seen in Figure 3.8. The major components of the ITB are labeled and will be discussed throughout the section. The ITB has been designed to allow an inlet air flow of 1 lbs/s, as the JetCat P-200 engine will be used to provide the vitiated air source. Figure 3.9 below provides some of the overall dimensions of the ITB that will accommodate the flow rate of the STE. The overall length of the ITB and STE is 27 inches with the STE accounting for the first 10 inches. The diameter of the ITB at its greatest is 10 inches. The diffuser inlet diameter is 3.469 inches which is equal to the STE exit area without the nozzle attached.

A general description of the flow through the ITB is discussed next, and then the

components of the ITB will be discussed in the following subsections.

Front Combustion Plate

Outer Ring

Back Combustion Plate

Tail

JetCat

Diffuser

Combustion Ring

Center Body

Exit Ring
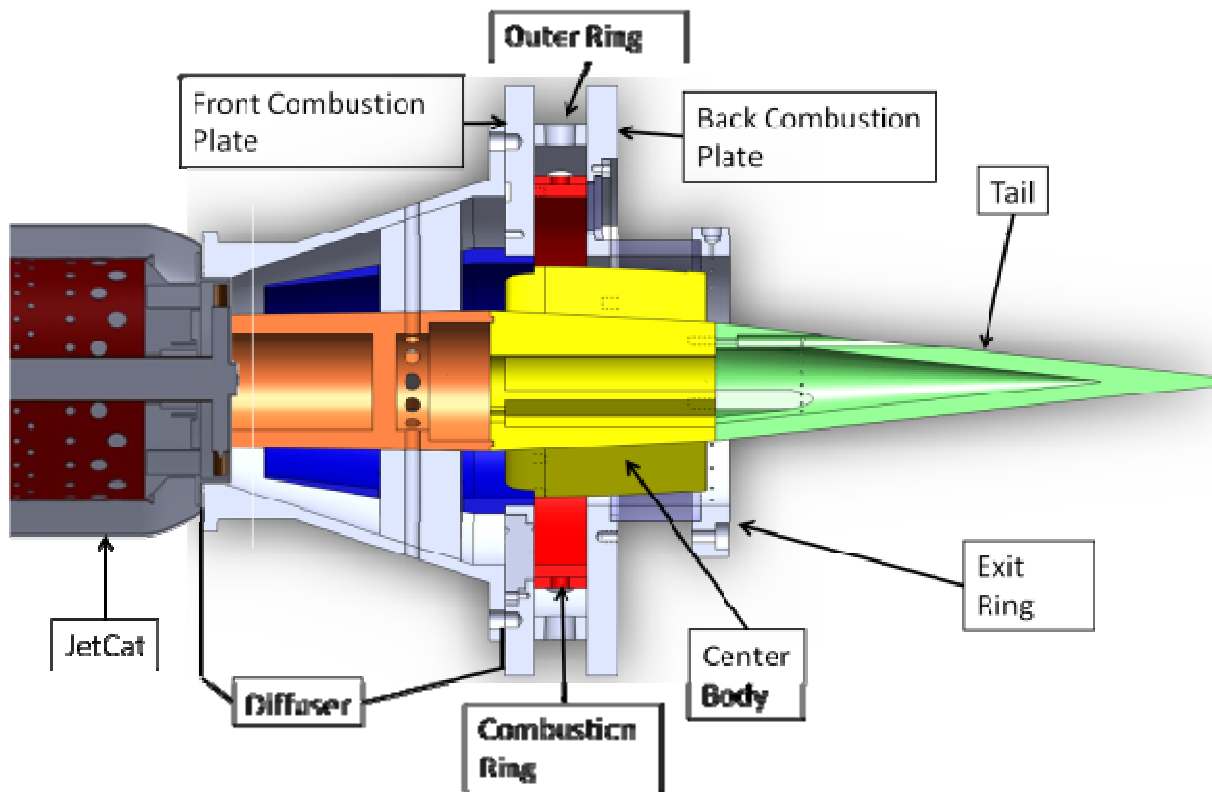
Figure 3.8: Crosscut of ITB

29
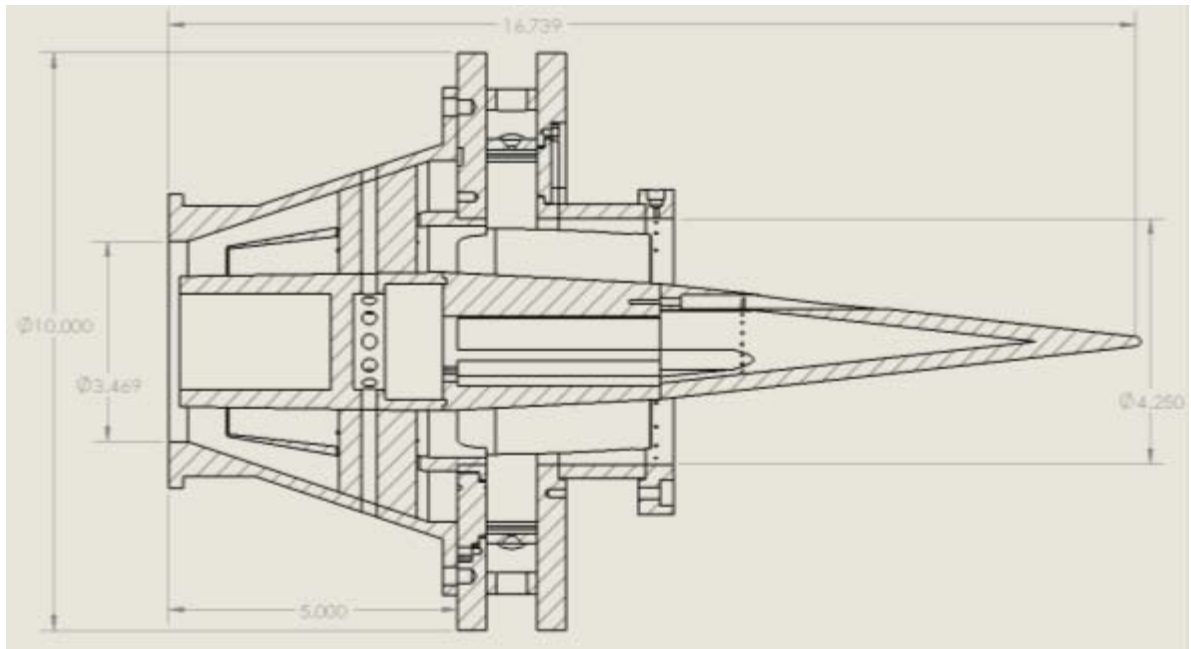
Figure 3.9: ITB dimensions

The flow through the ITB is shown moving from left to right in Figure 3.10.

Starting at the left is the inlet for flow into the diffuser. This flow represents the exit flow

from the STE. This flow splits into a core flow and a circumferential flow. The core

flow is diffused and brought into the center body. The circumferential flow is diffused

and brought to the circumferential injector plates where the flow is injected into the

circumferential cavity. The flow in the circumferential cavity is swirling around the

circumferential cavity. At this point fuel is injected into the circumferential cavity

through 6 atomizing fuel nozzles. The flow is ignited by an ethylene torch that is

mounted on to the back combustor plate. As the flow in the circumferential cavity burns,

the combusted gases rejoin in the center body with the core flow and exit the ITB. Figure

3.8 provides an exploded view of the all of the parts of the ITB. These ITB components are discussed in the following subsections.
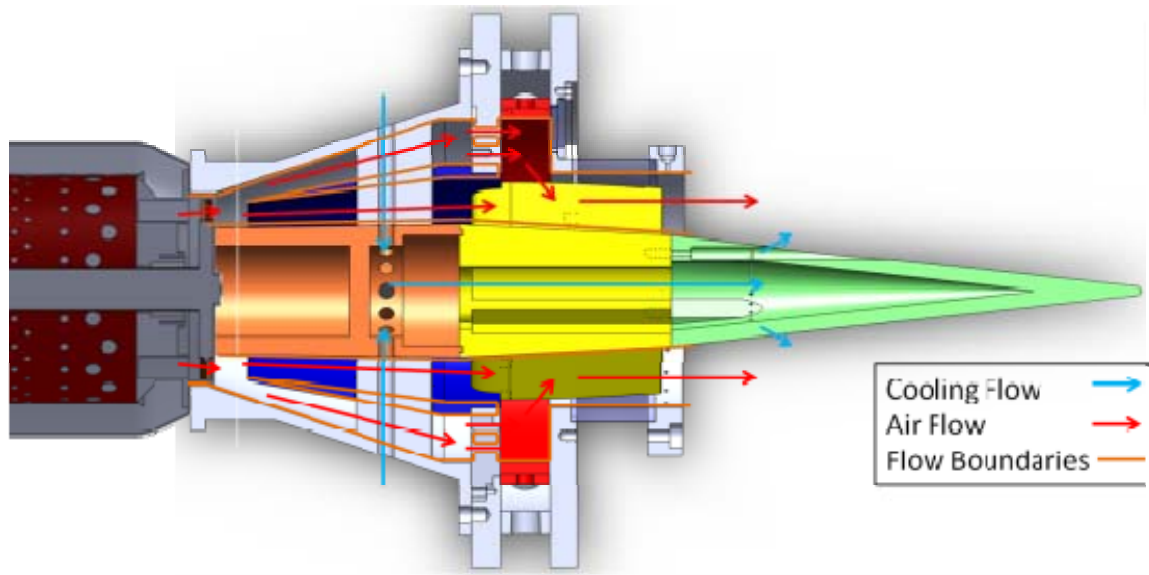
Figure 3.10: ITB flow pattern

3.4.1 Diffuser

The diffuser design was one of the critical aspects of this work. The diffuser needed to take the exhaust from the STE, slow it down, and split the flow. The Mach number of the flow exiting the STE is 0.71, without the nozzle. The exit Mach number will vary with the mass flow split in the diffuser as was shown in Table 1 and Table 2. The inlet to the diffuser is 3.45 inches in diameter and is designed to mount to the exit of the STE's turbine. The diffuser is 5 inches long. The exit of the diffuser is mounted to the front combustion plate. The flow splitter was designed to accomplish the flow splitting task while the outer and inner passages of the diffuser decelerate the flow. The splitter is rather simple in design. It consists of three major components and one additional set of structural components. The three main components are the outer

diameter (OD), inner diameter (ID) and the middle diameter (MD). Assembled and exploded view of the diffuser and its components can be seen in Figure 3.11 and Figure 3.12. The OD component houses the whole splitter assembly and connects the incoming flow source and the UCC chamber to the splitter. The ID component functions as a space holder to meet up with the center body of the UCC. The MD component is attached to the UCC on one end and the other end is unattached and used to split the flow into two flow paths, one for the core flow and a second for the circumferential cavity.

The additional set of structural components mentioned in the previous paragraph are for holding the three pieces together and consists of 12 airfoils to keep the flow moving downstream. Two sets of the 12 airfoils have been designed. The standard ITB configuration has airfoils that turn the flow 35° to provide the correct flow angle for the simulated turbine exit. The set for the augmenter configuration keeps the flow axial to minimize pressure losses through the diffuser. The standard and augmenter blades can be seen in Figure 3.13 for comparison. The chord of the straight airfoil is 0.47 inches and the length is 1.36 inches. The chord of the standard airfoil is 0.38 inches and the length is 1.53 inches.
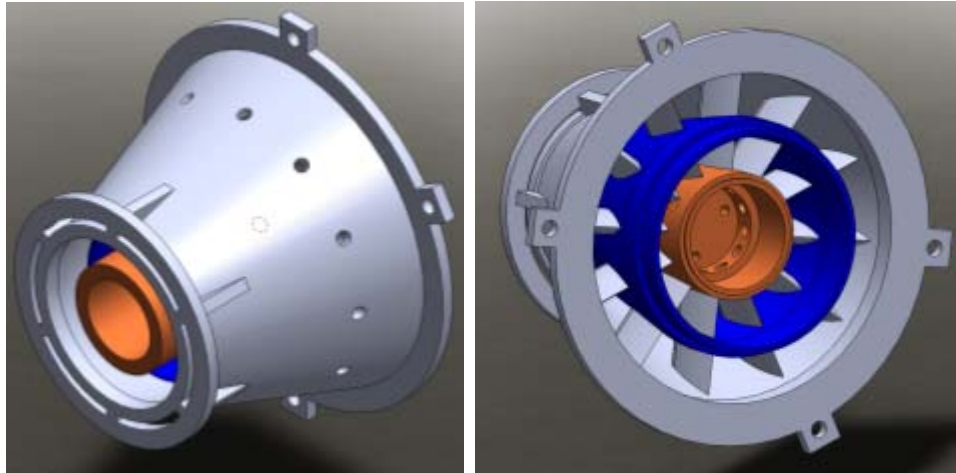
Figure 3.11: Diffuser assembled, front (left) and rear (right)
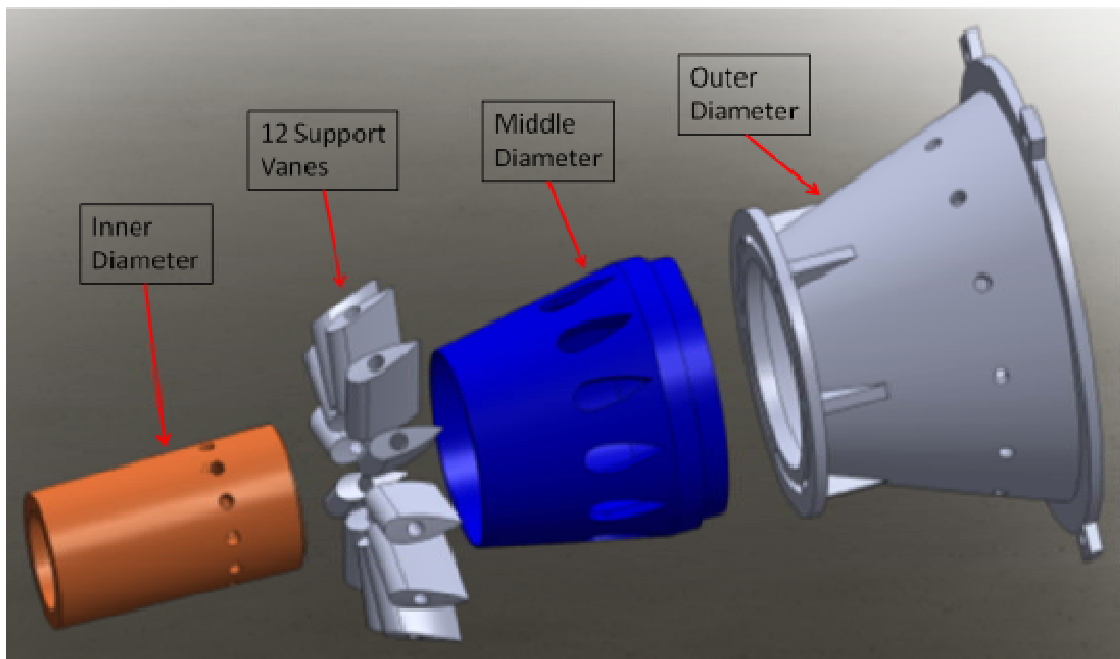
Figure 3.12: Diffuser exploded view
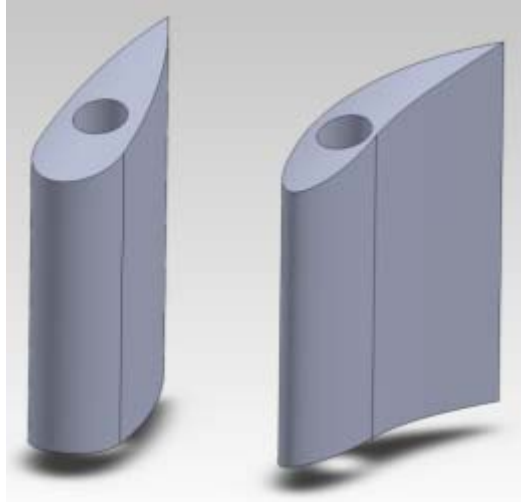
Figure 3.13: Standard and straight diffuser airfoils

The diffuser was designed using an Excel code created by David Burrus of ISSI, a
contractor within AFRL. The code allowed for the inlet geometry to be specified as well
as the inlet conditions. The inlet conditions used are the exit conditions from the STE.
The STE full throttle setting of 0.45 kg/s and the exit temperature is 1023 K was used as
the inlet condition to the diffuser. The exit pressure was assumed to be just a little bit
over ambient as the STE was designed to produce thrust to propel high performance RC
aircraft. From here the mass flow split could be set by the user. For this experiment
several mass flow splits between the core and cavity flows were chosen, an 80/20, a
70/30, and a 60/40. These flow splits were determined by looking at previous research
accomplished by Spytek [14] in UCC and ITB design. Spytek [14] was able to vary the
flow split from 0 to 50% into the cavity and determined for his engine a 23% flow split
into the cavity was the optimum. As will be discussed in Section 4.2, a combustion
analysis was conducted to examine the output of the ITB for the three mass flow splits
which corresponds to Spytek's range. The results of this analysis established the three

flow splits were chosen to look at values within his range to find narrow down the optimal flow split for the ITB. By setting the mass flow split the geometry downstream of the inlet began to be set. The user could then determine how much diffusion was required by configuring the exit-to-inlet area ratios. There are three exit-to-inlet ratios, core, upper bypass, and lower bypass that could be adjusted. The core and upper bypass ratios were used for the core and circumferential flows, and the lower bypass ratio was set to zero to keep the flow with only one split. The area ratios used can be seen in Table 4.

With the area ratios set, the diffuser design code calculated the exit geometry and flow conditions. The entrance geometry to the core and circumferential cavities to the UCC were already fixed by the UCC design of Wilson [13]. The inlet and exit dimensions were fixed to Wilson's design to reduce the number of parts to be manufactured for the experiment. This caused the diffuser exit geometry to also be predetermined so the diffuser could mate up to the UCC. The diffuser code was then manipulated to provide the correct exit geometry by adjusting the area ratio. Table 4 shows the diffuser inlet and exit dimensions and the location of the mass flow split. The diffuser length was set to 5 inches to keep the diffuser from becoming too long. Adding length to the diffuser would defeat the purpose of the ITB by adding additional weight to an engine which would reduce the performance gains.

Table 4: Diffuser code data

	Inner (in)	Outer (in)
	Inner (in)	Outer (in)
Inlet radius	1.13	1.735
Core Exit Radius	1.2	2
Cavity Exit Radius	2.25	3.125
	Axial distance from Inlet (in)	Area Ratios
80 / 20 Split Point	1.68	1.95 / 4.6
70 / 30 Split Point	1.625	2.29 / 3
60 / 40 Split Point	1.54	2.75 / 2.5

With the diffuser geometry configured to achieve the targeted flow splits with Dave Burrus's diffuser code, the geometry was converted into a design using SolidWorks. The SolidWorks model was then fabricated at AFIT's Model Shop. The diffuser was made from 316 stainless steel for its ease of machinability and lower cost than other materials such as to Hastelloy-X™. The diffuser was then able to be mounted to the STE and UCC. The OD component mounts to both the STE and the ITB by 3 M2.5 bolts. The MD component is held in place by fitting into the core opening on the ITB and the support vanes. The support vanes slide into the MD component in the airfoil shaped holes as seen in Figure 3.14. The ID component is then put inside the MD component so that the supporting vanes are in contact with the surface of the ID component and are lined up with the 12 threaded holes shown in Figure 3.15. Figure 3.16 shows the OD component slid over the supporting vanes and bolts are used to secure the diffuser assembly together.
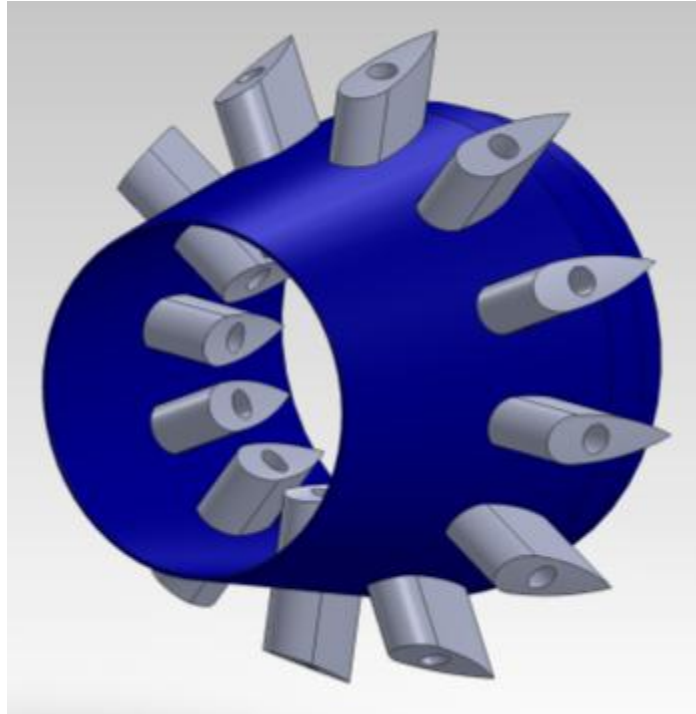
Figure 3.14: MD and support vanes
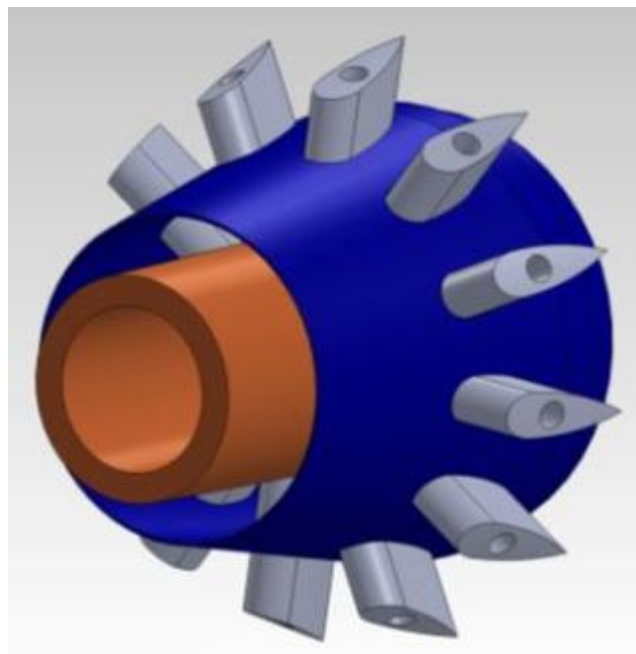
Figure 3.15: MD, support vanes and ID
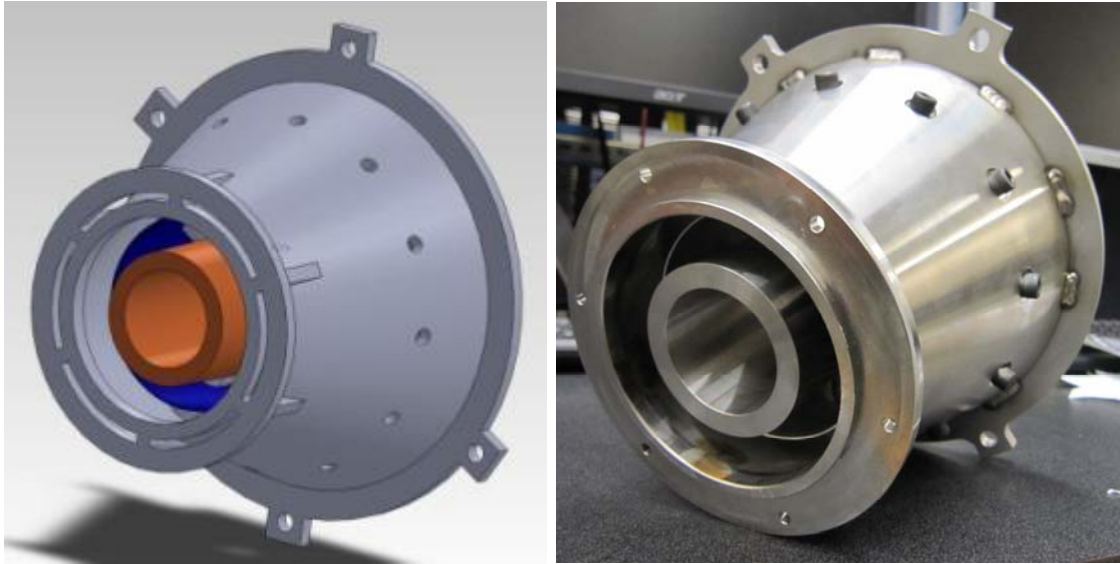
Figure 3.16: Fully assembled diffuser

A comparison of the three MD components can be seen in Figure 3.17. The three MD component designs are different by changing the point in the flow where the flow split occurs. The flows split were changed by disassembling the diffuser and replacing the MD component when required. The support vanes also allow for cooling air to be pumped into the ID component and then into the center body and the tail.
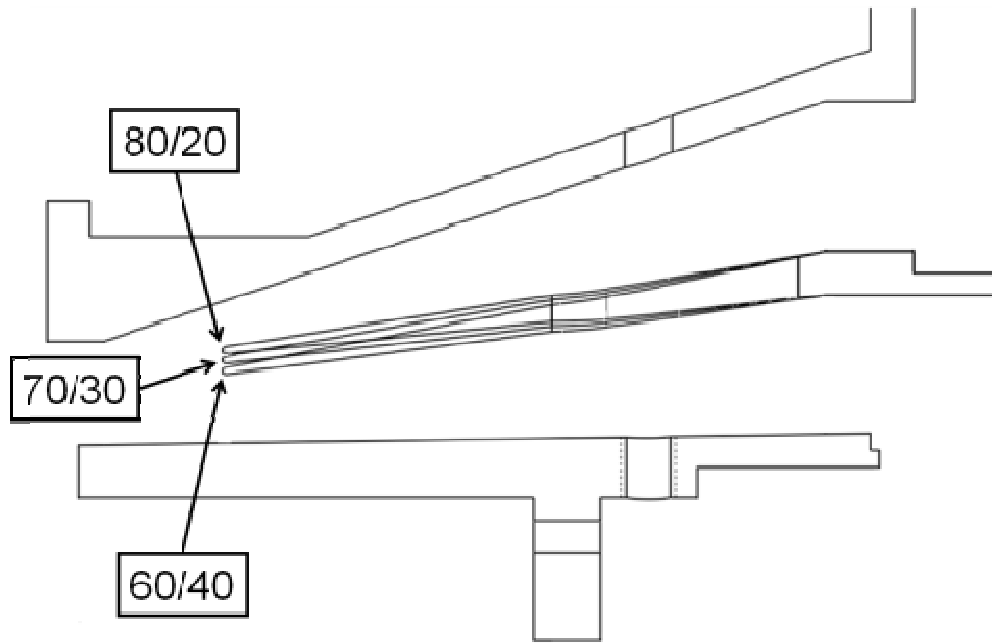
Figure 3.17: MD comparison, 80/20, 70/30, 60/40

3.4.2   Circumferential Cavity

As shown previous in Figure 3.10, the flow leaves the outer flow path of the diffuser into the circumferential cavity. The flow is mixed with fuel in the circumferential combustion cavity. The combustion chamber was created by the front and back combustor plates, the outer ring and the combustor ring.   The combustor ring can be seen in Figure 3.18. The combustion chamber is held together with a series of bolts connecting the front and back combustion plates to the outer ring and the combustor ring to keep it sealed tight. The outer ring and combustion plates can been seen assembled around the combustor ring in Figure 3.19 with the diffuser attached to the front of the cavity. The front and back combustor plates are also the points where the ITB is mounted to the thrust stand shown in Figure 3.2.

39
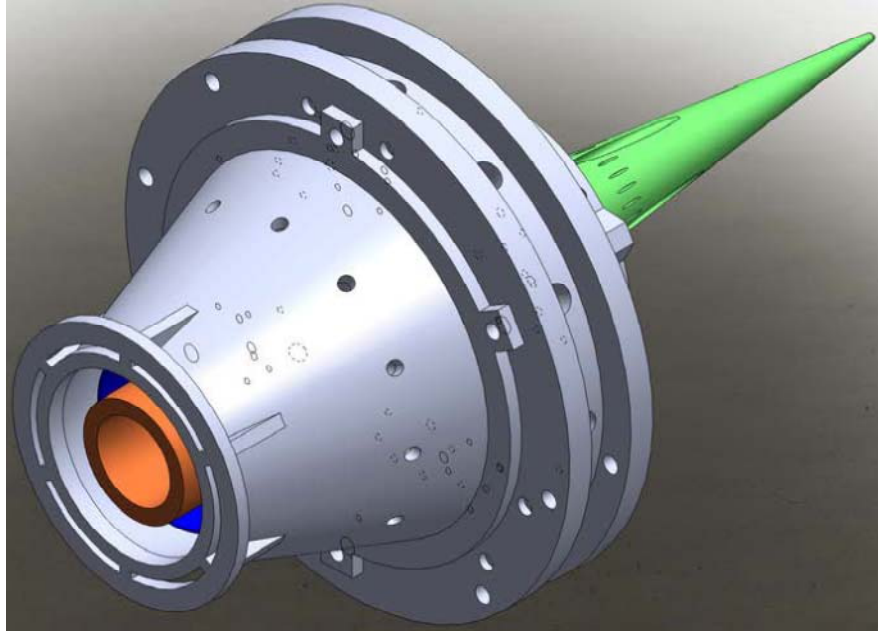
Figure 3.18: Assembled ITB minus STE

Figure 3.19: Combustor ring without top air inlets

The overall diameter of the UCC is 10 inches and the width of the UCC circumferential cavity is 2 inches. The circumferential chamber has a diameter of 6.25 inches and the cross sectional area is 1 inch by 1 inch shown in Figure 3.20. Liquid or

gaseous fuel can be used through the 6 fuel injector ports. The combustion chamber is machined from Hastelloy-X™ which allows the maximum temperature of the ITB to reach about 2600 K. The g-load in the cavity is set by the mass flow.   The combustion chamber was designed for a g-load from 0-3500, with a target of 1500.
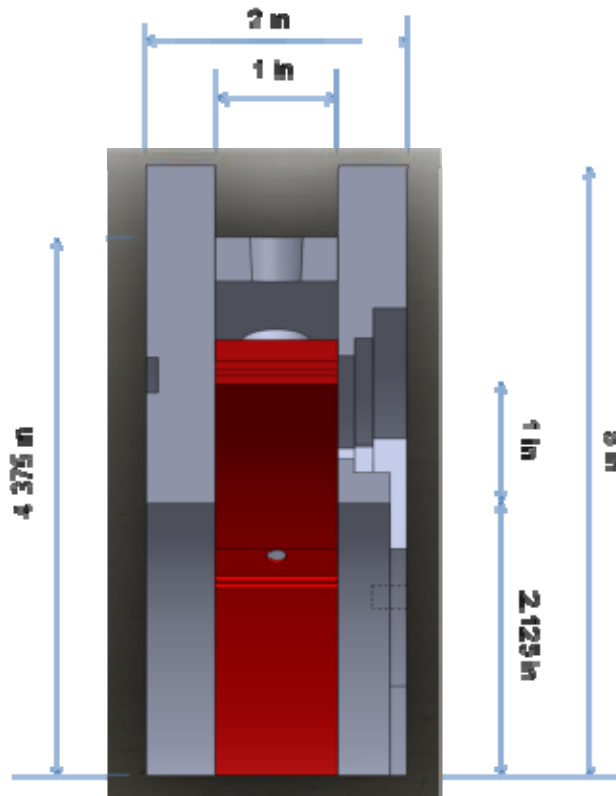
Figure 3.20: Dimensioned cavity cross section

A new combustor ring, shown in Figure 3.19, was redesigned to replace the one used by Wilson [13] shown in Figure 3.21. The air inlet holes were removed as the flow was now entering from the side verse the OD in Wilson's rig. The 8 point baffle gaseous fuel dispersion plates used by Wilson were also not installed as they were not required for liquid fuel. The ability to install the baffle plates in the future was integrated into the new combustor ring for possible future work with gaseous fuel. The 6 notches are the

41

locations of the fuel inlets. Each notch is able to have one baffle installed. For atomized

fuels, the baffles are not installed to allow the fuel to enter into the cavity unrestricted.

Figure 3.21: Combustor ring with top air inlets

3.4.2.1   Fuel Injectors

The 6 fuel injectors are mounted to the outer ring. Air can also be injected

through 6 additional holes in the outer ring with a different combustor ring. The fuel

injectors are made from stainless steel bolts that have their centers milled out and tapped.

The head of the bolt has a 1/8" Swagelok to NPT fitting installed to connect to the fuel

lines. The bottom of the bolt has a fuel nozzle installed. The assembled bolt is show in

Figure 3.22. The fuel nozzles are made by Goodrich and their part number is 46817-33.

Figure 3.23 shows the fuel nozzle uninstalled. The fuel nozzles have a nozzle flow

number of 0.3. A nozzle flow number is non-dimensional number used to rate atomizing

nozzles defined in Equation 2. Where $\dot{V}$ is the volumetric flow rate in gallons per minute

and P is the pressure in pounds per square inch. A nozzle number of 0.3 was chosen

based on the on the fuel-to-air ratio desired for the circumferential cavity. The fuel

nozzles designed to produce finely divided droplets in a fully developed cone with a

spray angle of 85° ± 5°. The fuel nozzles atomized the JP-8 as the fuel entered the

circumferential cavity dispersing the fuel into the swirling flow.

Figure 3.22: Fuel bolt assembly

Figure 3.23: Fuel nozzle

Equation 2: Nozzle Number

$$Nozzle\ Number = \dot{V} \times \sqrt{\frac{4000}{P}}$$

3.4.2.2 Insert Plates

The front and back combustor plates have 3 window frames. Each frame can

accept one of three different inserts. The first insert is a basic quartz window. The quartz

window can be used to visually inspect what is occurring in the combustion chamber or

to take optical diagnostic measurements into the cavity. The second insert is designed to

be loaded with pressure and temperature probes to examine the flow as it swirls around in the circumferential cavity shown in Figure 3.24 and Figure 3.25. The third insert plate was designed to work with the diffuser to allow air from the diffuser into the circumferential cavity as shown in Figure 3.26. Air was brought in the side through the insert plates to reduce total pressure losses from ducting to the OD of the rig where cavity flow typically enters.   The more total pressure loss experienced in the diffuser, the more difficult it will be to coerce the flow into the circumferential cavity. If the total pressure loss is too great not enough flow will enter the circumferential cavity to create a high enough g-load for the ITB to work correctly. Therefore the side of the circumferential cavity is the path of least resistance for routing the flow to the cavity. Total pressure losses in the diffuser are of concern as the flow exiting the STE does not exit at a very high pressure. In addition to minimizing the pressure loss in the cavity, adding ducting around to the top of the cavity would add addition weight and increase the size of the rig. The rig would also need even more parts fabricated to enable flow to enter the top of the cavity.

Figure 3.24: Instrumented inserts, outer face, front (top) and rear (bottom)

Figure 3.25: Instrumented inserts, inner face, front (top) and rear (bottom)
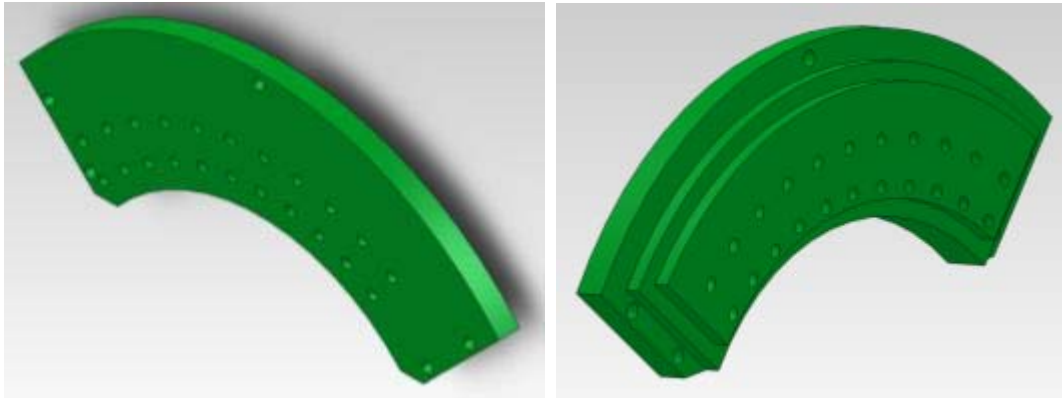
Figure 3.26: Air insert exterior (left) and interior (right)

There are 2 rows of 11 injection holes for this plate and they are set at 30° from axial to create the swirling flow in the circumferential chamber. The hole pattern was selected to allow as many holes as possible on the plate. The holes can always be made bigger in the future, but it is difficult add holes to the pattern once the pattern is made. Each hole has a diameter of 0.107 inches. The hole size was selected based on the AFRL UCC hole size of 0.22 inches. The AFRL UCC had a total of 24 holes compared to the AFIT design of 66 holes. This equates to a lower area for air to flow into the cavity for

the AFIT rig. Once installed on the rig, the g-load will be measured in the cavity for the new air inserts. The hole size can then be made larger if required to meet the desired g-load of 1500.

3.4.3   Center body

The straight center body, Figure 3.27, is held in place by mounting to the diffuser on the front and the back is fitted to the exit ring. The straight center body is machined from 316 stainless steel. The center body has 6 straight vanes to keep the core flow axial. An aerodynamic shape was used for the vanes. The vanes shape was set by the size required for the vane. The length of the vane was set by the distance between the front combustion plate and start of the UCC exit. The thickness of the vane was selected to achieve the desired Mach number through the core. By keeping the core flow axial there will be less total pressure losses through the core of the ITB.   Less total pressure loss was desired to increase the maximum thrust that could be output. The straight center body is 4 inches long and has a 4.25 inch diameter with the vanes and 2 inch core at the exit plane. The center body is also hollow to allow cool compressed air to flow through it from the diffuser. The cooling air is required when combustion occurs in the cavity. The hot core flow from the STE mixes with the higher temperature flow exiting the circumferential camber and flows over the center body. The cooling air is used to reduce heating effects on the center body to increase the life time of the part.
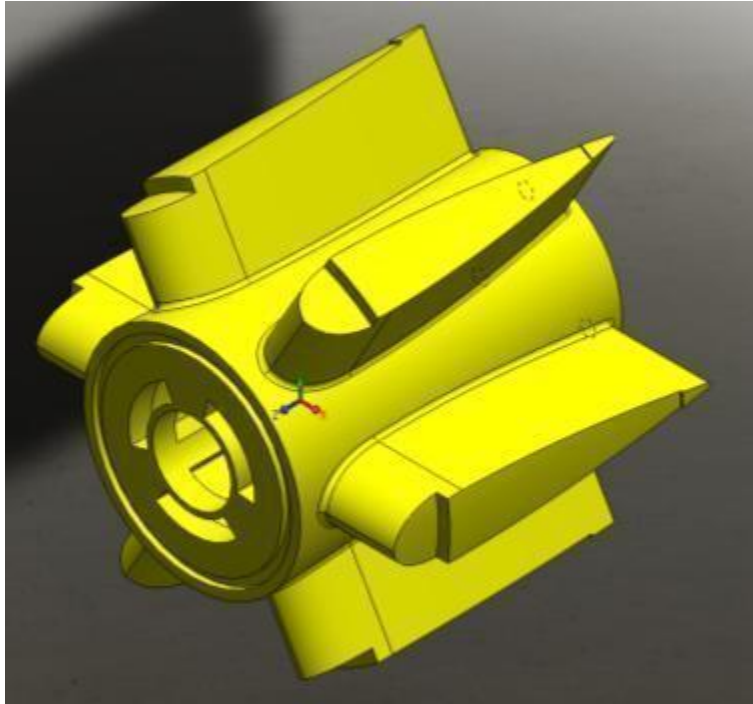
Figure 3.27: Straight Center body

The straight center body is different from Wilson's center body [13], shown in

Figure 3.28. Wilson's center body was designed to look at Rayleigh losses and

accurately representing engine swirl between the last compressor stage and the inlet to

the turbine. In Wilson's rig the center body rotated the flow so that it came out of the rig

with a 70° swirl angle. This large amount of swirl would have made measuring thrust

worthless for the purposes of the augmenter configuration experiment. Comparing the

STE and ITB thrust would be difficult if the ITB is not able to achieve an accurate thrust

value. The straight vanes in the ITB center body are expected to not reduce the thrust

like the curved vanes in Wilson's rig. The thrust however will not be optimized as a

nozzle has not yet been designed. Bolt holes were added to the exit ring to allow for a

future nozzle design. Another difference between the ITB center body and Wilson's

center body is there is less blockage. By not swirling the flow around the center body

and keeping the flow straight, total pressure losses through the center body will be lower.

When using the ITB in the augmenter configuration the straight center body is used. For

examining the ITB in a standard configuration Wilson's center body is used.
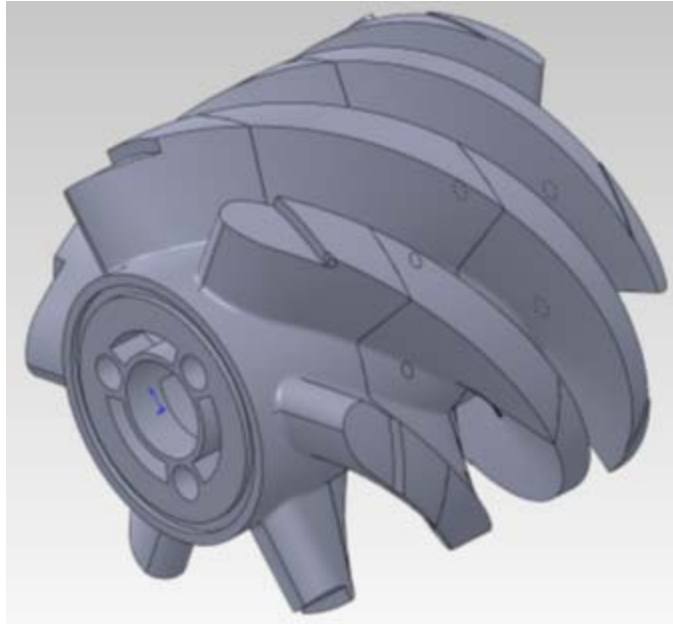
Figure 3.28: Wilson's center body

3.4.4 Exit Ring and Tail

The quartz exit ring, shown in Figure 3.29, is held in place by spring loaded

screws to prevent the ring from cracking due to expansion. The quartz ring allows the

core flow to be seen over the second half of the center body before it exits the ITB. The

exit ring flow path diameter is 4.25 inches. The exit ring has 21 taps, set in 3 groups of 7,

machined into its circumference. The taps are a 1/4inch NPT with a 1/16 hole to allow a

static pressure measurement, a small pitot probe to be inserted for total pressure

measurement, or a thermocouple to measure the total temperature.
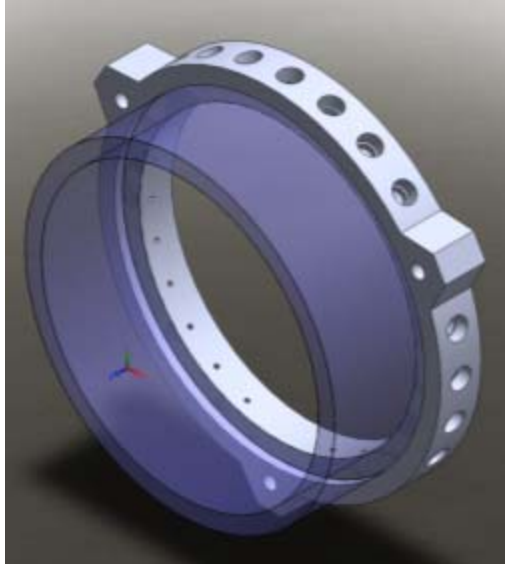
Figure 3.29: Exit ring and quartz ring

The tail, shown in Figure 3.30, has a 2 inches diameter, is 8.34 inches long and is made from 316 stainless steel. The tail bolts onto the rear of the center body. The cooling air flowing through center body is also able to flow into the tail and then exit through small film cooling holes in its surface.
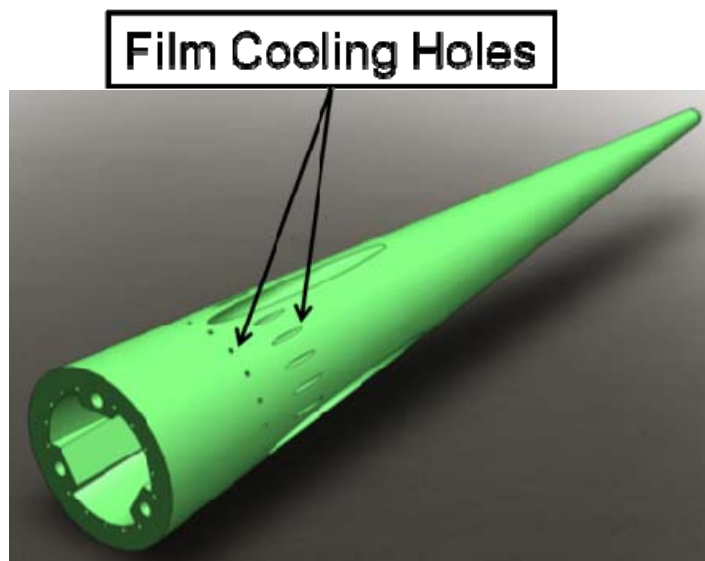
Figure 3.30: Tail

3.4.5 Igniter

The ethylene torch used to ignite the fuel in the circumferential cavity is shown in Figure 3.31 below. The ethylene is brought in the right side port and air enters from the bottom port. The spark plug ignites the mixture and the torch flame exits the left side. The igniter exit is connected onto the back plate of the circumferential cavity in the igniter attachment port. The air is supply by the shop control air. The ethylene is stored in a high pressure cylinder and is stored in the tank farm. The ethylene was acquired from Weiler Welding, INC. The spark plug is a Maxon 18075 Spark Igniter. The spark plug is powered by the Dongan interchangeable ignition transformer which is located in the control console. The ethylene torch was tested successfully using a 5 to 1 air to fuel ratio, which provided a stable flame jet as seen in Figure 3.32. The air and ethylene flow rates are controlled by the MKS Insturments flow control system via the LabVIEW code. The spark plug is activated using the LabVIEW code on the flow control tab.
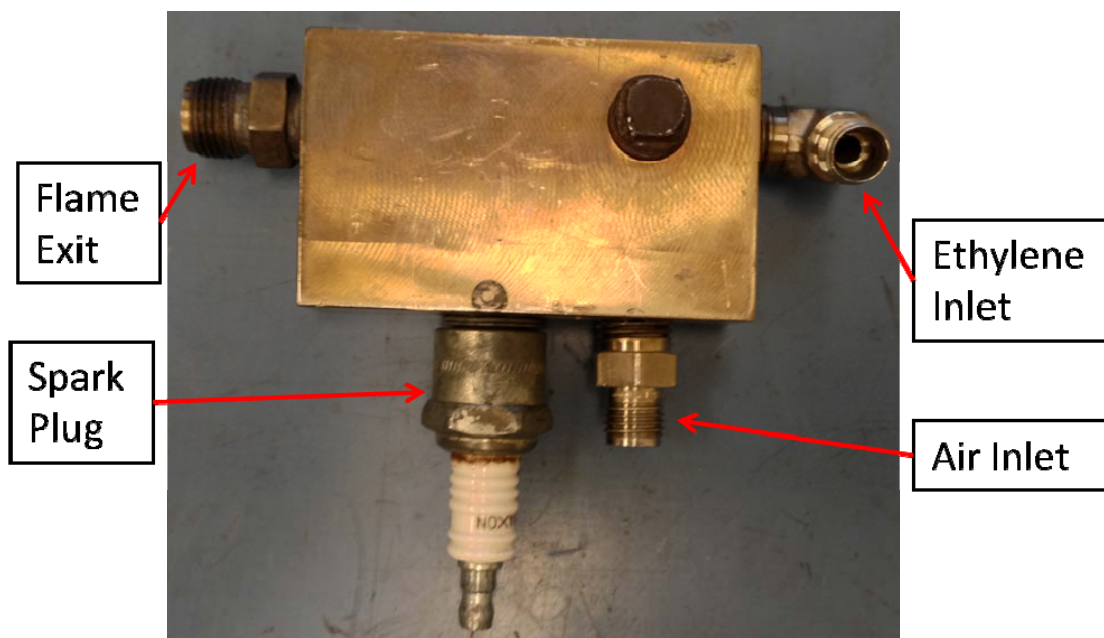
Figure 3.31: Ethylene torch

Figure 3.32: Ethylene torch with flame jet

3.5 Fuel Pump

The fuel pump supplying the JP-8 is a dual piston continuous pressure pump

shown in Figure 3.33. The manufacturer of the pump is ISCO and is a model 1000D dual

syringe pump. The pump system is controlled by the ISCO Series D pump controller.

The pump is capable of continuous flow of up to 408 mL/min. The maximum outlet pressure of the pump is 2000 psi. The pump is able to dispense from one syringe and fill the second syringe at the same time. The cycle of filling and dispensing is how continuous flow is achieved. Two sets of solenoids are used to control if a pump is filling or dispensing fuel. The solenoids are air actuated from the control air in the COAL lab.

Figure 3.33: ITB duel syringe fuel pump (left) and fuel tank (right)

Pump operation is fairly simple. First turn on the pumps and the control box by flipping the red power switches to "ON".   The startup screen will appear and then change to the control automatically, show in Figure 3.34. The pump can then be selected to operate on a constant pressure or constant volumetric flow rate. A constant volumetric flow rate was used for this experiment as it is more important to know how much fuel is entering the circumferential cavity. Next, open the ball valve that is connected to the fuel

in line. To select which pump to use press the "D" key the either "A" or "B" depending on which pump you wish to operate from. Now to fill the selected pump press the "REFILL" key, select the same pump that was selected previously. Next press the "A" key to set the flow rate. Using the number pad, enter the desired value and then press enter seen in Figure 3.35. Now press "RUN" to start flowing fuel. To stop flowing fuel press the red "STOP" key and select the pump that is to be stopped shown in Figure 3.36. Fuel will stop leaving the pump, though some fuel may continue to exit the fuel nozzle until the pressure in the line has dropped low enough.

Figure 3.34: Pump main screen
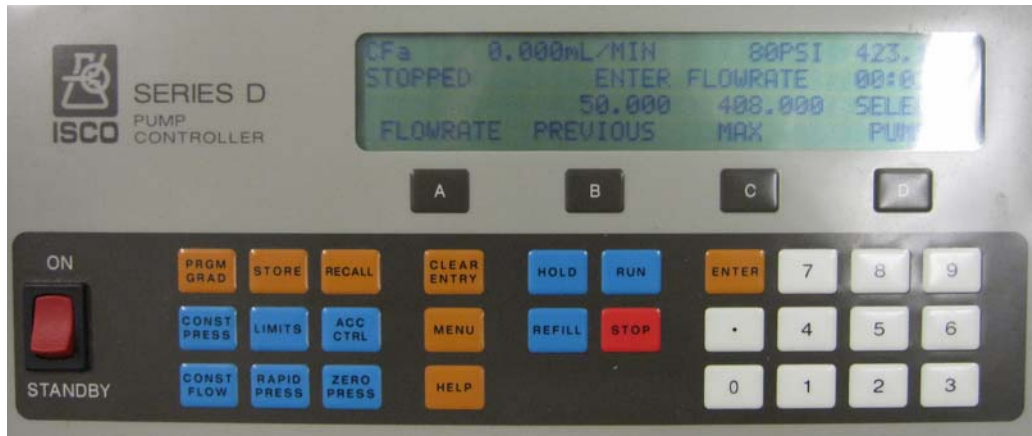
Figure 3.35: Pump flow rate select screen
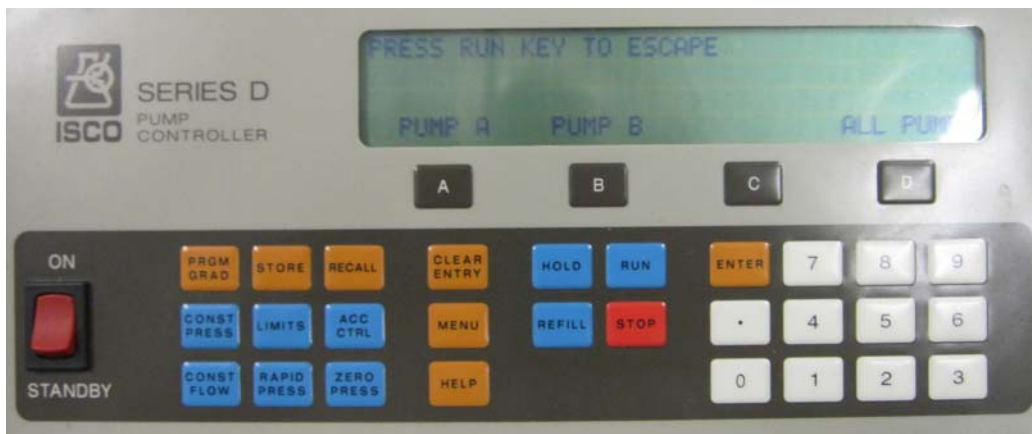
Figure 3.36: Pump stop screen

3.6   Instrumentation

The ITB rig has several types of instrumentation. There are thermocouples, pressure taps, emissions measurements, load cell, and mass flow meters. It was important to record the temperature and pressure of the flow exiting the STE as well as before entering the center body and circumferential cavity and at the exit of the ITB. The mass flow of the JP-8 into the STE and the ITB were also important measurements. The load cell was used to measure the thrust of produced by the experiment.

3.6.1 Optical Instrumentation

A high speed camera was used to examine flow in the cavity. Figure 3.37 shows
the camera used to collect imagery, a Phantom v12.1 monochrome. The memory for
camera is internal to the unit. The camera is connected through an Ethernet cable to the
Lenovo computer in the COAL laboratory. This computer has the PCC 1.3 software on it
able to control the camera. Several different lenses are available for use with the
Phantom camera. A Nikkor Micro 60mm f/2.8D lens was used in this experiment. It is
important that the lens cap be on the camera when the lens is not attached to prevent
overexposure from light to the internal components of the camera when not in use.

Figure 3.37: Phantom camera

3.6.2 Pressure and temperature instrumentation

The pressure measurement system is made by Esterline Pressure Systems. It is a
model DTC Initium show in Figure 3.38. The DTC Initium is able to measure 64

different pressures at once seen on the left in Figure 3.39. The system is used to measure the static pressure points on the exit ring and the measurement tapped insert. In addition the system has a pitot probe set up to measure the total pressure in the cavity to measure the tangential velocity. The system is calibrated with 80 psi control air. The system is self calibrating by running control air into the calibration ports on the collection node.

The thermocouple bank show in Figure 3.39 allows for up to 48 different temperatures to be measured. The thermocouples are K-type and the data is collect by the LabVIEW code to be saved with other data collected.

Figure 3.38: DTC Initium pressure system
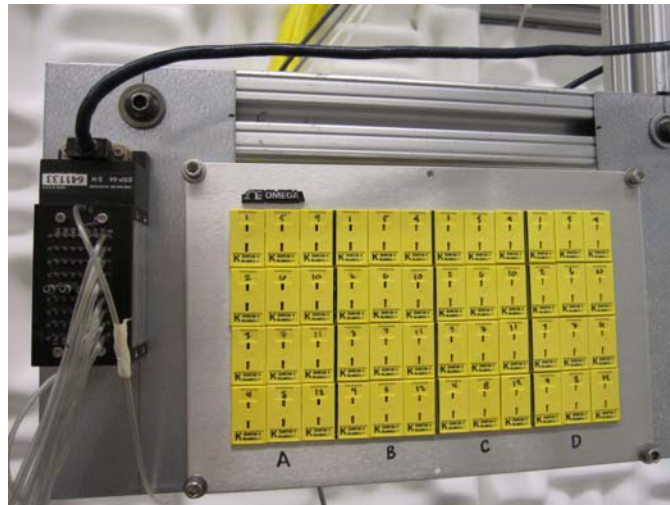
Figure 3.39: Pressure ports and thermocouple bank

3.6.3 California Analytical Instruments

The California Analytical Instruments (CAI) machine is used to gather emissions data. A large effort was put into rewiring, labeling, diagramming, and writing new LabVIEW code to collect data and control the outputs to the computer. The original wire diagram was found, which allowed for the modifications to the output of the CAI to be understood and incorporated into the upgraded lab. The new wiring diagram can be found in Appendix C. The rewiring and labeling required the entire wiring from the cDAQ to the CAI outputs to be replaced. During the process, an error in how the CAI communicates to with the LabVIEW code was corrected. The error was found in the OPTO22 relay board show in the wiring diagram and how it is controlled in LabVIEW. It was found that the old code was written to open the relays of the remote ranges that are supposed to be closed and close the relay of the remote range that is desired. By changing the sign in LabVIEW the error was corrected to allow the remote range control to function properly. The CAI can only send one output signal per gas being analyzed, THC, NO_x, CO_2, CO, and O_2. The CAI can output at different ranges depending on the gas. This is controlled by either manually setting the CAI on the front panel to the desired range or by setting the CAI to remote. Setting the CAI output to remote allows the LabVIEW code is able to select which range is desired from the main console. Using the remote setting allows for central control of the emissions measurements. More details on calibrating the CAI emissions machine can be found in Appendix C.

3.6.4 Thrust Stand

The thrust stand is used to support the ITB and STE as well as measure thrust. The thrust stand is able to measure a load in one linear direction. For the purposes of

testing the ITB that direction is setup in a horizontal axial orientation. The base of the

thrust stand consists of two mounting plates that support two rod clamps each. The rod

clamps are designed to hold 2 steel rods so that one rod clamp is at each end of the rod.

In-between the rod clamps are two air-bearings per rod. The air-bearings are then

mounted to the top mounting plate of the thrust stand, which supports the ITB seen in

Figure 3.40. The air-bearings are setup to the zero-air system in the COAL lab. This is to

make sure the air is properly filtered to prevent particulates in the air from clogging the

air-bearings. When the air-bearings are set at 60 to 80 psi, the air-bearings create a small

pocket of air around the rods allowing the top mounting plates slides smoothly along the

rods.
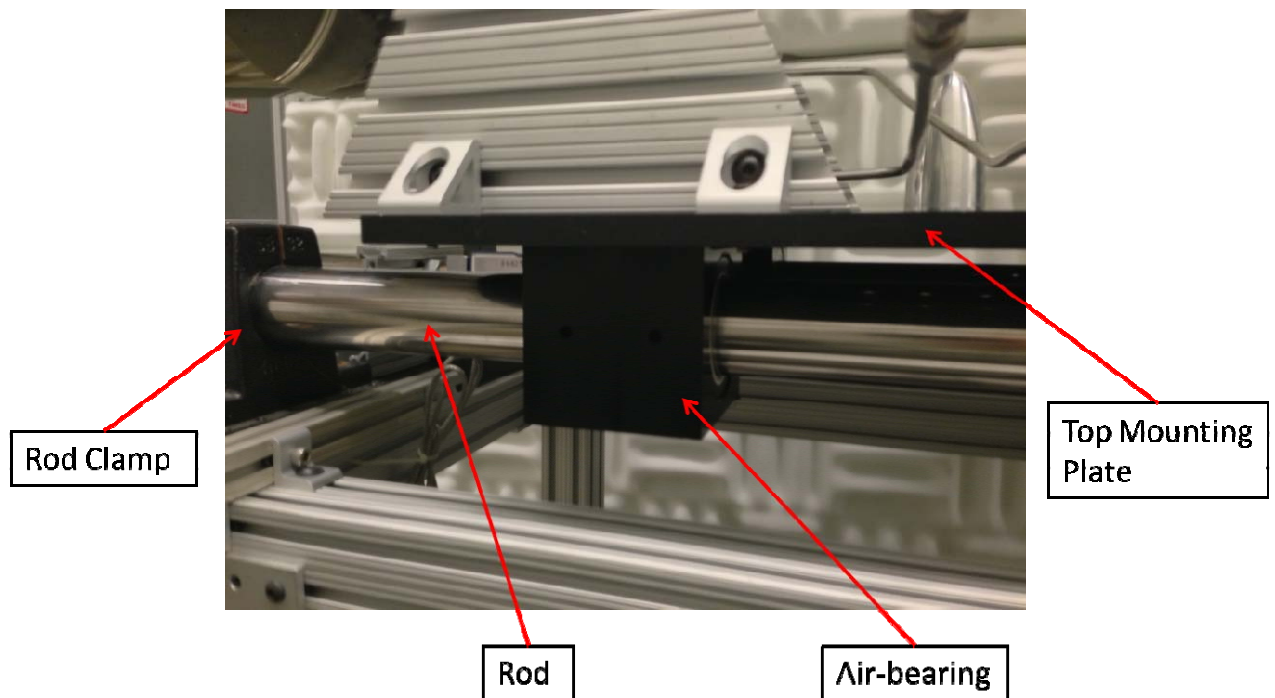
Figure 3.40: Air-bearings

To measure thrust on the stand, a load cell has been installed below the top mounting plate connecting the top and bottom plates as seen in Figure 3.41. The load cell used was an Interface SM-1000. The load cell can be configured for tension or compression; in the configuration used here the load cell is in tension. The load cell is rated to 250 lbf.

Figure 3.41: Load cell on the thrust stand

3.6.4.1 Thrust Stand Calibration

The thrust stand was calibrated using a set of calibrated weights. Air pressure was applied to the air bearings to reduce the friction in the system. Then the calibration weight hanger was attached to the thrust stand via Kevlar threads and a pulley to redirect the weight into the direction of the load cell as seen in below Figure 3.42. The calibration weight hanger, Figure 3.43, weighs 2 lbs and calibration weights, Figure 3.44, were added in 10 lb increments. The voltage of the calibrations was recorded for each weight added to the hanger. Weights were added up to 70 lbs. 70 lbs was chosen as the JetCat is only able to produce 52 lbs of thrust. Once 70 lbs was reached, the weights

were removed in 10 lb increments and the voltages recorded again to determine if hysteresis exists in the system. Hysteresis in the thrust stand could lead to inaccuracies when increasing and then decreasing the thrust. Special care will have to be taken to account for hysteresis when taking thrust measurements. The calibration curve generated can be seen in Figure 3.45.
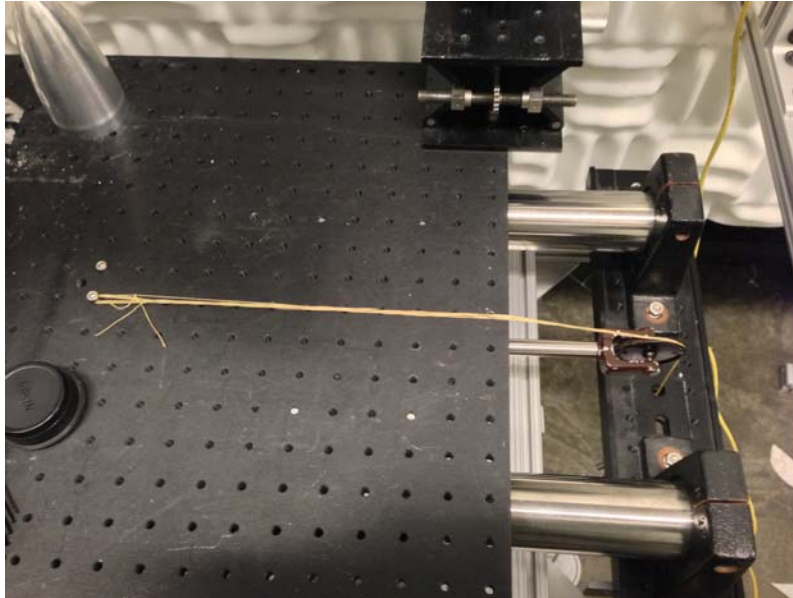
Figure 3.42: Calibration thread and pulley
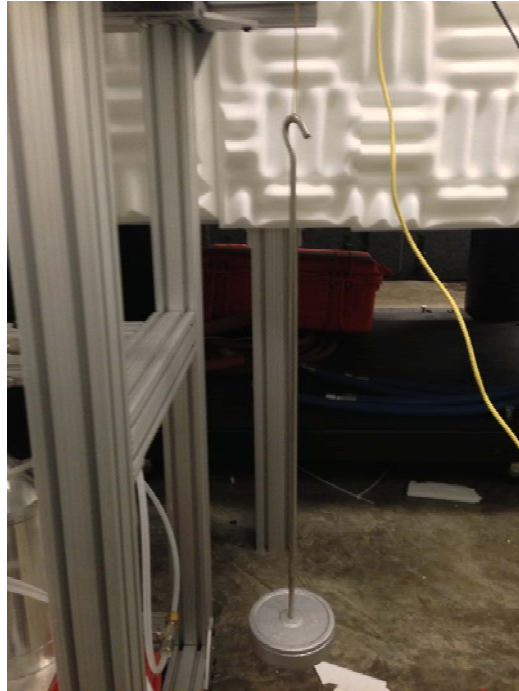
Figure 3.43: Load cell calibration hanger

Figure 3.44: Calibration weights

Load

y = 33.008x - 4.5622
R² = 0.9894
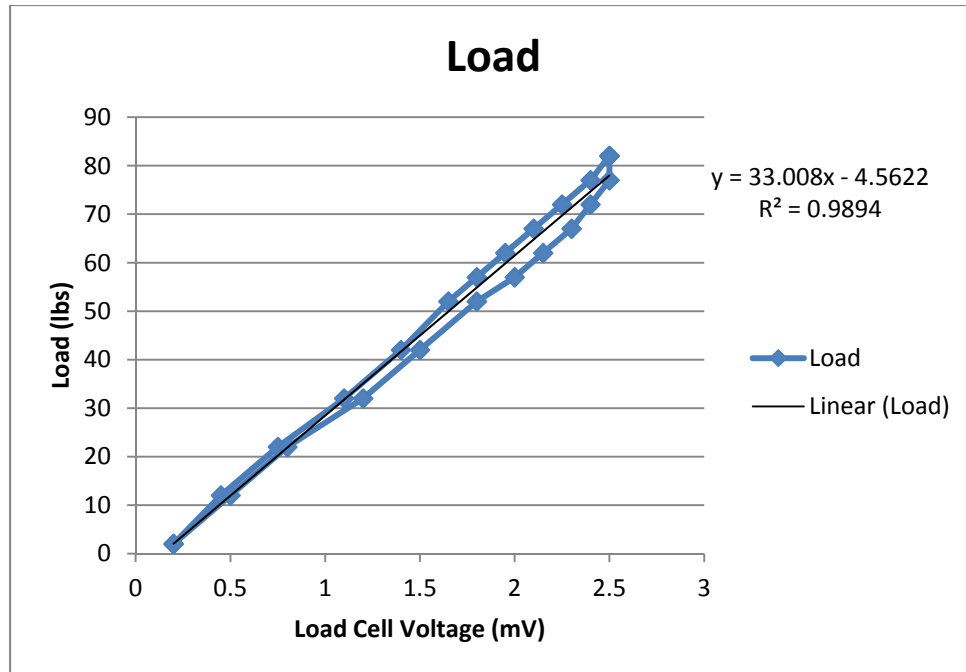
Figure 3.45: Load cell calibration curve

3.7   Summary

A significant amount of effort has been put into preparing the COAL laboratory for UCC and ITB testing. A new fully annular UCC has been designed as well as additional parts to make the UCC an ITB. Furthermore a diffuser which is capable of splitting the core flow into a core and circumferential cavity flow has been designed and built. This diffuser is the first to be made for an AFIT UCC and is modular in its design to allow easy modification to examine different flow splits. In addition to the UCC, the STE is the vitiated air source for future ITB testing. The STE will allow the option of varied amounts of vitiated mass flow rates providing addition capability to the COAL laboratory.

4   Analysis and Results

4.1   Chapter Overview

The objectives of this research effort are to examine how to integrate the UCC into a common flow source, examining the effect g-loading has on fuel sprays in the circumferential cavity, and create a vitiated air source for the UCC inlet. During this research a new facility was designed and built that was configured to accomplish these goals. Many pieces were put in place to evaluate the ITB as described in Chapter 3. This chapter will discuss some of the initial investigations that were accomplished to understand these objectives. Fuel spray testing was conducted in the circumferential cavity to examine the effects of g-loading. An analysis of the STE and ITB was carried out to estimate the emissions from both components and to predict the desired mass flow split.

4.2   Emission Results for the STE and ITB Configurations

An analysis has been conducted in CHEMKIN [15] to examine and predict the emissions results for the ITB with JP-8 as the fuel source. This model begins at the exit of the STE. Therefore, the ITB inlet flow composition needed to be specified.   The compounds that comprise this flow were found using CEA. CEA was able to calculate the combustion gases of the STE until actual emissions measurements are available. The inputs to CEA were consistent with the STE operation, namely an equivalence ratio of 0.3 between Jet-A fuel and air and assigned temperature and pressure model. The outputs from CEA can be seen in Table 5.

Table 5: CEA results

Compound	Mole Fraction
N_2	0.77
O_2	0.14
CO_2	0.04
H_2O	0.03
NO	0.0003

The CHEMKIN model developed can be seen in Figure 4.1. As such, there are two gas flow inlets which represent the flow split occurring after exiting the STE within the diffuser. A percentage is diverted into the circumferential flow while the rest passes through the core flow. The mass flow split can be easily adjusted by changing the mass flow in the inlet properties. The last inlet, fuel flow, is the fuel that is being added to the circumferential cavity. The mass flow rate for this inlet can be varied by inputting a range of values to achieve different air-to-fuel ratios. The fuel used can also be changed depending on the chemical data set used. For the purposes of this experiment $C_{12}H_{25}$ was used as it is similar to dodecane which can be used to approximate kerosene, which is the primary component of JP-8. Kerosene composition can vary greatly to include C_9 to C_{16} compounds according to OSHA [16].
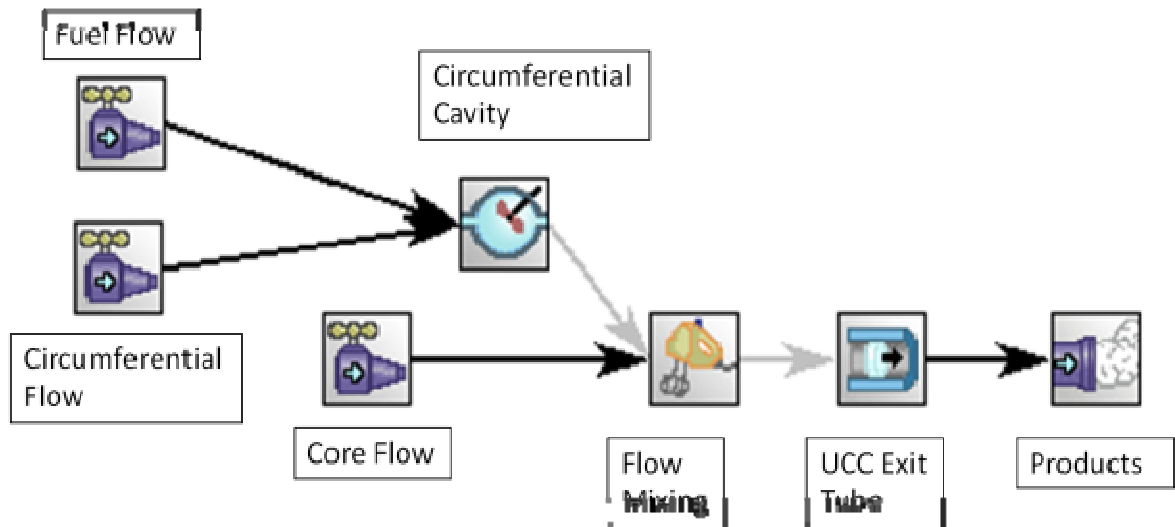
Figure 4.1: CHEMKIN model

The circumferential flow inlet and fuel flow inlet are combined in a well-stirred reactor which is being used to represent the circumferential cavity of the ITB. The well stirred reactor ensures complete combustion which is what is expected to occur due to the g-loading in the chamber, as discussed in Chapter 2. The products of the circumferential cavity are then recombined with the core flow inlet in the center body, here represented by a mixing chamber in CHEMKIN. With the two flows recombined, the mixed flow exits the ITB through a plug flow reactor representing the downstream tube that is the exit of the ITB.

The CHEMKIN software was able to produce a prediction of the exhaust from the ITB. Three mass flow splits were run: 60/40, 70/30, and 80/20 with a total mass flow rate of 1 lb/s matching the output of the STE. For each mass flow split the fuel flow rate was varied from 0.001 lb/s to 0.03 lb/s with increments of 0.001 lb/s. This resulted in equivalence ratios from 0.075 to 2.24 for the 80/20 split ranged, while the 70/30 split ranged from 0.05 to 1.49, and the 60/40 split varied from 0.04 to 1.12. The temperature

65

in the circumferential cavity can be seen in Figure 4.2 for the 3 mass flow splits. The

temperature gain is the same regardless of mass flow, as would be expected for a given

equivalence ratio in the cavity.   What is more interesting is that the exit temperature

shown in Figure 4.3 for the higher mass flow through the cavity achieves a higher

temperature for a given equivalence ratio. In other words, an equivalence ratio of 0.5

with 20% flow into the cavity yields an exit temperature of about 1200 K and for a 40%

flow into the cavity a exit temperature of nearly 1400 K. The 60/40 split is able to

produce a greater temperature gain because a larger percentage of the flow is undergoing

combustion. This in turn causes the total flow to have a larger temperature gain when the

two flows are recombined in the center body. It should also be noted that if the

equivalence ratio is too high, the cavity will become too rich and combustion

dramatically decreases as can be seen by the 80/20 split. The desired temperature gain of

300 K through the ITB will be possible within the range of equivalence ratios

investigated for the ITB. The 60/40 split with a 0.34 equivalence ratio, a 70/30 split with

a 0.45 equivalence ratio, or an 80/20 split with a 0.67 equivalence ratio will accomplish

the goal.
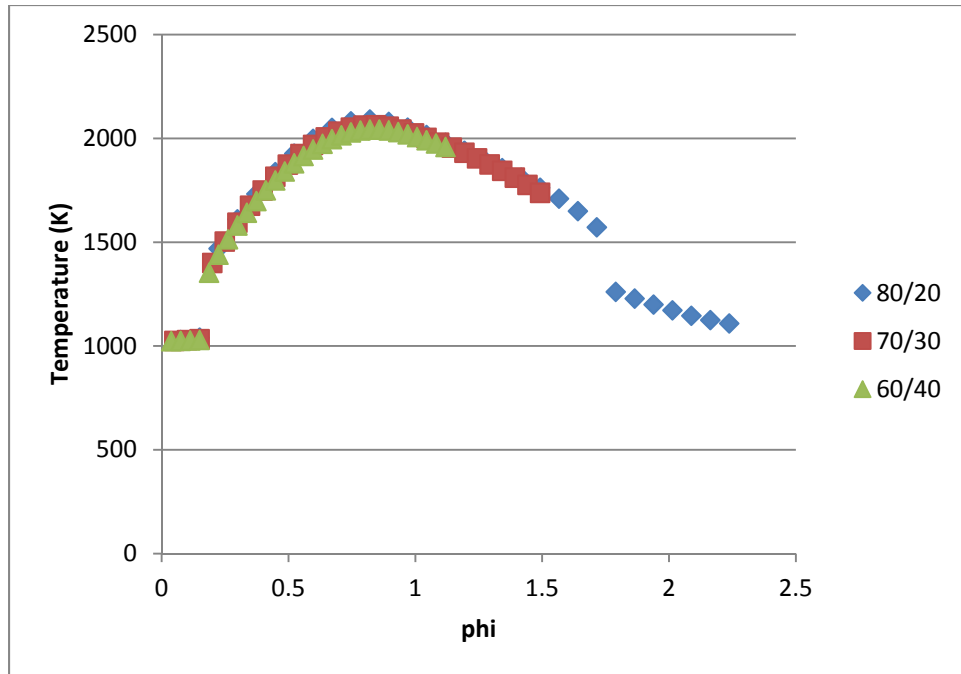
Figure 4.2: Cavity temperature
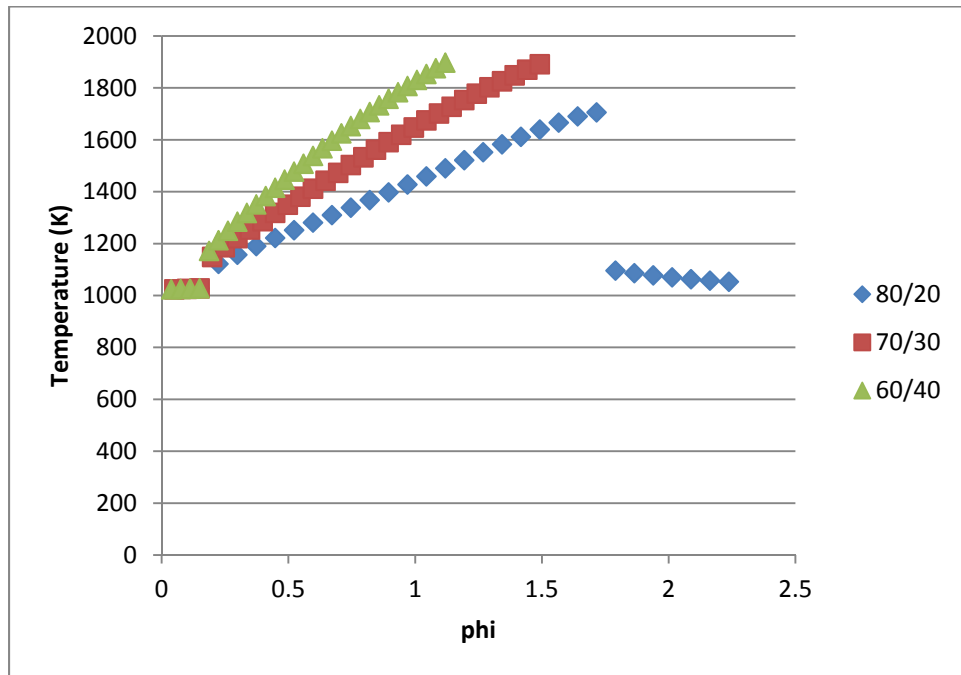
Figure 4.3: ITB exit temperature

The mole fraction ratios at the exit for O_2, H_2O, CO_2, CO, NO_x, and THC for the 80/20, 70/30, and 60/40 flow splits are shown in Figure 4.4 through Figure 4.9. Based on the THC emissions data it appears that almost all of the hydrocarbons will be burned within the range of equivalence ratio that are examined for the ITB. The NO_x levels are at their highest at an equivalence ratio of 1, which is the condition where the cavity is at its highest temperature. This trend follows what would be expected and because the goal is to run at lower equivalence ratios, lower NO_x emissions should be observed. From the O_2 plot it can be seen, that for the equivalence ratio range of interest, the CAI emissions analyzer should be kept in the 20% band as the 10% band would not capture the data. The CO and CO_2 ranges should be in the 5% band for emissions measurements. NO_x should be kept in the 100 ppm data band, and the THC should be in the 10 ppm data band.
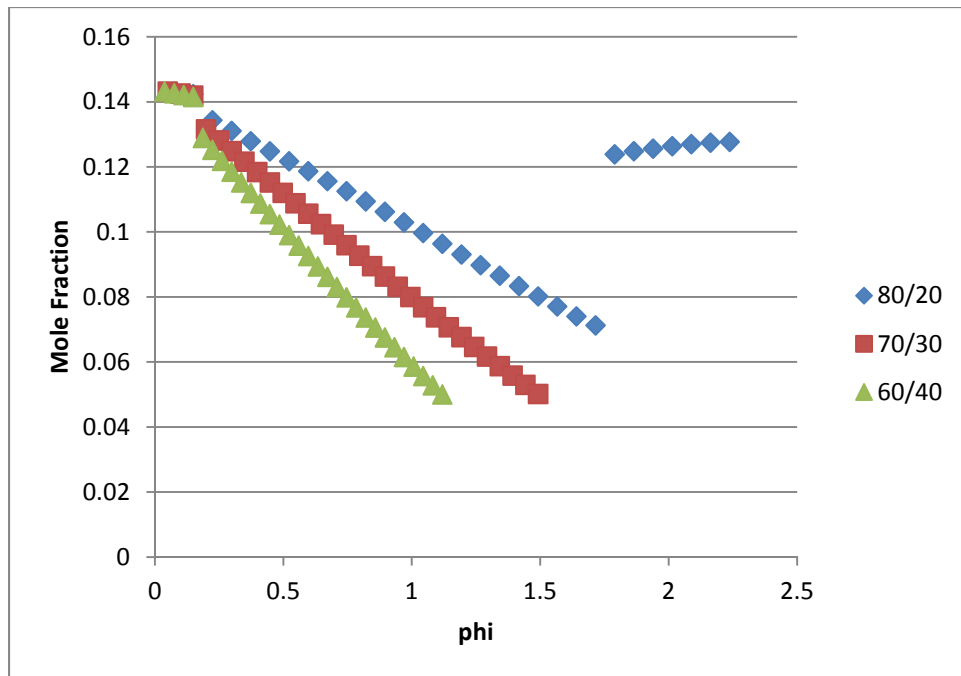
Figure 4.4: O_2 emissions
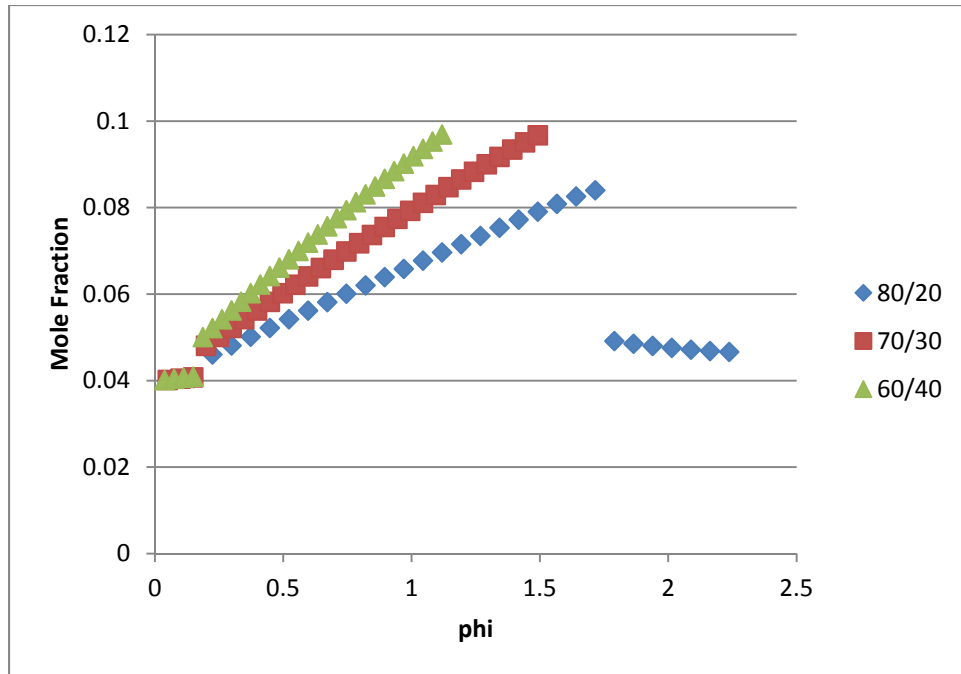
Figure 4.5: H₂O emissions
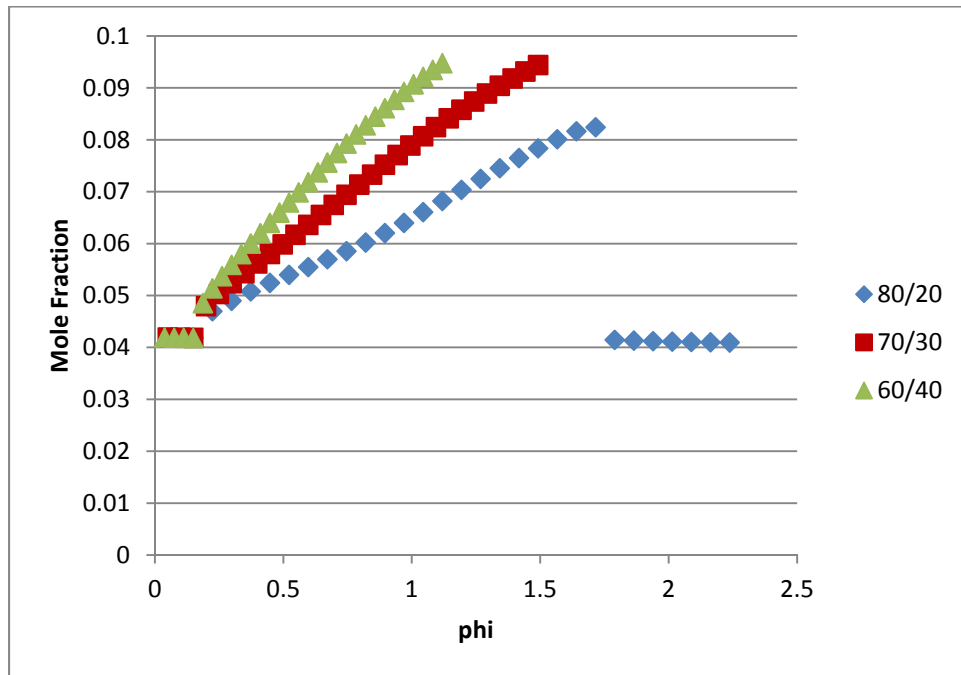
Figure 4.6: CO₂ emissions
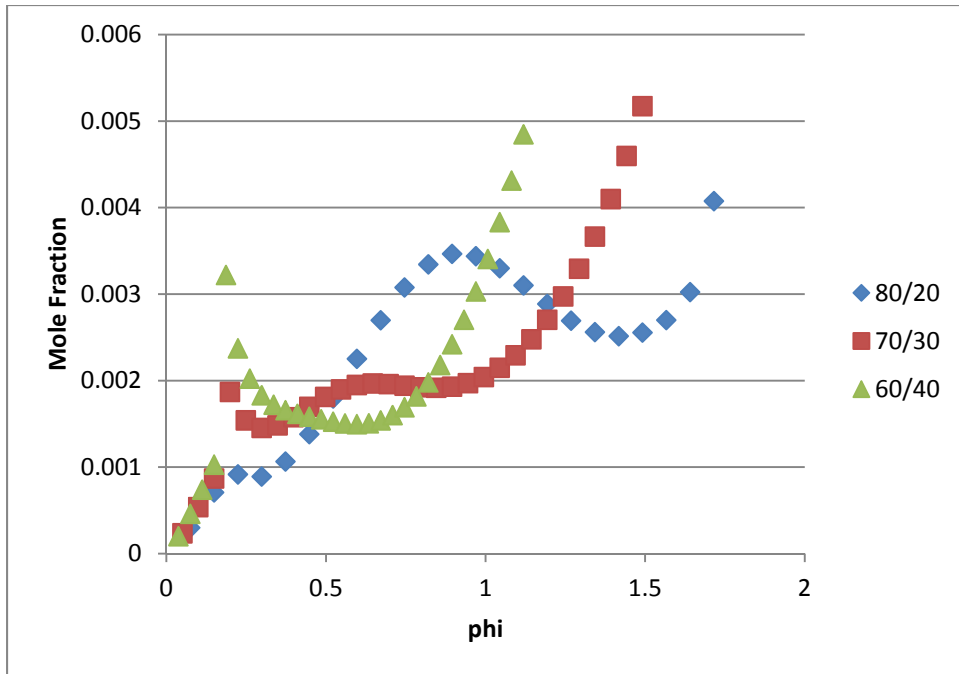
Figure 4.7: CO emissions
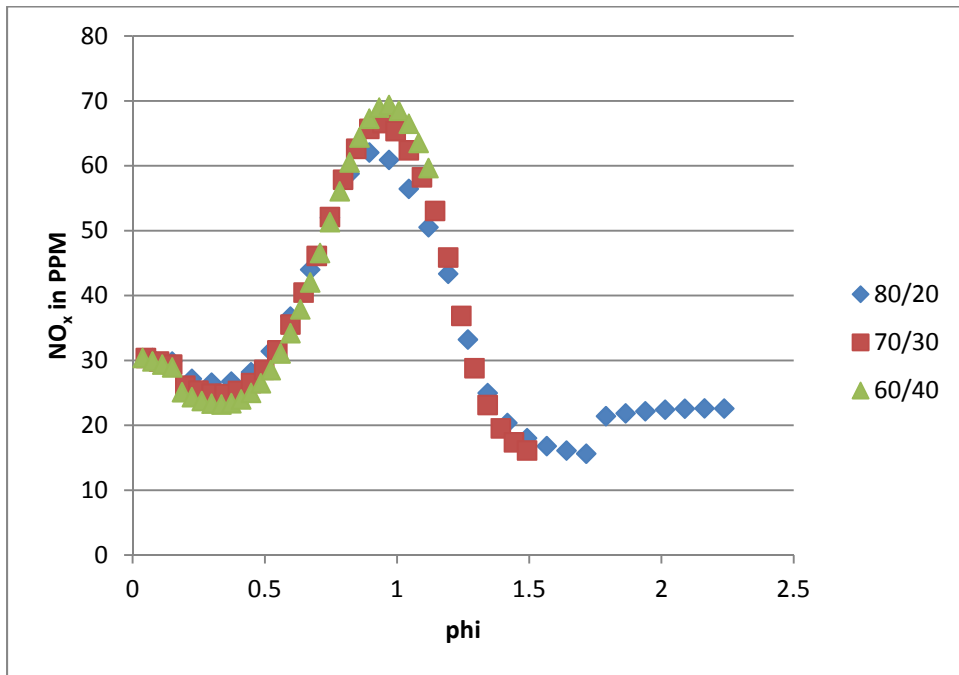
Figure 4.8: NO$_x$ emissions
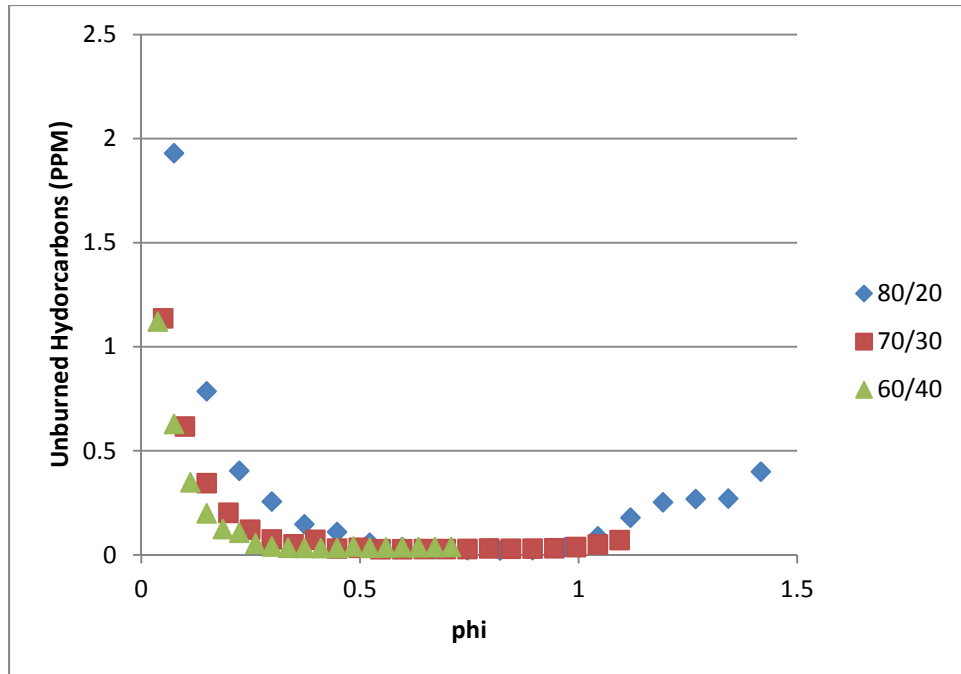
Figure 4.9: THC emissions

By taking the temperature and emissions data from CHEMKIN and comparing the two, a flow split can be selected that is most likely to achieve the 300 K temperature increase and keep pollutant emissions low thus producing an efficient combustion process. Table 6 below shows the three flow splits with the corresponding equivalence ratio, temperatures and emissions data. The 80/20 flow split has the highest efficiency of combustion, but is significantly worse in NOx and CO emissions compared to the 70/30 and 60/40 splits. The 70/30 split's NO_x emissions are 5 ppm higher than the 60/40 split, the THC is 6 ppm lower while achieving the desired temperature increase. The CO emissions are also lower for the 70/30 split by 25 ppm. The 70/30 split was chosen because it provides the best blend of efficiency and emissions output.

Table 6: CHEMKIN results

	80/20	70/30	60/40
φ	0.67	0.45	0.34
Temperature (K)	1310	1319	1318
NO_x (ppm)	63.98	38.74	33.92
THC (ppm)	0.15	1.14	7.03
CO (ppm)	2865	1803	1828

4.3   G-load testing

The total and static pressure were measured in the cavity to examine what g-loads were capable of being achieved in the cavity with the current configuration. The 0.75" air line was used and operated at 50%, 75% and 100% of the flow avaiable on the 0.75" air line, equating to 0.990 kg/min, 1.496 kg/min and 1.991 kg/min. The air line flow percentage was set using the LabVIEW code on the main computer. A pitot tube and a static port were used to measure the total and static pressure at the three conditions shown in Figure 4.10. The measurement was taken three times for each condition. The average pressure for each condition is shown in Table 7. The pressures were used to determine the tangential velocity in the cavity using Equation 3. The tangential velocity was then able to be used to calculate the g-loading in the cavity using Equation 4. The results from the g-loading measurements can be seen in Table 7.

Figure 4.10: Pitot and static port locations

Equation 3: Tangential velocity

$$V_{tan} = \left[\left(\left(\frac{P_T}{P} \right)^{\gamma-1/\gamma} - 1 \right) \frac{2}{\gamma - 1} \right]^{1/2} [\gamma R T]^{1/2}$$

Equation 4: G-loading

$$g = \frac{V_{tan}^2}{g_c r_{cav}}$$

Table 7: G-loading for given cavity flow

Cavity flow %	50%	75%	100%
Cavity flow rate (kg/min)	1.004	1.496	1.991
Total Pressure (Pa)	99119	99457	100174
Static Pressure (Pa)	98712	98698	98678
Tangential Velocity (ft/s)	85.94	122.42	164.99
G-load	882	1789	3249

4.4   Impact of G-Load on Fuel Sprays

The goal of the circumferential cavity is to swirl the flow and create an elevated centripetal loading. The swirling helps mix the fuel and air in the cavity while the g-loading keeps the unburned mixture towards the OD while the burned gases move into the center body. The swirled mixture of air and fuel will result in a specific equivalence ratio set by the amount of air in the cavity and the amount of fuel being pumped in through the fuel nozzles. Equivalence ratios less than 1 were examined ranging from 0.2 to 0.5. Low equivalence ratios were examined because only a small temperature rise is required in an ITB and keeping the equivalence ratio low uses less fuel. By varying the air flow rate into the cavity g-loads of 822 to 3249 were examined. It was determined that before fuel was pumped into the cavity, the fuel nozzles should first be tested outside the rig to learn more about fuel pump control and flow rates required to achieve an atomized cone of fuel.

4.4.1   Initial fuel spray testing

Fuel spray tests were conducted initially outside the rig with JP-8. These tests were used to examine the angle of the spray cone and to determine the fuel flow rate to achieve atomization. A test rig was used that mounted the fuel nozzle in the center of a plate as shown in Figure 4.11. Beneath the plate a series of rings were drawn to help quantify the spray angle. Each fuel nozzle was evaluated over a range of pressures as provided by the ISCO fuel pump.

Figure 4.11: Fuel spray test rig

Each spray nozzle was able to produce a uniform spray cone with a minimum

flow of 50 mL/min corresponding to a pressure of 364 psi shown in Figure 4.12. The

spray angle was nominally 90° at this flow rate. When the flow rate was reduced to 20

mL/min, corresponding to a pressure of 43 psi, the cone shape degraded as can be seen in

Figure 4.13 yielding a spray angle of 35°. At 10 mL/min corresponding to a pressure of

13 psi the flow reduced to a drip with no cone development. These results were

consistent for all 6 nozzles tested. The appearance of a cross flow in Figure 4.13 is

caused by the exhaust duct used to remove the atomized fuel from the laboratory.

Figure 4.12: Fully developed fuel spray cone

Figure 4.13: Partially developed fuel spray cone

A second experiment was performed to evaluate the flow rates with two spray nozzles. The setup for the 2 spray test can be seen in Figure 4.14. This test produced similar results with the major difference was lower pressures were required to achieve the same total flow rate. Figure 4.15 provides the corresponding pressure versus flow rate curves for the single and dual jet tests. The results of the test show that for a given pressure the addition of a second fuel nozzle provides twice the mass flow rate. As a note of safety, the tests were only conducted for a short time as they produced a cloud of atomized JP-8. The exhaust vent was used to reduce the cloud. As expected, two fuel nozzles produced a larger cloud than one nozzle.
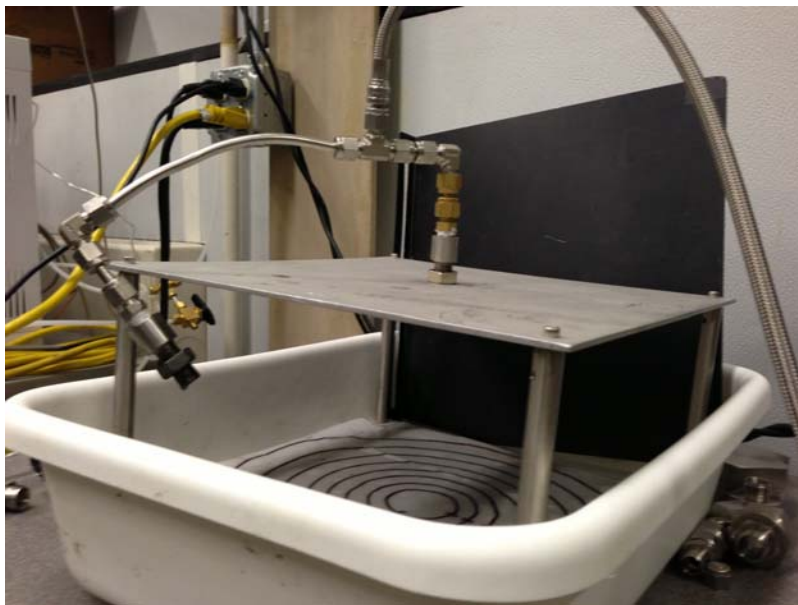
Figure 4.14: 2 fuel nozzle spray test
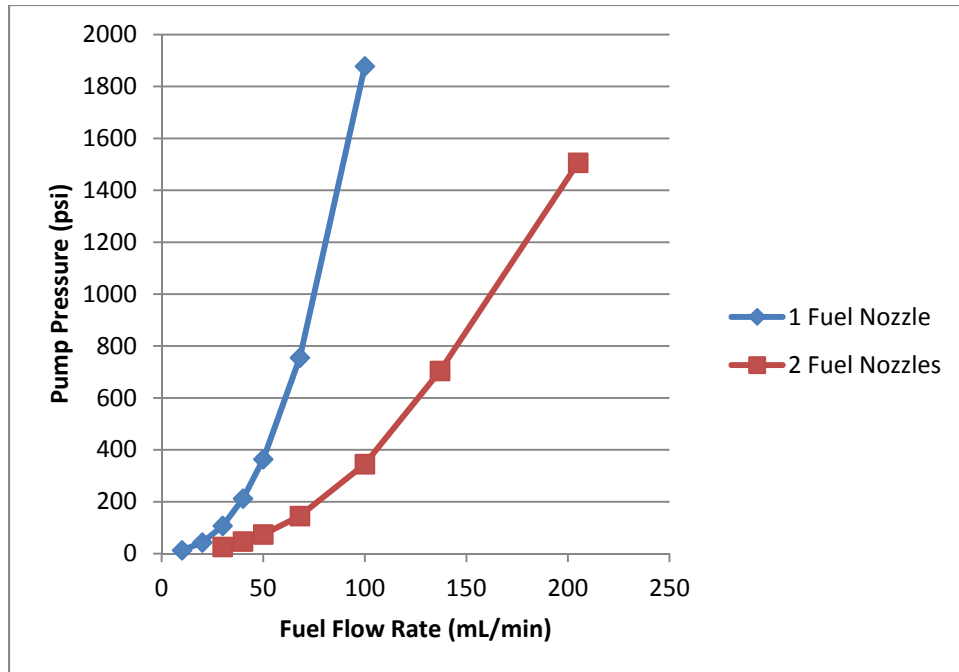
Figure 4.15: Fuel nozzle pressure vs. flow rate curves

The six fuel nozzle experimental setup is shown in Figure 4.16. The single and dual fuel nozzle tests were conducted with 2 existing fuel nozzle bolts from an old experiment, of which there are only 3 existing fuel nozzle bolts. The six fuel nozzle test required new bolts as there were not enough exiting fuel bolts to complete the test. The newly fabricated fuel nozzle bolts used to hold the fuel nozzles were unable to be achieve an adequate seal. Teflon tape was used with some limited success until the JP-8 began to break down the tape. At this point the system began to leak again. A nickel anti-seize which has some ability to act as a seal was also used, but when put under pressure was squeezed out of the threads and leaked. Six new bolts will need to be fabricated to tighter tolerances to correct this problem.

Figure 4.16: 6 nozzle spray test rig

4.4.2 Circumferential cavity fuel spray testing

Having successfully evaluated the flow ranges that produced quality sprays, a

single fuel nozzle was installed in the ITB circumferential cavity using the functional

older bolts. The fuel nozzle was positioned 60° degrees clockwise from top dead center.

Figure 4.17 shows the configuration of the spray nozzle in the rig and the viewing angle

of the Phantom camera through one of the optical windows. Also shown in Figure 4.18

are the location of the fuel nozzle, the 6 air lines feeding the cavity and the quartz

window that was used to look into the cavity. The test was run at constant air flow rates

of 0.0165 kg/s in the cavity and a nominal 0.05 kg/s in the core to simulate an axial flow

through the core. The mass flow split between the cavity and the core flow is a 25%

cavity and 75% core. This created a g-load of 882 in the circumferential cavity. Of note

is that there was no center body during these tests and as such no airfoils to help pull the

79

flow out of the cavity. The fuel was run at 25 mL/min, 50 mL/min and 100 mL/min

providing a nominal equivalence ratio of 0.22, 0.44, and 0.88 locally. For the given fuel

flow rates blowing ratios were able to be determined of 10.4, 20.8, and 41.7 respectively.

Figure 4.17: Fuel spray rig setup
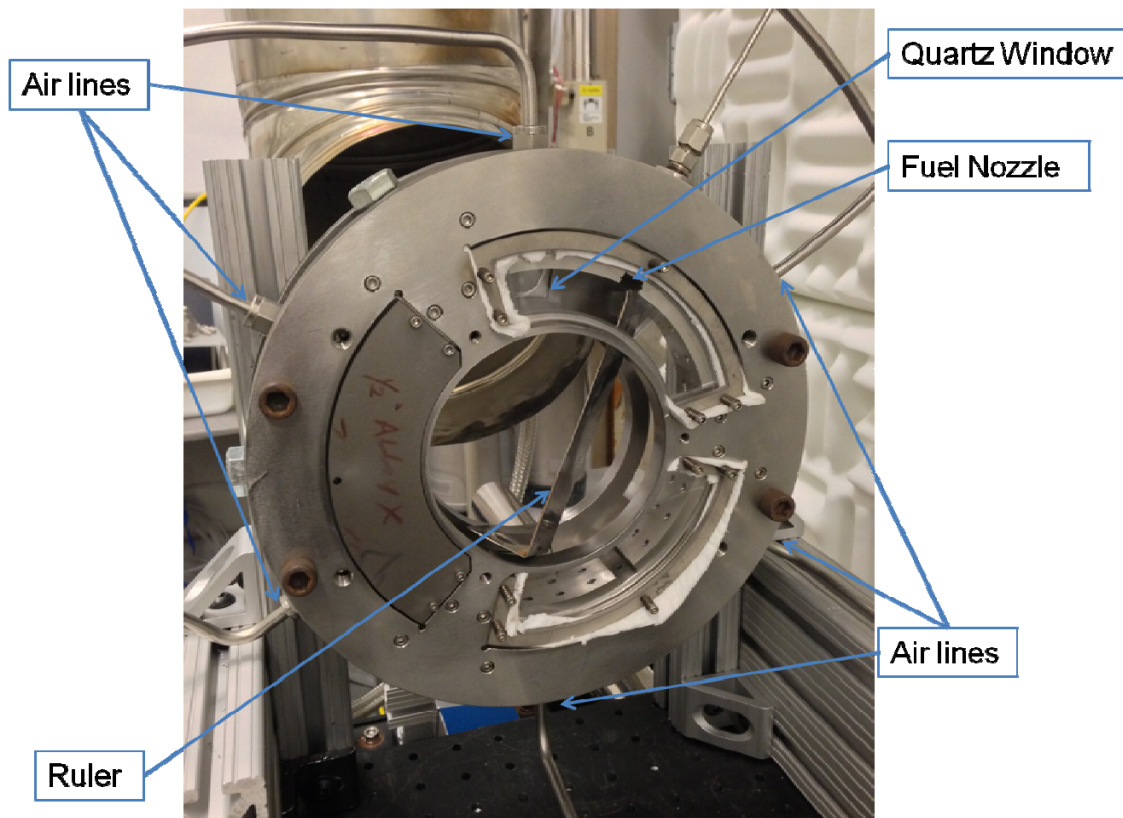
Figure 4.18: Fuel spray rig w/o inlet

High speed video of the three test cases was taken with the Phantom camera. The

camera settings were 11,001 fps, 10µs exposure time, and 800x600 resolution for

acquiring this data. This allowed for 3.851 seconds of data to be captured. Still images of

the three flow rates can be seen in Figure 4.19. Red lines have been added to aide in

viewing the atomized fuel spray. Visible in these pictures are the atomized fuel particles.

By tracking the particles, the penetration and spray pattern of the fuel nozzle could be

evaluated. The 50 mL/min flow is 24° from the nozzle exit centerline and the 25 mL/min

flow is 34° from the nozzle exit centerline. The 100 mL/min fuel flow rate condition was

unable to have its trajectory angle determined due to the large quantity of fuel in the

cavity. The fuel in the cavity was drained and the window was cleaned. The 100

mL/min test was preformed 2 more times with similar results. The fuel was not burned in this test. Therefore the fuel was not exiting the circumferential cavity due to the buoyancy created by the g-load. The atomized fuel not exiting the cavity then mixed with the fuel cone that was examined, distorting the cone. The atomized fuel was also coating the quartz window making visibility poor in the cavity which is seen in Figure 4.19.
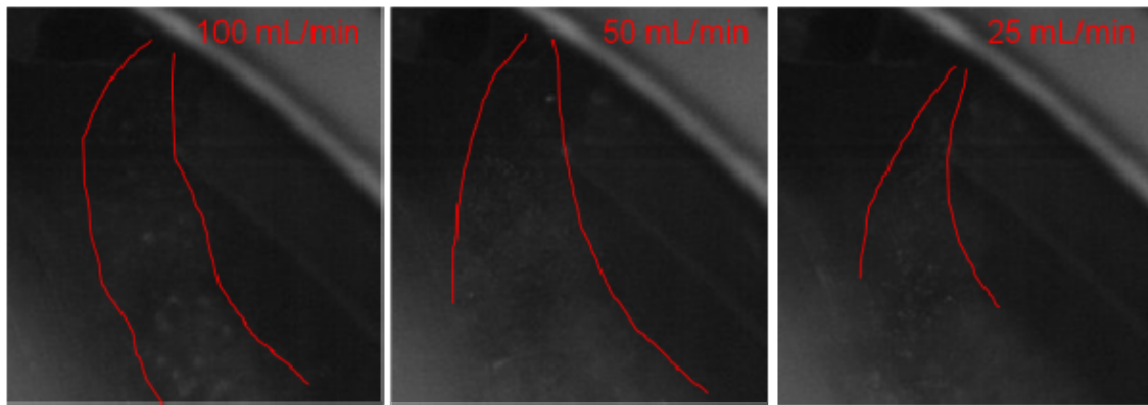
Figure 4.19: Camera still images

Digital particle image velocimetry (DPIV) software was provided by Dr. Larry Goss of ISSI and was attemped for the three conditions. DPIV is a method where two consecutive frames from high speed video are captured and two images are correlated using correlation software. By comparing the two images the software is able to calculate velocity vectors of particles as they move from frame to frame. The distance the particle travels between two frames can be measured by knowing the number of pixels the particle moved. The pixel count can be converted into a distance with a calibration image showing a known distance determining the distance per pixel. The velocity can be obtained by dividing the distance the particle traveled over the change in

time from one frame to the next. The atomized fuel particles were not discrete enough to be tracked by the DPIV software. This may be caused by inadaqute lighting, the frame rate may be too slow, the particles are not well enough defined to track, fuel on the windows preventing a clear image, or exposure time being too long. This software and technique is typically used to track the CH radical in combusting flows. The chemiluminescence from the CH radical is much more distinct than the atomized fuel droplets. A Phase Doppler Particle Analyzer (PDPA) system will be utilized in the future to attempt to better quantify the spray droplet sizes and velocities.

Addition fuel spray testing was conducted with the fuel flow held constant and the g-load varied. For these tests the flow rate was kept at 20 mL/min to reduce the effects of excessive fuel coating the window. The g-load was tested at 0, 822, 1789, and 3249, again without a center body. Figure 4.20 shows the results from the 4 g-loads. The phantom camera was not used for these tests as the data was too difficult to interpert. Instead a standard digital camera was used to take still images of the fuel sprays. The fuel sprays are move visible from this test and were able to provide greater detail of the fuel spray pattern. The 0 g-load case looks as expected, a simple cone. The cone however is not at the maximum spray angle possible as the fuel flow rate is too low to achieve a full cone. The 822 g-load condition has a significant amount of atomized fuel heading slightly upstream while in the recess of the combustor ring. This is interesting as the non g-loaded case did not have as wide of a cone as the 822 g-load case. It is believed that the recess is creating a low pressure pocket on the upstream side of the recess causing the fuel to be drawn into a broader pattern before flowing into the cavity. The 1789 g-load case experieances the same phenomena but to a lesser extent as the fast

moving cavity flow is not affected by the recess as much as the lower g-load case. The 3249 g-load case has almost no signs of the fuel spray broadening.

The atomized fuel swept towards the OD of the combustor ring the more the g-load was increased due to in increase in cross flow velocity. This trend follows what would be expected. The penetration depth of the 822 case was 0.26 inches, the 1789 case was 0.22 inches and the 3249 case was 0.19 inches. The penetration depth was measured from the outer wall to the middle of the fuel spray pattern. It is expected that by adding the center body less migration from the cavity will occur, causing the fuel to become more swept into the cavity, reducing penetration depth, for a given mass flow rate.
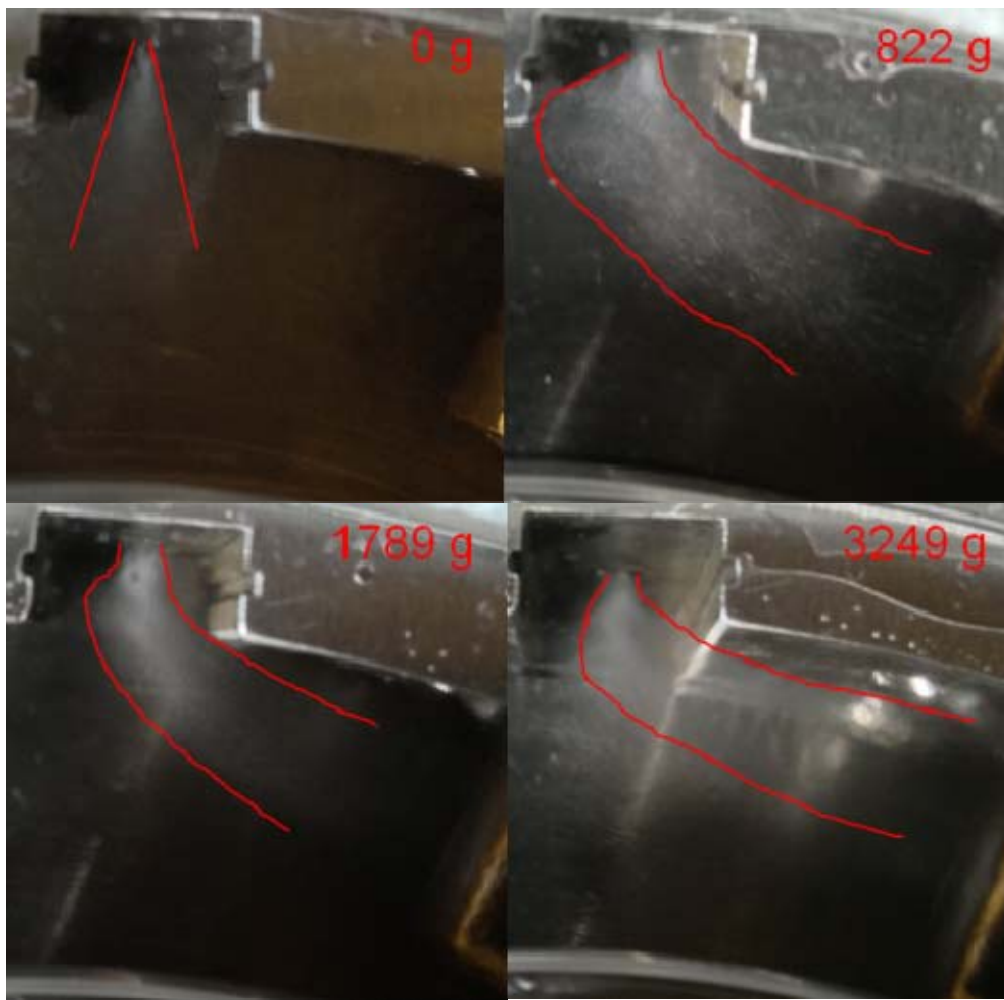
Figure 4.20: Constant fuel flow rate spray test

4.5   UCC combustion testing

With the g-loading and fuel spray testing complete, combustion testing of the single fuel nozzle was conducted. The ignition of the fuel was unsuccessful. The igniter is located on the back combustion ring in the lower left quadrate of the cavity when looking from the rear of the UCC. The fuel injection port was tried at three different locations of 0°, 60°, and 120° upstream of the igniter.   Many different combinations of fuel and air flow rates were attempted with no success. Fuel flow rates were varied from 20 to 100 mL/min and air flow rates were varied from 0.4 to 1.5 kg/min. It is interesting to note that when the fuel nozzle was turned off and the igniter left on, small bursts of combustion occurred from the residual JP-8 in the cavity. At this point, one possible explanation was that the cavity was running too fuel rich of an environment to combust with the fuel pump running. Once the fuel pump was off, the equivalence ratio in the cavity was correct for combustion but did not have a steady flow of fuel for combustion to be stable. The fuel flow rate could not be lowered more to test the fuel rich idea as the fuel would not be atomized. A solution to test this would be to find a fuel nozzle with a lower flow number. A second hypothesis is that the fuel was not flowing into the path of the igniter. This seems very unlikely as the fuel spray testing showed that the fuel would pass right through the igniter path when the JP-8 was injected at the fuel port in line with the igniter. A third hypothesis was the fuel migrated prematurely into the core flow and out of the engine because the center body was not installed. This third hypothesis was tested by changing the fuel source from JP-8 to propane as previous UCC research had

85

success with propane in sectional rigs in the past even though ignition was difficult to achieve. The fuel nozzle was removed and the propane tube attachment was installed. The propane was set to a volumetric flow rate of 40 L/min with a cavity flow of 25% or 0.8 kg/min. The core flow was at 1.5 kg/min and the equivalence ratio was 0.51. The propane was entering the cavity at the fuel port in line with the igniter. The propane had great success at lighting off as can be seen in Figure 4.21. The propane was most likely successful because the propane was exiting as a jet into the cavity. This caused the propane to directly intersect the igniter port. Based on the propane tests, the JP-8 was not coming in contact with the igniter seemed more plausible for the cases of 60° and 120° upstream of the igniter. By adding the center body, the JP-8 should be able to come in contact with the igniter due to the reduced migration from the cavity. For the case of the fuel injecting in line with the igniter, it is believed the flow is too rich for combustion to occur.
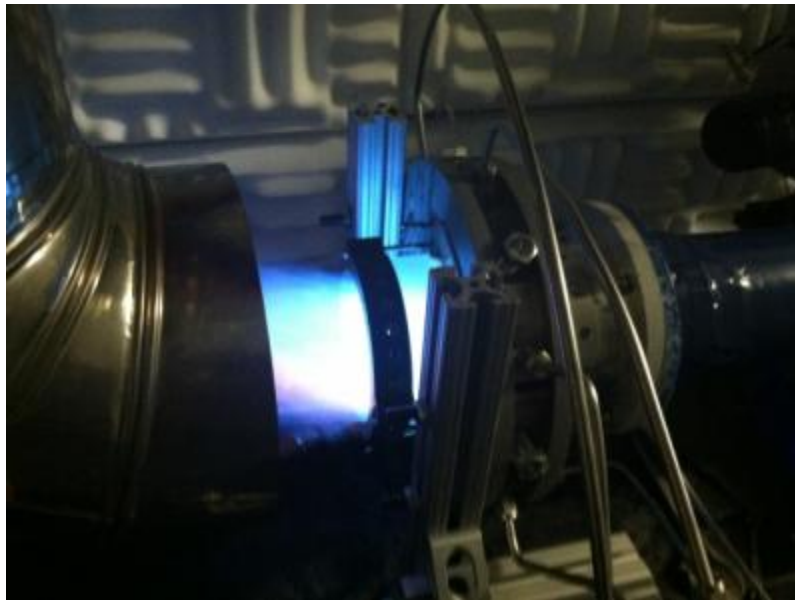
Figure 4.21: UCC with propane combustion

With combustion occurring in the UCC, additional photos were taken, the most interesting of which are Figure 4.22 and Figure 4.23. Figure 4.22 shows the front window where the igniter can be seen. It shows that the fuel is igniting in the cavity, but is quickly migrating into the core flow. Figure 4.23 shows there is no combustion occurring in the cavity at the next window downstream, 120° from the previous window. From what was observed during the test, the core flow drew the combusting gas into the core. It is believed that this is because the center body is not in place to keep the flow moving tangentially within the circumferential cavity versus quickly exiting into the core flow. The igniter was placed inline radially with the fuel port. By doing so, flow could move clockwise or counterclockwise in the cavity and the igniter would still come in contact with the fuel. The igniter flame acts as a jet of fire perpendicular to the circumferential flow. The tip of the flame was observed bending slightly at the tip in the direction of the circumferential flow.
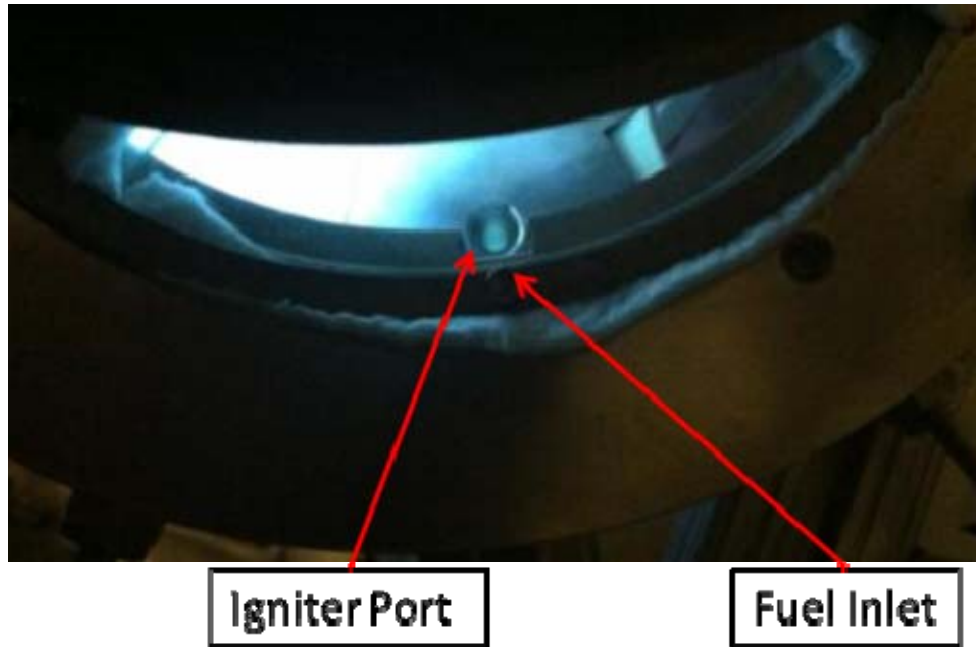
Figure 4.22: Igniter window

Figure 4.23: Front top window

Having successfully ignited propane in the UCC, combustion with JP-8 was

attempted again. During this combustion test three fuel nozzles, of flow number 0.3,

were used to inject atomized JP-8 into the circumferential cavity. The fuel nozzles were

set 120 apart with the igniter centered between two of the fuel nozzles. The JP-8 did not

ignite as quickly as the propane, but after adjusting the cavity air flow rate and the fuel

flow rate combustion was achieved. Combustion occurred at a total JP-8 flow rate of 100

mL/min, 1.1 kg/min of air in the cavity and 1.5 kg/min of air for the core flow. The g-

load in the cavity was 1066. The equivalence ratio in the cavity was 1.09 and the overall

equivalence ratio of the UCC was 0.46. Much of the combustion took place in the center

body region. It was noticed that some combustion was occurring in the circumferential

cavity immediately downstream of the fuel injectors and continuing about 1 to 2 inches in

the cavity before migrating into the core flow shown in Figure 4.24. The igniter is

located 180 from the fuel inlet. The flame was downstream of the fuel inlet. The flow

direction was counterclockwise in Figure 4.24. The flow exiting the UCC can be seen in

Figure 4.25. The flame exiting the UCC was swirling as would be expected without the

straight center body. The flame exiting the UCC is undesirable as burning at this point

would not increase thrust for the augmenter configuration and for the standard

configuration the flame would enter the LPT.
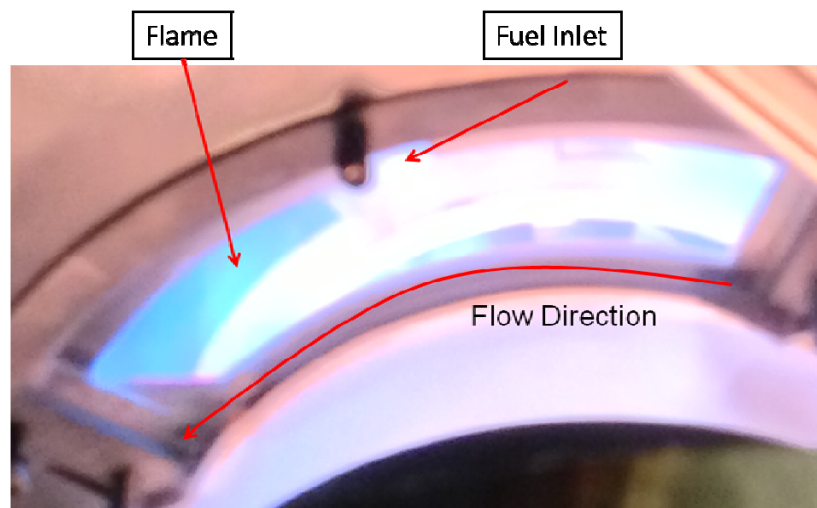
Figure 4.24: JP-8 three fuel nozzle test
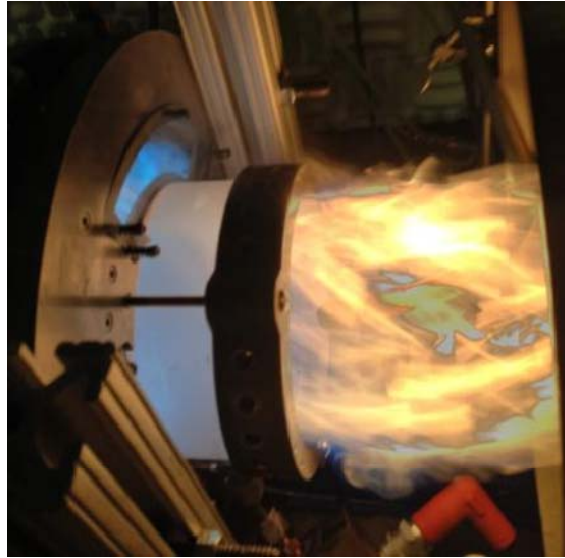
Figure 4.25: JP-8 exit flame

4.6   Summary

The CHEMKIN emissions data has provided several useful pieces of information. First, the data provided ranges for the CAI emissions machine to be set to for testing of the ITB. Second, equivalence ratios for the 3 mass flow splits were found to provide the 300 temperature increase at the exit of the ITB. This will allow for more accurate starting points for ITB testing in the future.

The fuel spray tests produced some very useful data for future testing. First the initial spray testing provided pressure and volumetric flow rates for the fuel nozzles. Second the initial spray testing confirmed the spray cone angles of the nozzles. Third, the cavity spray nozzle test showed how g-loading affects penetration depth of the atomized fuel into the cavity. This is exceptionally important to ensure the fuel is not pumped at too high a rate for a specific g-load. The higher the fuel flow rate, the more likely fuel will flow into the center body rather than stay in the circumferential flow.

5   Conclusions and Recommendations

5.1   Chapter Overview

This chapter covers conclusions from the research, significance of the research, recommended actions, and recommendation for future research. The objectives of the research were to integrate the UCC to a common source, conduct fuel spray tests to examine the effect g-loading has on the atomized fuel, and setup a vitiated air source for the ITB.

5.2   Conclusions of Research

Several conclusions can be drawn from the diffuser design, CHEMKIN results, fuel spray testing and combustion tests. First, the goal of integrating the UCC into a common flow source has been successful. This is the first time the UCC has been built for a full annular rig for the COAL laboratory. A diffusing flow splitter has been designed and fabricated to allow the UCC to operate from a common flow source. Three flow splitters have been designed to allow for different cavity g-loads for a given total mass flow.

Second, the CHEMKIN results gave predictions that the 70/30 mass flow split will provide the best results. The emissions data from CHEMKIN will also be useful to narrow the band for examine NO_x, CO, CO_2, O_2 and THC with the CAI emissions analyzer. The CHEMKIN data also provided the equivalence ratio needed for a given flow split to achieve the 300 K temperature increase that is desired for the ITB.

Third, the fuel spray testing showed that as the g-load increased the atomized fuel was pushed towards the OD of the circumferential cavity. Also for a constant g-load as

the amount of fuel being sprayed into the cavity increases the atomized fuel is less affected by the g-load. Both of these conclusions were expected.

Fourth, the combustion testing showed that JP-8 was able to be ignited in the circumferential cavity. All of the combustion testing showed that the center body would need to be installed into the UCC to function as intended. The combustion tests did provide valuable experience for igniting the flow in the cavity which will be able to be used once the center body is installed.

5.3   Significance of Research

AFIT now has the ability to run a full annular UCC from a common flow source. This has been a significant accomplishment in that it will allow many future AFIT students to conduct research on the UCC as both a main combustor and ITB combustor configuration.

The laboratory has been rebuilt to facility future UCC research. The emissions analyzer is functional and calibration procedures have been documented. Fuel nozzle spray testing has been conducted with varying degrees of success, but has provided valuable data to improve future experiments.

5.4   Recommendations for Action

There are several actions that need to be addressed before future research is conducted. First, the center body needs to be constructed. The center body is critical flow migration from the cavity. Without the center body, flow is migrating from the cavity earlier than desired. Second, the fuel pump needs to be added to the LabVIEW code. The fuel pump is currently operated from the fuel pump control panel. To increase

safety and functionality of the laboratory the fuel pump needs to be operated from the main control terminal. Third, the regulators on the 3" and 1.5" air lines need to be examined as they are constricting the flow more than is needed and preventing the air lines from providing the maximum flow desired. Fourth, the STE needs to be run and baseline thrust measurements taken. Fifth, changes to operation of the Phantom camera are necessary for the experiment. It will need to be oriented so that it is as close to perpendicular to the cavity as possible. Furthermore additional lighting will be needed to reduce the exposure time of the camera to allow for more clear images to be taken. Sixth, it was also found that the fuel bolts will need to be re-fabricated to tighter tolerances before all six fuel nozzles can be used.

5.5 Recommendations for Future Research

There are several recommendations for future research. First, the fuel spray testing needs to be reexamined with the center body. This would allow the effects of the center body addition to be examined. Second, using the STE as the vitiated air source, run the ITB and collect emissions measurements and compare them to the CHEMKIN analysis. This will allow the CHEMKIN analysis to be validated and determine if the model in CHEMKIN is accurate for providing other estimates. Third, examine the effects of the spacing and number of fuel nozzles. This would allow the affects of nozzle placement to be observed and determine the best fuel nozzle configuration for the straight center body. Fourth, examine the difference between flows coming in the side vs. the top of the circumferential cavity. By comparing the two cavity flow injection configurations, losses from the diffuser could be examined.

5.6   Summary

In conclusion the research conducted has been valuable to the further development UCC technology. A new UCC rig has been developed and initial testing of the rig has been conducted. The new rig will provide research opportunities for years to come.

Appendix A: JetCat P-200 Operating Procedures

The JetCat P-200 procedures in Appendix A are for proper operation of the JetCat

P-200 to ensure it is safely operated. Procedures include pre-ignition checks, starting

procedures, shut down procedures and routine checks.

<u>**JetCat P-200 Setup Procedures**</u>

Connect ECU (Engine Control Unit) and GSU (Ground Support Unit) with 7.5V
line from JetCat Power Relay
Check glow plug if needed (See JetCat Systems Routine Checks)
Mount JetCat on test stand, ensure glow plug is within 45 degrees of vertical
Check jet fuel line to make sure it is in good condition
Check starting gas line to make sure it is in good condition
Connect jet fuel tank to fuel line and solenoid valve line
Prime jet fuel line by running a little fuel into a cup (This is done by accessing the
Test-Functions Menu and then going to the **Pump TestVolt (Purge Fuel)**
option. Use the **Change Value/Item** button and the arrow keys to change the
pump voltage and run fuel through the lines.) **IMPORTANT: Make sure that
the fuel line is NOT connected to the turbine when you run fuel through the
lines. This will flood the turbine with fuel.**
Connect the fuel lines to JetCat
Connect starting gas line to JetCat
Connect ECU and GSU to turbine
Connect Butane fuel tank (make sure it is somewhat full) and refill if necessary
Check level of jet fuel
Shake (or stir) jet fuel to mix in oil
Connect nitrogen pressurization line to fuel tank
Open nitrogen supply valve for Jet Cat
 Ensure fuel is pressurized by checking gauge on fuel tank (ensure nitrogen
 valve is open and regulator is set to ~2 psi)
 Adjust bleed air to electronics and fuel boxes using needle valve
Open the manual fuel valve
Open the manual propane valve
Turn on exhaust fans
Check all connections to make sure everything is connected properly

JetCat P-200 Starting Procedures

Make sure "Emergency Stop" is in the out position
Turn on "JetCat Power"
Check to make sure jet fuel valve has switched to open
Check to make sure propane valve has switched open
Verify that ECU is powered by checking GSU via camera
Option A: DAQ and Labview control
Check the COM channels and select the correct ones for the ECU and Enerac
Set the Baud Rate to 9600
Press "Stop Program"
Restart the program
Verify that all the data reads correctly
Option B: Terminal program (no DAQ)
Start Termite 3.0
Select COM Port of ECU (usually 5), 9600 BAUD, 8 data bits, parity none, stop bits 1
Check ECU communication send <1,RAC,1> Response <1,HS,OK,…>
Open cameras and set view
Option A: DAQ and Labview control
Press "Write Data" in program
Press Start Turbine
Option B: Terminal program (no DAQ)
Set serial control of ECU <1,WSM,1> Response <1,HS,OK,…>
Other useful serial commands:
- o Start JetCat <1,TCO,1>
- o Stop JetCat <1,TCO,0>
- o Throttle <1,WTH,value> Value = 0..100
- o Aux <1,WAU,value> Value = 0..100

JetCat P-200 Power-down Procedures

Flip "Turbine 1" switch off or send <1,TCO,0>
Allow ECU to run the automatic cool down process
When the turbine has stopped turning, turn off "JetCat Fuel"
Turn off "JetCat Power"
Turn off the three DC power supplies
Close manual fuel valve
Close manual propane valve
Close nitrogen supply valve

JetCat P-200 Systems Routine Checks

Check jet fuel filter every ten tests and change if necessary

Check the glow plug every ten tests and change if necessary (See page 21 in manual)

Calibrate thrust stand (hit with rubber hammer after placing each weight on; this loosens the bearings up to give a more accurate reading)

Note: Run at idle for 2 minutes when testing new fuel to allow old fuel to be used from

fuel lines.

Appendix B: Laboratory Upgrades

Several upgrades to the COAL laboratory were required. These included sound absorption, increased air flow capacity, new data acquisition software and hardware, and rerouting of wires and flow lines in the laboratory. All of these topics will be discussed in more detail in the following sections.

B.1 Sound Absorption

The JetCat P-200 produces significant noise measured at 100 dB at 25 feet. Table 8 shows a range for the noise at various distances from the STE. Due to high noise level of the STE, sound absorbing panels were installed around the thrust stand area as can be seen in Figure B.1 to reduce the dB level in the vicinity of the experiment. The panels are made from semi-rigid melamine foam and are 3 inches thick. The fire retardant version was selected to reduce the risk of the panels igniting. They are rated to 422 K. The panels were purchased from McMaster-Carr and are called Fire Retardant Sheet Sound Absorbers, part number 9162T271. The panels were installed using zip ties to secure them to the frame surround the testing area. It should be also noted that even with the sound absorbing panels installed around 3 sides of the test area, additional hearing protection should be used to reduce the risk of hearing damage from the sound that will come from the top, bottom and rear of the test area.

Table 8: STE noise levels [17]

Distance from STE in feet	dB
2	114.4
12	105.6
25	11.5
50	97.5

Figure B.1: Sound absorbing panels

B.2 Air Lines

A 3" air line was installed to provide a greater mass flow rate to the rig. This 3" air line will allow the ITB to be run without the STE so clean flows can be examined. The higher flow rate was required to be able to match the flow rate of the STE to give accurate comparison of the vitiated and clean air. The new air line required a new compressor be installed to supply the air. A dryer system is also installed to remove excess water from the air which is condensed during the compressor process. In addition to the compressor and dryer, new regulators, values and flow meters were installed to complete the new air line.

B.3 Data Acquisitions System

The data acquisition software and hardware was updated. The hardware needed

to be upgraded because additional pressure and temperature probes were needed to

properly instrument the ITB. One of the major advantages of the new hardware is that it

is modular and plug-n-play. This will make future updates to the lab easier to execute.

The old hardware was National Instruments SCXI data acquisition cards and the new

hardware are National Instruments compact data acquisitions cards (cDAQ). The new

cDAQs can be seen in Figure B.2.
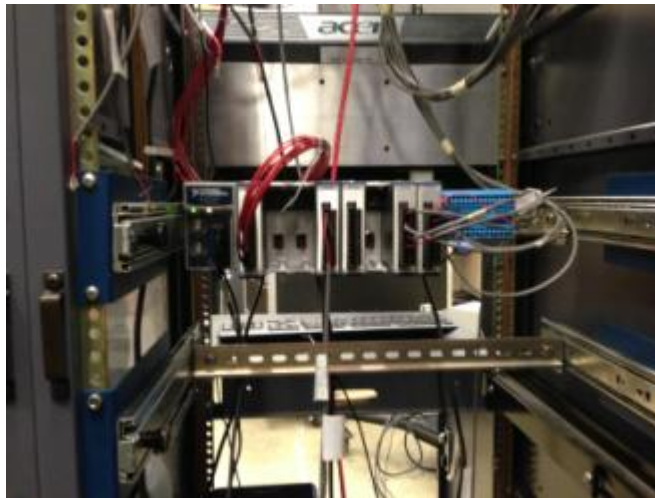
Figure B.2: New cDAQ

The data acquisition software, LabVIEW, was also updated. The LabVIEW code

was updated to version 11. The LabVIEW code was updated to keep the code modern

and needed to be updated for use with the new hardware. During the hardware and

software upgrades the Lab was also rewired. Wilson [13] has more on the rewiring of the

lab. This was an extensive effort to ensure capability was not lost and the improvements

functioned correctly.

Furthermore, a new mass flow controller box was created to allow easier connects to the experiment and to future rigs in the COAL lab as seen in Figure B.3 below. The mass flow controllers are located in front of the thrust stand. The new mass flow controller box is capable of controlling 8 different gases at once. The mass flow solenoids in the box are controlled through the LabVIEW program. The MKS mass flow control system, show in Figure B.4 below, is also programmed into LabVIEW.
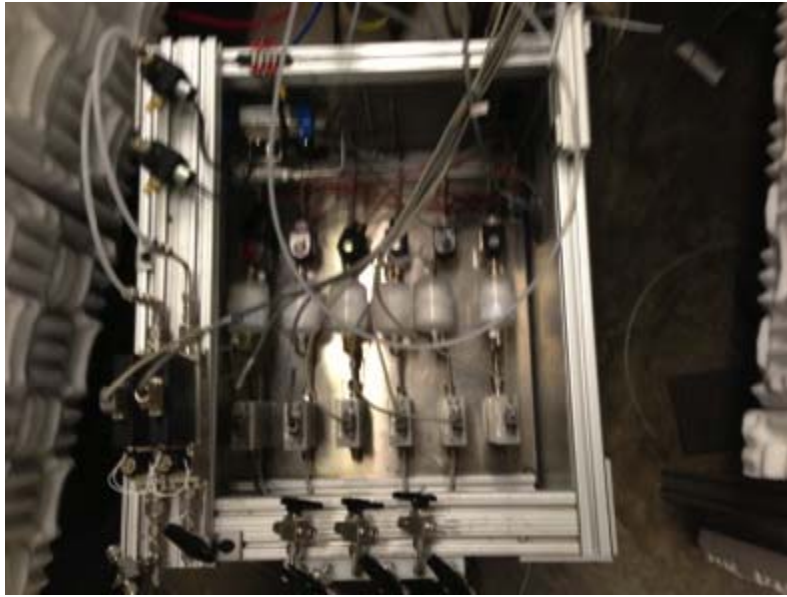
Figure B.3: Mass flow controllers

Figure B.4: MKS mass flow control system

B.4 Line Rerouting

The rewiring of the lab was a huge undertaking. With 10 years of student run experiments and limited documentation of what was changed from the original setup, a lot of time and effort was put into making sure capability in the lab was not lost when upgrading the data acquisition hardware and software. All of the power and instrumentation lines in the COAL laboratory were rerouted. This allowed for old unused lines to be removed and all active lines to be labeled and incorporated into the current laboratory setup. Furthermore, new wiring diagrams are provided outlining the changes and upgrades undertaken over the last year. Wiring diagrams and information for the CAI emissions analyzer can be seen in Figure B.5, Figure B.6, Table 9, and Table 10.
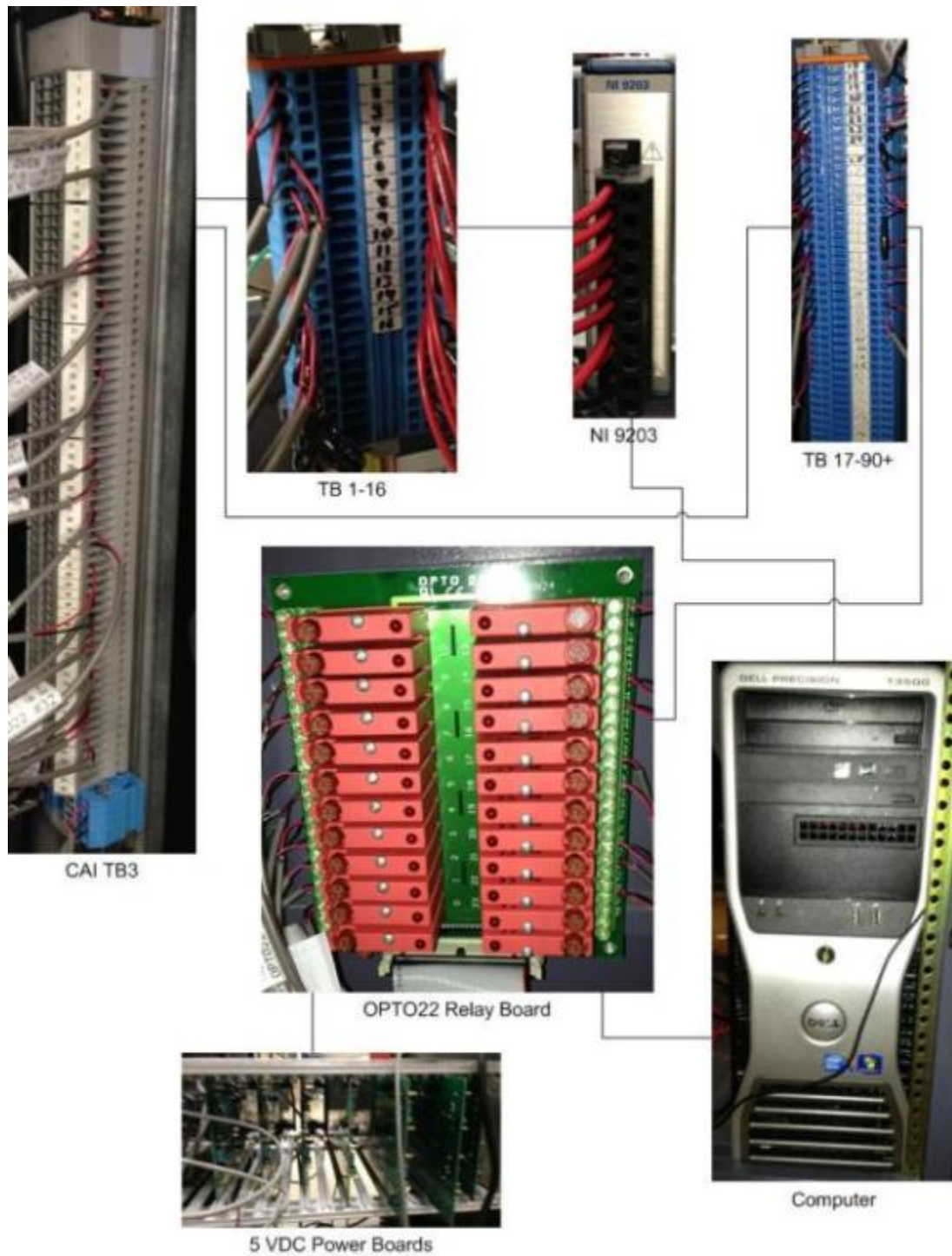
Figure B.5: CAI pictographic wire diagram
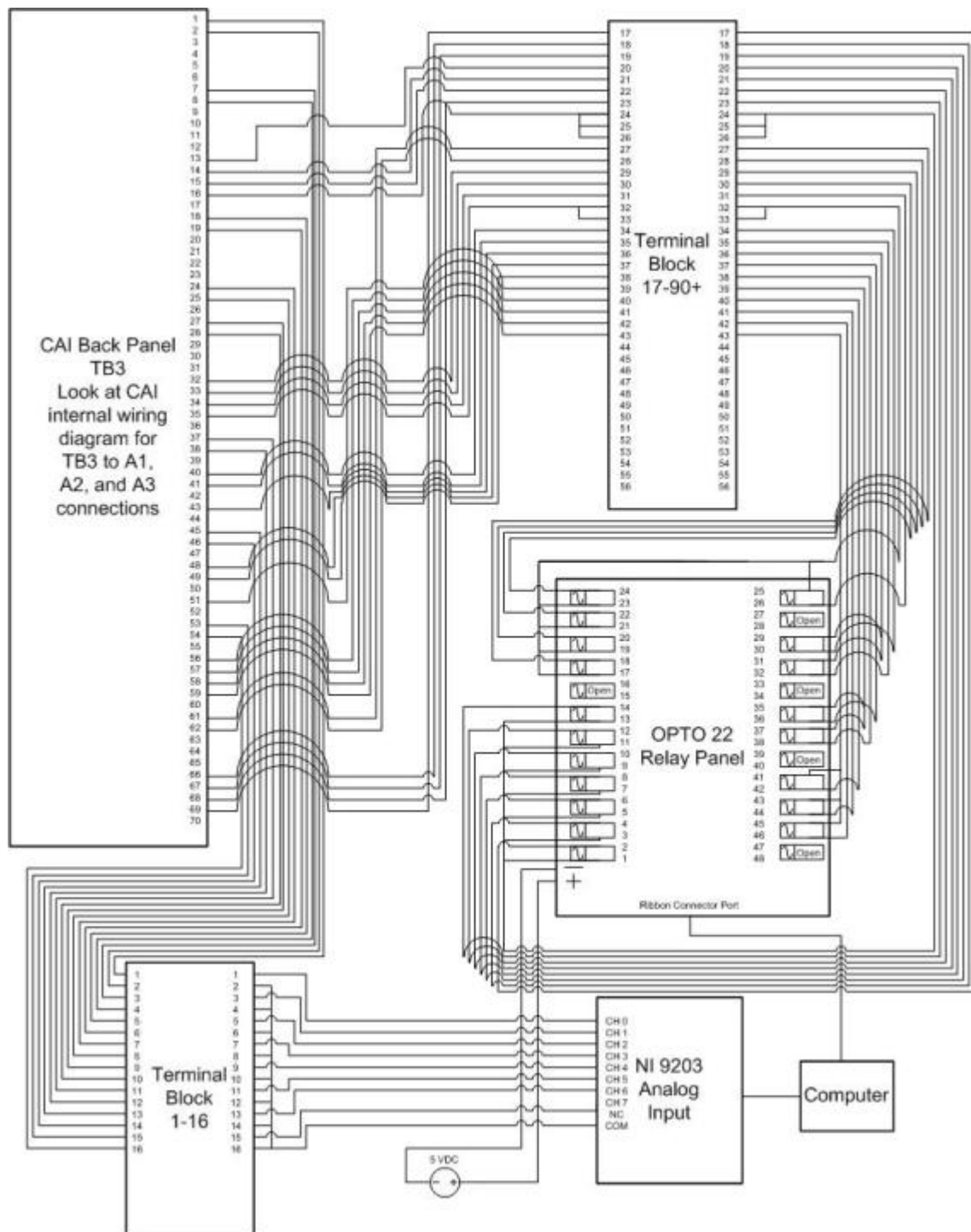
Figure B.6: CAI wire diagram

104

Table 9: CAI Back Panel

Port Number	New Label	Wire Color
1	THC Analyzer Out CAI #1,2 -- TB 1,2 cDAQ2 NI 9203 Ch 0	R
2		B
3		
4		
5		
6		
7	THC Oven Temp CAI #7,8 -- TB 3,4 cDAQ2 NI 9203 Ch 1	R
8		B
9		S
10		
11		
12		
13	THC Range 4 CAI #13 -- TB 20 OPTO22 #8	R
14	THC Range 5 CAI #14 -- TB 21 OPTO22 #10	B
15	THC Range 6 CAI #15 -- TB 22 OPTO22 #12	R
16	THC Remote CAI #16 -- TB 24 OPTO22 #1,3,5,7,9,11,13	B
17		
18	NOX Analyzer Out CAI #18,19 -- TB 5,6 cDAQ2 NI 9203 Ch 2	R
19		B
20		S
21		
22		
23		
24	NOX Conv Temp CAI #24,25 -- TB 7,8 cDAQ2 NI 9203 Ch 3	R
25		B
26		S
27	NOX Oven Temp CAI #27,28 -- TB 9,10 cDAQ2 NI 9203 Ch 4	R
28		B
29		
30		
31		
32	NOX Range 3 CAI #32 -- TB 29 OPTO22 #22	R
33	NOX Range 4 CAI #33 -- TB 30 OPTO22 #24	B

34	NOX Range 5 CAI #34 -- TB 31 OPTO22 #26	R
35	NOX Remote CAI #35 -- TB 32 OPTO22 #17,19,21,23,25	B
36		
37	CO2 Analyzer Out CAI #37,38 -- TB 11,12 cDAQ2 NI 9203 Ch 5	R
38		B
39		
40	CO2 Range 1 CAI #40 -- TB 34 OPTO22 #30	R
41	CO2 Range 2 CAI #41 -- TB 35 OPTO22 #32	B
42		
43	CO2 Remote CAI #43 -- TB 36 OPTO22 #29,31	R
44		
45	CO Analyzer Out CAI #45,46 -- TB 13,14 cDAQ2 NI 9203 Ch 6	R
46		B
47		S
48	CO Range 1 CAI #48 -- TB 37 OPTO22 #36	R
49	CO Range 2 CAI #49 -- TB 38 OPTO22 #38	B
50		
51	CO Remote CAI #51 -- TB 39 OPTO22 #35,37	B
52		
53	O2 Analyzer Out CAI #53,54 -- TB 15,16 cDAQ2 NI 9203 Ch 7	R
54		B
55		S
56	O2 Range 1 CAI #56 -- TB 40 OPTO22 #42	R
57	O2 Range 2 CAI #57 -- TB 41 OPTO22 #44	B
58	O2 Range 3 CAI #58 -- TB 42 OPTO22 #46	R
59	O2 Remote CAI #59 -- TB 43 OPTO22 #41,43,45	B
60		
61	NOX Range 1 CAI #61 -- TB 27 OPTO22 #18	R
62	NOX Range 2 CAI #62 -- TB 28 OPTO22 #20	B
63		
64		
65		
66	THC Range 2 CAI #66 -- TB 18 OPTO22 #4	R
67	THC Range 3 CAI #67 -- TB 19 OPTO22 #6	R
68	THC Range 7 CAI #68 -- TB 23 OPTO22 #14	B
69	THC Range 1 CAI #69 -- TB 17 OPTO22 #2	B
70		

Table 10: CAI OPTO22 board

OPTO 22 Port Number	Wire Name	OPTO 22 Port Number	Wire Name
1	THC remote	25	NOX remote
2	THC 1	26	Nox 5
3	THC remote	27	
4	THC 2	28	
5	THC remote	29	CO2 Remote
6	THC 3	30	CO2 1
7	THC remote	31	CO2 Remote
8	THC 4	32	CO2 2
9	THC remote	33	
10	THC 5	34	
11	THC remote	35	CO remote
12	THC 6	36	CO 1
13	THC remote	37	CO remote
14	THC 7	38	CO 2
15		39	
16		40	
17	NOX remote	41	Oxygen Remote
18	Nox 1	42	Oxygen 1
19	NOX remote	43	Oxygen Remote
20	Nox 2	44	Oxygen 2
21	NOX remote	45	Oxygen Remote
22	Nox 3	46	Oxygen 3
23	NOX remote	47	
24	Nox 4	48	

Appendix C: CAI Emissions Analyzer

Appendix C contains equipment descriptions and calibration procedures for the California emission equipment. The CAI range data bands can be seen in Table 11.

Table 11: CAI ranges

Range	THC (ppm)	NOx (ppm)	CO2 (%)	CO (%)	O2 (%)
1	10	30	5	5	5
2	30	100	20	10	10
3	100	300			20
4	300	1000	N/A	N/A	N/A
5	1000	3000	N/A	N/A	N/A
6	3000	N/A	N/A	N/A	N/A
7	10000	N/A	N/A	N/A	N/A
8	30000	N/A	N/A	N/A	N/A
RMT					

It was also found that the vacuum pump to the oven was broken on the CAI. The pump was sent back to the CAI factory for repairs and was reinstalled. A new resistance temperature detector (RTD) and a new heater were also installed in the NO_x analyzer as they were not functioning correctly.

Emissions measurements are taken by a probe located in the exhaust path of the flow seen in Figure C.1below. The probe is heated by using a hot oil pump system, the MOKON HTE System, shown in Figure C.2. The heated probe is required to allow accurate measurements of unburned hydrocarbons. If the line is not heated the particles will cool and change composition as they do so giving inaccurate results.

Figure C.1: Emissions probe

Figure C.2: MOKON HTE system

The CAI emissions machine is made up of several modules. They are the Power /
Machine Diagnostics, Emissions Analyzers, Flow Meters, Flow Switches, and Sample
Oven and can be seen in Figure C.3. The power and diagnostics panel shown in Figure
C.4 is where the power to the CAI machine is turned on. It also has the power switch for
the pump. The diagnostics on the panel are used to ensure different parts of the machine
are operating at the correct temperature. The CAI analyzer controls are where the
emissions outputs are controlled and display on the machine. The different knobs on the
analyzers are shown in Figure C.5. The CAI flow meter panel, Figure C.6, is where flow
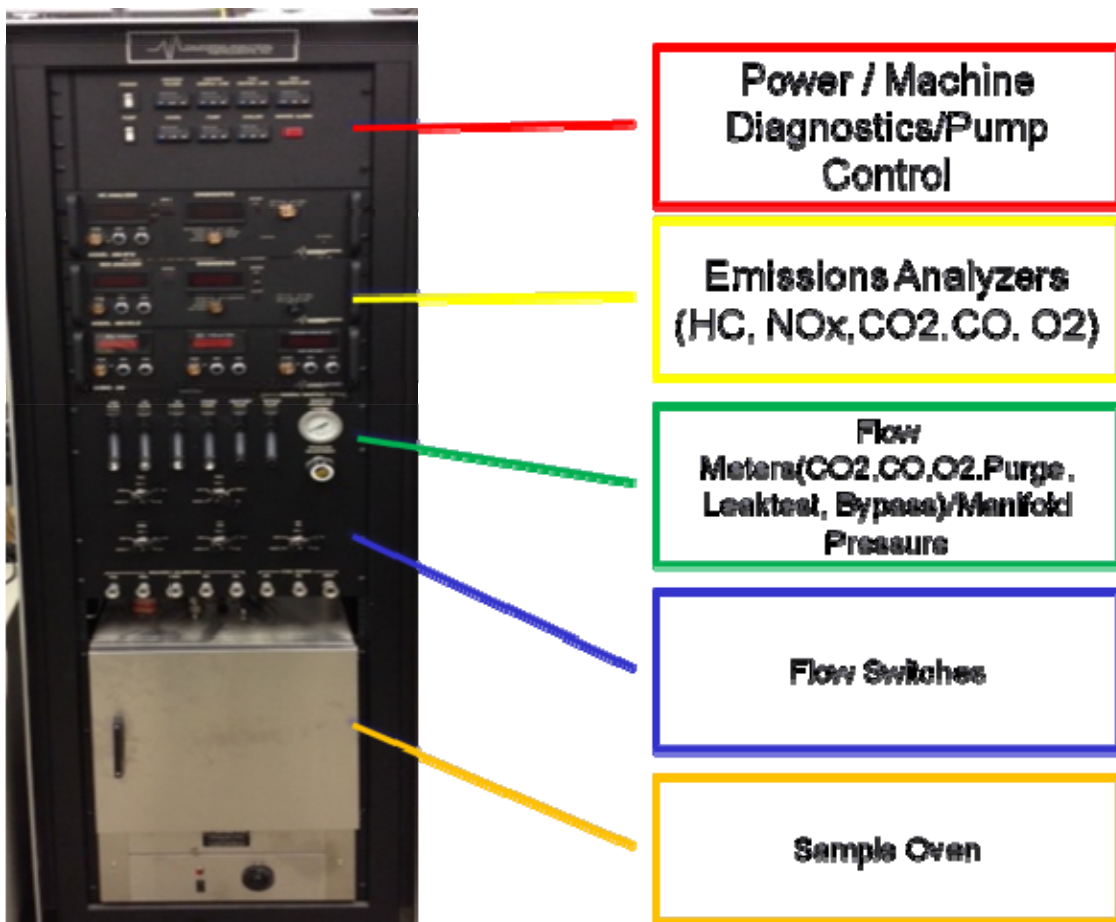rate are adjusted and displayed.

Figure C.3: CAI modules

Figure C.4: CAI power and diagnostics panel
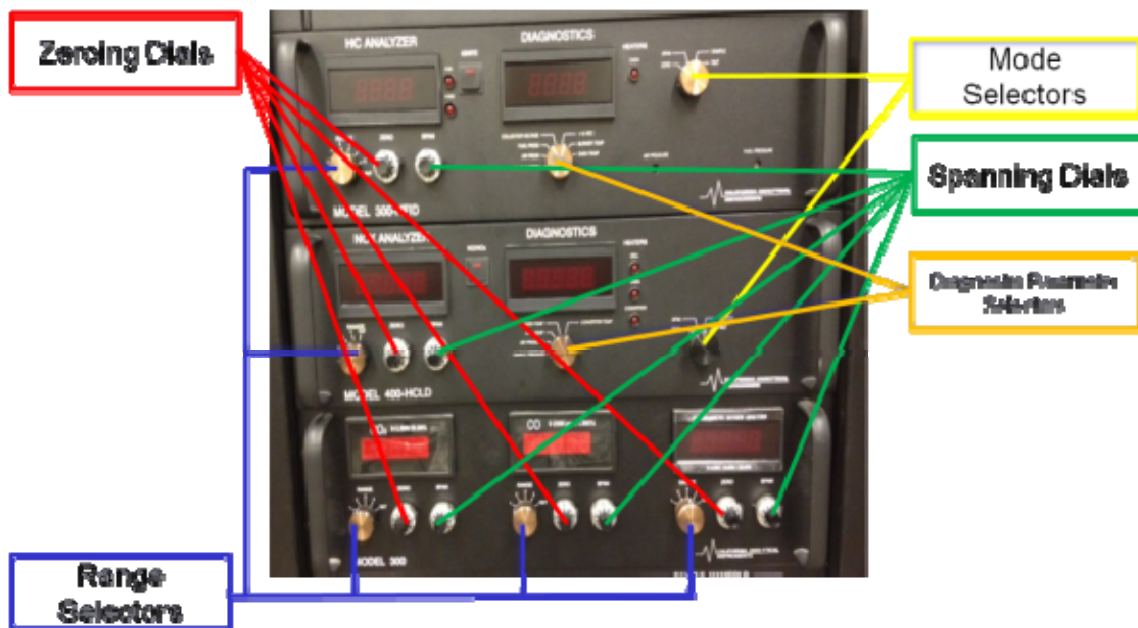
Figure C.5: CAI analyzer controls

Figure C.6: CAI flow meter panel

The CAI flow switch panel shown in Figure C.7 is where the source gas can be selected to go to the analyzers. Sample is the setting used for taking data. Zero, Span 1 and Span 2 are for calibration of the CAI emissions machine. The CAI emission machine is equipped with an oven, the insides of which can be seen in Figure C.8.

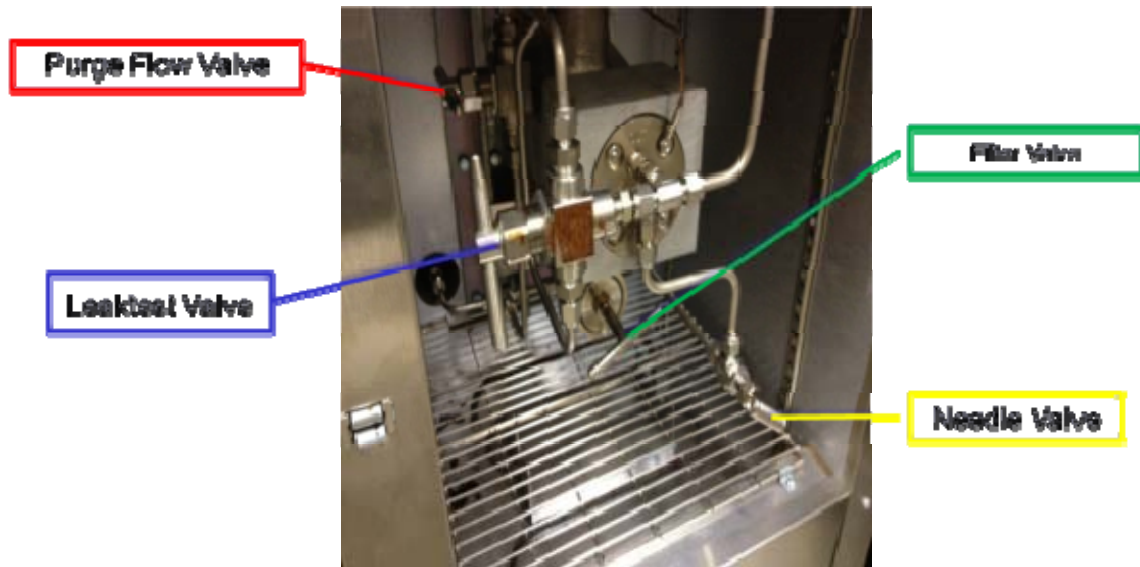**Figure C.7: CAI flow switch panel**

Figure C.8: Inside CAI sample oven

C.1 CAI Calibration Procedures

Calibrating the CAI emissions machine is a fairly simple process. Before beginning calibration it is important to ensure span gases are available in the tank farm shown in Figure C.9. The span gases are short tanks and can be seen in Figure C.10. In addition to the span gases, continuous emissions monitoring (CEM) air and a helium hydrogen fuel blend are also required to complete the calibration shown in Figure C.11. Specifics on the composition of span gases, CEM air, and helium hydrogen blend can be found in the CAI binder in the COAL laboratory as they will change with each new bottle that is used. It is very important to have accurate records of these gases as it has a direct impact on the calibration of the CAI machine.

Figure C.9: Fuel farm

Figure C.10: Span gas tanks, O$_2$, CO, CO$_2$

Figure C.11: CEM air tank

The calibration proceedures are as follows.

1) Bleed fuel line to remove excess air from the line

2) Set the range selector to the correct concentration number

3) Set the Diagnostic Selector to "Sample Pressure"

4) Set the Mode Selector to "Span"

5) Set the Flow Switch to "Zero"

6) Adjust Zero Dial to bring indicator to 0.0

7) Set the Flow Switch to the appropriate span, either "Span 1" or "Span 2"

8) Adjust the Span Dial to bring the indicator to specified concentration

9) Set the Flow Switch to" Zero

10) Verifiy 0.0 state on indicator, if incorrect repeat steps 6 to 10 until correct values are

obtained

Appendix D: Fuel Flow Calculation for the ITB and STE

The below Matlab code is able to calculate the fuel flow rates for the ITB need for operating the fuel pump for a given equivalence ratio.

```
clc
clear

%% Conversion Factors and Constants
oz_mL = 29.573529563; % mL/oz
gal_L = 3.785411784; % L/gal
lb_kg = 0.453592; % kg/lbs
C_K = 273.15;

rho_JP8 = 0.804; % kg/L
q_fuel = 43600000; % J/kg
CP = 1106.85; % J/kg K
pump_pres_max = 2000; % psi
pump_Vdot_max = 0.408; % L/min

MW_C = 12.011;
MW_H = 1.008;
MW_air = 28.85;

nozzle_pressure = 300; % psi
nozzle_mdot = 5.4*lb_kg/60/rho_JP8*1000; % mL/min
5.4*lb_kg/60/rho_JP8/gal_L;

%% Variables

T_jetcat = 750 + C_K; % K
mdot_air = .2; % lbs/s
mdot_split_factor = 0.3;
phi_jetcat = .3;
vdot_fuel_jetcat = 24.7*.2; % fl oz / min
n = 6; % number of nozzles
nozzle_number = 0.3;
phi_cav = .4; % cavity phi

den_cav = 0.1; %lbm/ft3
xarea_cav = 1/12*1/12; %ft^2
beta = 28; %degrees
gc = 32.174; %gravitational
r_cav = (6.25/2)/12; %ft
```

```matlab
%%% phi and mdot fuel calc

MW_fuel = 12*MW_C+26*MW_H;
AF_stochiometric = 4.76*18.5*MW_air/MW_fuel;

AF_jetcat = AF_stochiometric / phi_jetcat;

AF_cav = AF_stochiometric / phi_cav;
mdot_air_cavity = mdot_split_factor * mdot_air; % lb/s
mdot_fuel = mdot_air_cavity / AF_cav; % lb/s

T_cavity = q_fuel*mdot_fuel*lb_kg/(mdot_air_cavity*lb_kg*CP) + T_jetcat; % K

AF_overall = mdot_air/mdot_fuel;
phi_overall = AF_stochiometric/AF_overall;

a1 = sprintf('The phi in the cavity is %g',phi_cav);
a2 = sprintf('The temp in the cavity is %g K',T_cavity);
a3 = sprintf('The air to fuel ratio in the cavity is %g',AF_cav);
a4 = sprintf('The overall phi is %g',phi_overall);
a5 = sprintf('The overal air to fuel ratio is %g',AF_overall);
%%% fuel pump calc
pump_mdot_max = pump_Vdot_max * rho_JP8 / 60; % kg/s

%%% fuel nozzle calc

mdot_fuel_injector = mdot_fuel*lb_kg / n; % kg/s

Vdot_nozzle = mdot_fuel_injector/(rho_JP8*gal_L)*60; % gph
Vdot_nozzle_mL = Vdot_nozzle*gal_L*1000; % mL/min

vdot = mdot_fuel*lb_kg/(rho_JP8*gal_L)*60; % gpm
vdot_mL = vdot*gal_L*1000; % mL/min
a6 = sprintf('The total volumetric flow rate is %g mL/min',vdot_mL);
a7 = sprintf('The volumetric flow rate per nozzle is %g mL/min for %g
nozzles',Vdot_nozzle_mL,n);

pressure = (vdot/nozzle_number)^2*4000;

a8 = sprintf('The pressure on the fuel pump should be %g psi',pressure);
%%% JetCat fuel flow
vdot_fuel_jetcat_mL = vdot_fuel_jetcat * oz_mL; % mL/min

a9 = sprintf('The JetCat volumetric flow rate is %g mL/min',vdot_fuel_jetcat_mL);
```

```matlab
%% g-loading nonsense

vtan = (mdot_air_cavity + mdot_fuel)/(den_cav * xarea_cav) * (1 / tand(beta));
gload = vtan^2 / (gc*r_cav);

a10 = sprintf('The g-load in the cavity is %g',gload);

%% Results
disp(a1)
disp(a2)
disp(a3)
disp(a4)
disp(a5)
disp(a6)
disp(a7)
disp(a8)
disp(a9)
disp(a10)
```

Appendix E: Air lines

A 3" air line was installed into the lab with a higher mass flow rate for the increased size of the rig. The new full annular rig requires a higher mass flow rate of 1 lb/sec. The 3" air line is capable of provide this larger amount of air flow. The previous mass flow rate available was 0.3 kg/s. The new 3" air line was installed by John Hixenbaugh, a laboratory technician at AFIT. The addition of the 3" air line required installation of new flow controllers, flow meters, a regulator, and an air compressor. The new air compressor is located in the shipping crate outside of the COAL laboratory shown in Figure D.1. It is capable of compressing air to 120 psig. The compressed air is stored in an air tank outside between the exterior wall of the COAL laboratory and the air compressor shipping container shown in Figure D.2. The air then comes into the COAL lab to the flow control tree seen in Figure D.3. The flow control tree allows the 3" air line compressor to provide air to the 1.5" and 0.75" air lines in the case of a failure in their primary air source. The 3" air line then proceeds to the new regulator which is capable of reducing the pressure down to 100 psig seen in Figure D.4. Downstream of the regulator is the new Foxbox air flow meter measures the flow rate in kg/s seen in Figure D.5. After the flow meter is the new air flow controller which is capable of allowing 0.675 kg/s of air flow seen in Figure D.6. The addition of the 3" air line caused the 1.5" and 0.75" air lines to be rearranged in the COAL laboratory. This allowed all three air lines to be mounted on the same wall and be integrated into the flow control tree shown in Figure D.**7**.

Figure D.1: Air compressor housing outside COAL lab
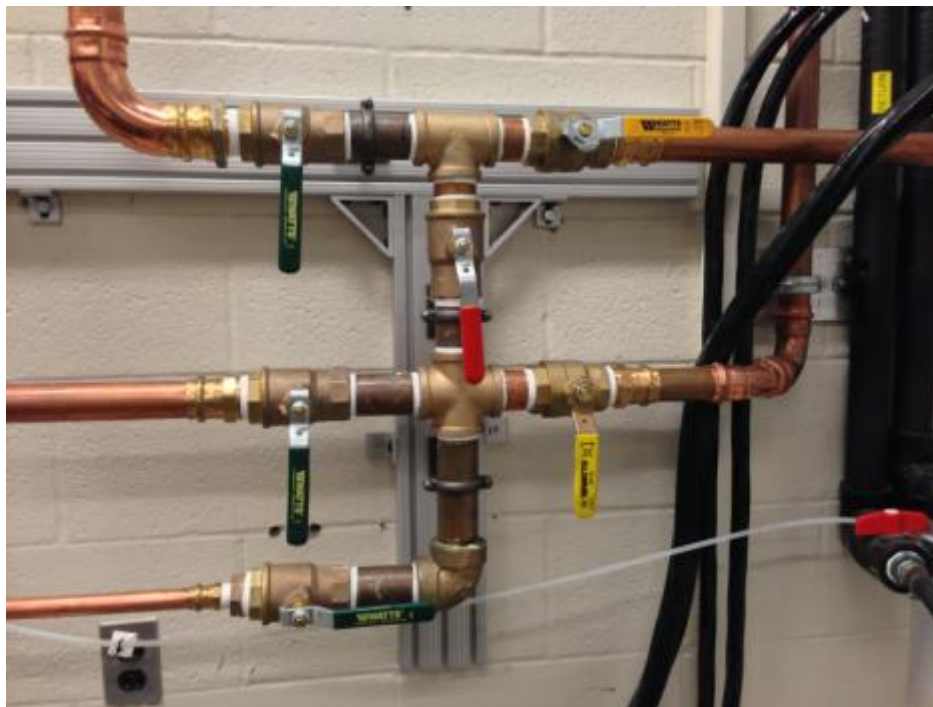

Figure D.2: 3" air line tank

Figure D.3: Air flow control tree

Figure D.4: 3" air line regulator

Figure D.5: Fox box mass flow meter

Figure D.6: 3" air line mass flow controller

Figure D.7: 0.75", 1.5", and 3" air lines

Bibliography

1. Lewis, G. D., "Swirling-Flow Combustion – Fundamentals and Application", AIAA/SAE 9th Propulsion Conference, 1973, AIAA-1973-1250.

2. Bohan, B. T., Polanka, M. D., "Analysis of Flow Migration in an Ultra-Compact Combustor Part", *Journal of Engineering for Gas Turbines and Power*, 2013

3. Sirignano, W. A., Liu, F., "Performance Increases for Gas-Turbine Engines Through Combustion Inside the Turbine", *Journal of Propulsion and Power*, 1999, Vol. 15, No. 1

4. Wilson, D. G., Korakianitis, T., "The Design of High-Efficiency Turbomachinery and Gas Turbines", Upper Saddle River, NJ, Prenice-Hall, 1998

5. Sirignano, W. A., Delphanque, J. P., Liu, F., "Selected Challenges in Jet and Rocket Engine Combustion Research", 33rd AIAA/ASME/SAE/ASEE Joint Propulsion Conference & Exhibit, 1997, AIAA-97-2701.

6. Zelina, J., Shouse, D. T., Hancock, R. D., "Ultra-Compact Combustors for Advanced Gas Turbine Engines", ASME Turbo Expo, 2004, 2004-GT-53155.

7. Zelina, J., Sturgess, G. J., Shouse, D. T., "The Behavior of an Ultra-Compact Comubstor Base on Centrifugally-Enhanced Turbulent Burning Rates", 40th AIAA/ASME/SAE/ASEE Joint Propulsion COnference and Exhibit, 2004, AIAA-2004-3541.

8. Zelina, J., Shouse, D. T., Stutrud, J. S., Sturgess, G. J., Roquemore, W. M., "Exploration of Compact Combustors for Reheat Cycle Aero Engine Applications", ASME, 2006, GT2006-90179.

9. Liew, K. H., Urip, E., Yang, S. L., Mattingly, J. D., Marek, C. J., "Performance Cycle Analysis of Turbofan Engine with Interstage Turbine Burner", *Journal of Propulsion and Power*, 2006, Vol. 22

10. Zelina, J., Sturgess, G. J., Mansour, A., Hancock, R. D., "Fuel Injection Design Optimization for an Ultra-Compact Combustor", ISABE, 2003, ISABE-2003-1089

11. Thornburg, H., Sekar, B., Zelina, J., Greenwood, R., "Numerical Study of an Inter-Turbine Burner (ITB) Concept with Curved Radial Vane." 45th Aerospace Sciences Meeting & Exhibit, 2007, AIAA-2007-649.

12. Baranski, J. A., Hoke, J. L., Litke, P. J., Schauer, F. R., "Preliminary Characterization of Bio-fuels using a Small Scale Gas Turbine Engine." AIAA

13. Wilson, J. D., Polanka, M. D. "Analytical and Experimental Study of Pressure Losses due to Rayleigh Effects", IGTI, 2013, GT2013-94795

14. Spytek, C. J., "Application of an Inter-Turbine Burner Using Core Dirven Vitiated Aire in a Gas Turbine Engine." Proceeding of ASME Turbo Expo 2012, 2012, GT2012-69333.

15. Reaction Design, "CHEMKIN-PRO", San Diego, CA, 2010, www. reactiondesign.com

16. United States Department of Labor. *Kerosene.* US Governement. http://www.osha.gov/dts/sltc/methods/partial/pv2139/pv2139.html (accessed Jan 17, 2013).

17. 88 AMDS/SGPB to AFRL/SE, "Noise Survey Turbine ENgine Division (0206-RDLA-092A)", May 19, 2009

Vita

    Captain Matthew M. Conrad graduated Northville High School in Northville, Michigan in 2003. Upon graduation, he attended Purdue University to pursue a degree in Aeronautical and Astronautical Engineering. In 2008, he completed his undergraduate work and was commissioned as a Second Lieutenant in the United States Air Force.

    His first assignment was to the United States Air Force Test Pilot School at Edwards AFB, California. He was assigned to the Education Division, Flying Qualities Branch as the Assistant Branch Chief. He led the short course program, conducted research into parameter identification for flight control systems and co-taught the capstone flying qualities project. In August 2010, he received a permanent change of assignment to the F-22 Combine Test Flight where he worked as a performance and flying qualities developmental engineer. His focus was on increasing test card standardization to improve testing safety and streamline new software updates to the warfighter.

    In May 2011, he entered the Graduate School of Engineering and Management at the Air Force Institute of Technology to pursue a Master's Degree in Aeronautical Engineering. Upon graduation, Captain Conrad will be assigned to the Air Force Research Laboratory, Wright-Patterson Air Force Base, Ohio to conduct research in hypersonic combustion.

1. REPORT DATE *(DD-MM-YYYY)* 21-03-2013	2. REPORT TYPE Master's Thesis	3. DATES COVERED *(From – To)* May 2011 – March 2013

TITLE AND SUBTITLE Integration of an Inter Turbine Burner to a Jet Turbine Engine	5a. CONTRACT NUMBER
	5b. GRANT NUMBER
	5c. PROGRAM ELEMENT NUMBER
6. AUTHOR(S) Conrad, Matthew M., Captain, USAF	5d. PROJECT NUMBER
	5e. TASK NUMBER
	5f. WORK UNIT NUMBER

7. PERFORMING ORGANIZATION NAMES(S) AND ADDRESS(S) Air Force Institute of Technology Graduate School of Engineering and Management (AFIT/ENY) 2950 Hobson Way, Building 640 WPAFB OH 45433-8865	8. PERFORMING ORGANIZATION REPORT NUMBER AFIT-ENY-13-M-06

9. SPONSORING/MONITORING AGENCY NAME(S) AND ADDRESS(ES) Air Force Office of Scientific Research – Energy, Power and Propulsion 875 N. Randolph St. Suite 325, Room 3112 Arlington, Virginia 22203 (703) 696-8574 Chiping.Li@AFOSR.AF.MIL Dr. Chiping Li	10. SPONSOR/MONITOR'S ACRONYM(S) AFOSR/RTE
	11. SPONSOR/MONITOR'S REPORT NUMBER(S)

12. DISTRIBUTION/AVAILABILITY STATEMENT
   APPROVED FOR PUBLIC RELEASE; DISTRIBUTION UNLIMITED.

13. SUPPLEMENTARY NOTES
This material is declared a work of the U.S. Government and is not subject to copyright protection in the United States.

14. ABSTRACT
As aircraft power requirements continue to grow, whether for electrical systems or increased thrust, improved engine efficiency must be found. An Ultra-Compact Combustor (UCC) is a proposed apparatus for accomplishing this task by burning in the circumferential direction as a main combustor or an Inter-Turbine Burner (ITB). In order for the UCC to be viable it is important to study the effects of feeing the core and circumferential flows from a common gas reservoir. This research effort has developed a diffuser, for the AFIT Combustion Laboratory, that is capable of 80/20, 70/30, and 60/40 mass flow splits between the core and cavity for flow emanating from a single source. The diffuser was fabricated robustly so that the single flow source may consist of a vitiated air, such as that from a small jet engine, or a clean air source of compressed air. Chemical analysis software (CHEMKIN) was applied to assist in the prediction of which flow split would produce the best results and testing of this prediction was initiated. A second important issue for UCC development is the assessment of the effects of g-loading on atomized fuel sprays within a UCC because it is important to stabilize the flame in the cavity. To this end, fuel spray experiments have been conducted over a g-load range of 0 to 3000 to examine how atomized fuel behaves within the circumferential cavity. Results gathered from high speed imaging showed that as g-load increased, fuel carried toward the outside diameter of the circumferential cavity. Results were obtained for combinations of fuel pressure, and cavity air mass flow rate. In summary, a new rig has been developed that will facilitate future endeavourers into UCC research.

15. SUBJECT TERMS
   Combustion, Combustor, Experimental, Ultra-Compact Combustor, Fuel Spray

16. SECURITY CLASSIFICATION OF:			17. LIMITATION OF ABSTRACT	18. NUMBER OF PAGES	19a. NAME OF RESPONSIBLE PERSON Dr. Marc D. Polanka, ENY
a. REPORT	b. ABSTRACT	c. THIS PAGE	UU	143	19b. TELEPHONE NUMBER *(Include area code)* (937) 255-3636, ext 4714 (marc.polanka@afit.edu)
U	U	U			